UNIVERSITÀ POLITECNICA DELLE MARCHE

SCUOLA DI DOTTORATO DI RICERCA IN SALUTE DELL'UOMO

XV° CICLO

# *Osteoclast-specific Tsc2 deletion in mice increases bone mass: a model for the study of sclerotic bone lesions in Tuberous Sclerosis*


Presentata da: Dr. Nicola Alesi

Relatore : Chiar.mo Prof. Antonio Domenico Procopio


Triennio Accademico 2013-2016

# *Index*

# *1. Introduction*

## *1.1 Tuberous Sclerosis: Historical Notes*

Tuberous sclerosis or Tuberous Sclerosis Complex is an autosomal dominant, multisystemic disorder with high penetrance and variable expression, which can cause benign and less commonly malignant lesions in any organ (1, 2).

The term "tuberous sclerosis of the cerebral convolutions" was used for the first time more than a century ago to describe the distinctive autopsy findings in some patients presenting with symptoms of seizures and mental abnormality (3, 4).

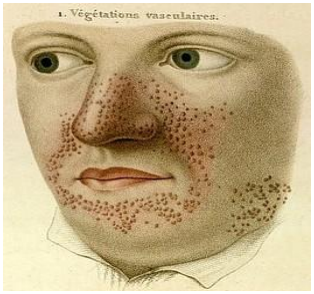


Fig.1. Atlas of skin by Rayer: vegetations vasculaires

Tuberous Sclerosis is also known as Bourneville-Pringle Disease, although, these two physicians were not the first who reported patients with signs that later were considered to be the diagnostic criteria.

Fig.2.Von Recklinghausen

Reports of the disease started to be published in the 19th century and were based on the descriptions of clinical and pathological findings. The first lesions to be described were the characteristic skin lesions, mentioned in 1835 in Rayer's atlas of skin diseases. He named the facial lesions ''ve´ge´tations vasculaires''. In 1862 Von Recklinghausen, was the first to observe the cerebral involvement after performing an autopsy of a newborn that died few minutes after birth in which he found cardiac myomata and sclerotic brain lesions (5).

However, the description of the cerebral pathology and neurological signs in Tuberous Sclerosis is credited to Désiré-Magloire Bourneville in 1880. He described the case of a 15-year old girl with a history of seizures, psychomotor retardation and “confluent vascular papulous eruption of the nose, the cheeks, and forehead” (6). Bourneville proposed the term “scle´rose tube´reuse des circonvolutions ce´re´brales” to characterize the large islets of sclerosis with potato-like consistency he found in the cortical gyri.

Fig.3. Desire’-Magloire Bourneville

In 1890 Scottish dermatologist John James Pringle described the butterfly-pattern facial rash of a 25-year-old woman, who also presented with subnormal intelligence and rough lesions on the arms and legs. Pringle believed the facial glands to be the source of the problem, leading to the eponym Pringle’s adenoma sebaceum. This is a misnomer as the papules are neither adenoma nor derived from the sebaceous glands but rather facial angiofibroma, one of the benign lesions frequently observed in patients with Tuberous Sclerosis (8, 9). Pringle was the first to associate skin lesions and mental abnormality.

Fig.4. John James Pringle

Van der Hoeve, who characterized the retinal hamartomas in Tuberous Sclerosis and Neurofibromatosis, introduced the name phakomatosis (phakos means spot), comprehensive of both diseases (10).

It was the German pediatric neurologist Heinrich Vogt, in 1908, which recognized the facial rash, the intellectual deficits and the seizures as part of the same condition, known as Vogt's triad. Vogt's triad defined the diagnosis of Tuberous Sclerosis for the next 70 years (11-12). Nine years later, Shuster proposed the existence of a variant of Tuberous Sclerosis, after observing a young male patient with angiofibromas and epilepsy but no mental retardation (13).

We must wait until 1979 with Gomez, "the Godfather of Tuberous Sclerosis" to have a complete clinical description of Tuberous Sclerosis (14, 15), he described in details all the diagnostic features of the disease, in various organs, dividing them in: definitive, presumptive and suspect (fig. 5).

**TABLE 1.** Hierarchy of Clinical or Imaging Features for the Diagnosis of TSC

| | Diagnostic Features | | |
|---|---|---|---|
| Organ | Definitive | Presumptive | Suspect |
| CNS | Cortical tuber<br>Subependymal nodules<br>Giant cell astrocytoma | | Infantile spasms<br>Gnzld/part seizures |
| Retina | Hamartomas | Hamartoma | |
| Skin | Facial angiofibromas<br>Ungual fibroma<br>Fibrous forehead plaque | Confetti-like spots | Hypomelanotic macules |
| Kidneys | Multiple angiomyolipo-mas | Angiomyolipoma | Cysts |
| Heart | | Multiple rhabdomyomas | Rhabdomyoma |
| Lungs | | Lymphangiomyomatosis | Spontaneous pneumothorax<br>Chylothorax<br>Honeycomb image |
| Teeth | | | Enamel pits |
| Gingiva | | | Fibromas |
| Rectum | | Polyps | |
| Thyroid | | | Adenoma |
| Adrenal | | | Angiomyolipoma |
| Gonads | | | Angiomyolipoma |
| Liver | | | Angiomyolipoma |
| Bones | | | Cysts<br>Osteom thickening |

Fig. 5. Diagnostic Features of Tuberous Sclerosis by Gomez. 1991 (15)

## *1.2 Genetics of Tuberous Sclerosis*

The probable link between Tuberous Sclerosis (TSC) and a gene on chromosome 9q34 was first described in 1994 (16). This gene was called *TSC1* but linkage with this region of the genome was not found for all affected families. Therefore, it was theorized that there must be at least one other locus associated with the disease. In the same year, the locus 16p13 was linked to Tuberous Sclerosis, and the gene involved was named *TSC2* (17, 18, 19). Many scientists have suggested the presence of a third locus, but the current studies consider this possibility high unlikely (fig. 6).

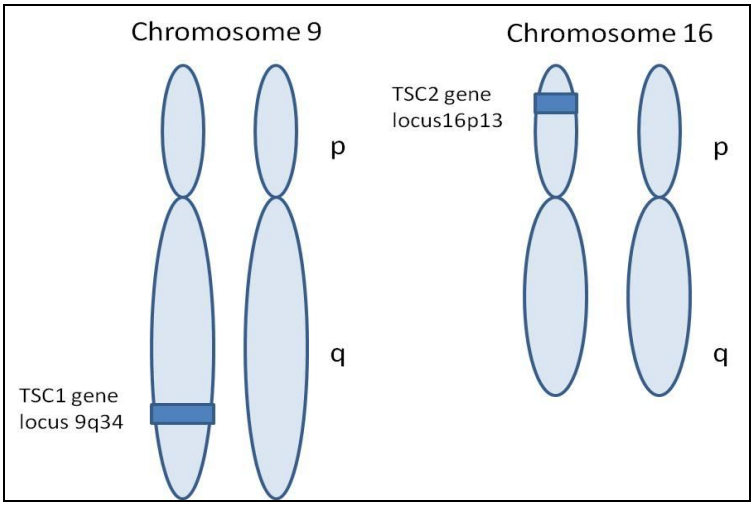


Fig. 6. Position of *TSC1* and *TSC2* genes.

Further observations concluded that the *TSC1* mRNA encoded a protein of 130 kDa that was named HAMARTIN. The *TSC2* mRNA was predicted to encode a 198 kDa protein that was named TUBERIN (20).

The *TSC1* gene consists of 23 exons, 53284 nucleotides; *TSC2* consists of 42 exons, 40723 nucleotides; The 3' UTR of *TSC2* lies together with the 3' UTR region of the *PDK1* gene, this interconnection between the two genes has important therapeutic consequences. Within the *TSC2* gene the highest level of conservation across species is in the GAP domain, showing the importantance of this region for the function of the protein. In *TSC1*, regions of high conservations between species lie in the N-terminal and C-terminal regions of the gene.

TSC1 and TSC2 proteins interact to form a complex, with the binding region consisting of amino acids 1-418 in TSC2 and 302-430 in TSC1. Both proteins can be phosphorylated at multiple sites, regulating, through the GAP domain of TSC2, the activity of another protein: RHEB. These phosphorylation sites are highly conserved among species.

Large deletions and rearrangements in *TSC2* are frequent, and many extend beyond the gene, affecting the *PDK1* gene as well, event known to be associated with early onset polycystic kidney disease. Large deletions are less frequent in *TSC1*. Polymorphism is very common in the *TSC2* gene, but less in *TSC1* (22). TSC-causing mutations have been identified in all the exons of the two genes except for the exon 23 of *TSC1* and the exons 25 and 31 of *TSC2*.

In the general population of individuals affected by Tuberous Sclerosis, mutations in *TSC1* are less commonly observed than mutations in *TSC2*, 26% versus 74%. Mosaicism is described in Tuberous Sclerosis patients in both forms: somatic mosaicism (generalized) and germline (only gonadal). Somatic mosaicism is quite common in Tuberous Sclerosis patients with large deletions, less common in patients with small deletions (23). Early reports suggested a high frequency (10%) of mosaicism, more recently the frequency was observed to be around

1% (24). The severity of the disease correlates with the level of mosaicism; however, some mosaic patients have a full and severe phenotype. Germline mosaicism has been characterized in Tuberous Sclerosis as well, since around 2% of Tuberous Sclerosis families have at least two members affected in a generation, without any mutation found in the genomic DNA of either parent. Nowadays, mutations are discovered in 90% of the patients with a phenotype of Tuberous Sclerosis. Patients in whom a specific mutation is not found usually present with milder symptoms. Mosaicism and errors in mutation detection (if the mutation is in a remote non-coding region of the genes) might explain why it is impossible to describe a mutation in almost 10% of Tuberous Sclerosis patients (25-27).

The genotype-phenotype correlation in Tuberous Sclerosis has been analyzed extensively. *TSC2* mutations correlate with a more severe phenotype since almost all the clinical features are more common in *TSC2* patients, compared to patients with a *TSC1* mutation. Familial Tuberous Sclerosis has a milder phenotype than sporadic Tuberous Sclerosis. This has been noted in several studies, and for different features like mental retardation, hypomelanotic macules, retinal phakomas, subependymal nodules and renal angiomyolipomas. Mutation in the *TSC1* gene is more likely to be familiar, whereas mutation in *TSC2* is more frequently sporadic. Male sex correlates with a worse phenotype in Tuberous Sclerosis. In fact, all the manifestations of Tuberous Sclerosis are more common in males than females except for lymphangioleiomyomatosis (LAM) (28-30). However, there is great variability of the phenotype, even in patients of the same family expressing the same mutation. Several studies have suggested correlations between the nature of the mutations in both genes with neurologic and psychiatric symptoms such as the severity of epilepsy and mental retardation (31-33).

Individuals with Tuberous Sclerosis are heterozygous for *TSC1* or *TSC2*. It is well recognized that in order to develop a lesion a second somatic mutation in the other copy of the gene must occur. Loss of heterozygosity is therefore necessary for the development of the phenotype.

## *1.3 Epidemiology and Criteria for Diagnosis*

The term Tuberous Sclerosis Complex (TSC) was proposed by Molten to account for the multiple organs involved in the disease (4). Tuberous Sclerosis affects 2 million individuals worldwide and the incidence is approximately 1 case per 6,000-10,000 live births (34-36).

Approximately 96% of patients with TSC have one or more skin lesions, 90% have symptoms of cerebral involvement, 85% history of seizures, 60% show renal involvement, 50% retinal pathology. Almost every organ can be affected, the only tissues never reported to be involved in TSC patients are skeletal muscles and peripheral nerves.

The diagnosis of TSC can be hard, since only a few patients express the Vogt triad of seizure, mental retardation and skin abnormalities. Therefore, radiology (brain, heart, lung and kidneys) or genetic testing is, nowadays, necessary for the diagnosis. The genetic counselling can be requested because of family history of the disease, although several of the patients affected represent new mutations. Cognitive and developmental examination should always be performed. The identification of a mutation in either *TSC1* or *TSC2* is considered sufficient for the diagnosis, though in more than 10 percent of the patients no mutation is identified. The identification of a mutation is particularly important in that subclass of *TSC2* patients in which the mutations extend into the *PDK1* gene, since these patients will show a particularly severe kidney phenotype (35, 37).

Based on the 2012 TSC Consensus Conference, Northrup et al updated the clinical diagnostic criteria as stated below (38).

*Genetic diagnostic criteria*

Normal Tissue identification of either a *TSC1* or *TSC2* pathogenic mutation is sufficient to make a definitive diagnosis of TSC. A pathogenic mutation is defined as a mutation that clearly inactivates the function of the TSC1 or TSC2 proteins. Approximately 10% of patients with TSC do not have a mutation that can be identified by testing; therefore, a normal result is not enough to exclude the disease and a clinical deep evaluation is needed" (38).

*Clinical diagnostic criteria*

Diagnosis of TSC is certain if a patient presents two major features or one major and two minor. Diagnosis of TSC in possible if the patient presents either one major feature or at least two minor features. (38).

## Major features:

Hypomelanotic macules (≥3 of ≥5 mm in diameter)

Angiofibromas (≥3) or fibrous cephalic plaque

Ungual fibromas (≥2)

Shagreen patch

Multiple retinal hamartomas

Cortical dysplasia (includes tubers and cerebral white matter radial migration lines)

Subependymal nodules

Subependymal giant cell astrocytomas

Cardiac rhabdomyomas

Lymphangioleiomyomatosis (LAM)

Angiomyolipomas (≥2)

Minor features:

‘Confetti’ skin lesions

Dental enamel pits (>3)

Intraoral fibromas (≥2)

Retinal achromic patch

Multiple renal cysts

Non-renal hamartomas.

A combination of LAM and Angiomyolipomas without other features does not meet criteria for a definitive diagnosis since they are considered one the metastatic manifestation of the other (38). Cystic bone lesions, previously included as minor criteria, are no longer considered for the diagnosis of TSC since they are nonspecific.

Rapamycin (sirolimus) started to be used clinically in 1999 as an immunosuppressant, and has been used since 2003 in the treatment of Tuberous Sclerosis. Nowadays, not only sirolimus but also is derivative, everolimus, are effectively used in long-term therapy of Tuberous Sclerosis.

## *1.4 Common Manifestations of Tuberous Sclerosis and Their Treatment*

Tuberous Sclerosis can affect multiple organs, the most common are: Brain, Kidney, Lung, Skin, Heart and eye. Some of the features are summarize in fig. 7.

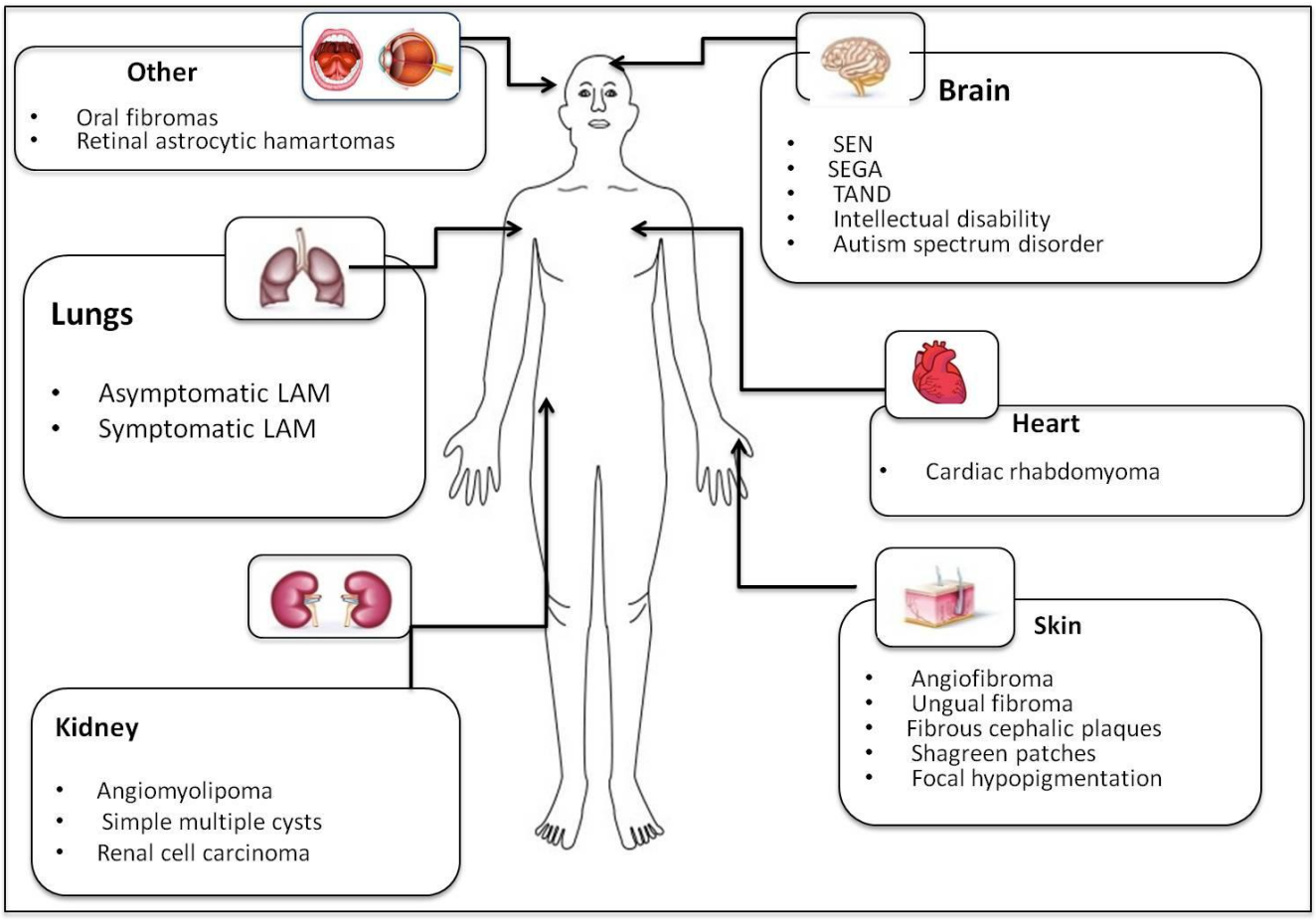


Fig. 7. Common manifestations of TSC.

*Brain*

Neurological manifestations are the most frequent morbidities in patients with TSC. Epilepsy is the most common symptom, affecting 8 out of 10 patients and frequently represents the first sign of the disease (39). The earlier it develops, the more it will be followed by severe developmental problem such as speech impairment, neurophysiologic disorders and autistic behavior (35, 40-42). In one third of patients, the initial partial seizures will develop into West Syndrome (infantile spasm), events that correlate negatively with the prognosis and the efficacy of the therapy (43).

The anticonvulsant drug vigabatrin, an irreversible inhibitor of GABA transaminase should be used as a first-line treatment (44, 45). Unfortunately, epilepsy becomes resistant in more than 50% of the patients. Rapamycin in combination with anticonvulsivant as a new therapeutic approach is under investigation on clinical trials (35, 46, 47). Dietary therapy (ketogenic diet, and low glycemic diet) was seen demonstrated to be very effective, as was vagal nerve stimulation (48-50). The role of mTOR inhibitors like rapamycin in combination with anticonvulsant in the treatment of refractory epilepsy in TSC is under investigation (49, 50). The last available therapeutical option is represented by surgical resection (51).

SEGAs (subependymal giant cell astrocytomas) are present in 10–15% of individuals with TSC, they usually develop during the first two decades of life, and curiously they stop growing and usually calcify after the second decade of life (52). SEGAs localize under the ependymal lining of the ventricular wall, in the region of the foramen of Monro. Sub

Ependymal Nodules (SEN) are considered the precursors of SEGAs and are very common in TSC, with almost 90% of the patients showing at least one.

Resection was the only option to manage symptomatic SEGAs in the past. Nowadays, everolimus is approved by FDA in the treatment of SEGAs (35, 53).

*Neuropsychiatric Disorders*

TSC-associated neuropsychiatric disorders (TANDs) are present in half of the individuals with TSC (54). The incidence of autism is 40% in individuals with TSC (55). 5 out 0f 10 individuals with TSC will develop anxiety; moreover, obsessive-compulsive behavior is frequently observed. Unfortunately, no specific treatments are available for TANDs.

*Lung*

Lymphangioleiomyomatosis (LAM) is the most frequent pulmonary manifestation of TSC. LAM is characterized by cysts formation, spontaneous pneumothorax, and chylous pleural effusion. Asymptomatic LAM (presence of multiple lung cysts without symptoms) occurs in up to 90% of women with TSC, whereas symptomatic LAM (presence of cysts and symptoms like chest pain and shortness of breath) occurs in about 10% of women with TSC and can lead to respiratory failure (35, 56, 57).

Curiously LAM progresses more quickly in premenopausal women than in postmenopausal women, raising the question of whether estrogens are involved in the pathogenesis of the disease. There have been many reports describing a worsening of LAM symtoms during pregnancy, again suggesting a causal relationship between LAM and the estrogen production (58). A very small percentage of men with TSC present with asymptomatic

lung cysts and it has never been reported a man with symptomatic LAM (59, 60). Multifocal micronodular pneumocyte hyperplasia (MMPH) is another possible manifestation of TSC in lung.

A large percentage of women with LAM also present with a single renal angiomyolipoma. The presence of identical somatic mutations in LAM cells and in renal AMLs has led to the hypothesis that LAM cells metastasize to the lungs from kidneys.

Bissler et al published a clinical trial of rapamycin for renal angiomyolipomas (AMLs) associated with tuberous sclerosis or lymphangioleiomyomatosis (LAM), a year rapamycin manifestation showed 50% decrease in AML volume. The study also reported amelioration in forced expiratory volume (FEV1), forced vital capacity (FVC) and residual volume (RV) in patients with pulmonary LAM (61).

*Kidney*

Renal lesions in TSC are extremely common and present since childhood, angiomyolipomas (AMLs) a tumor characterized by the presence of different cells: blood vessels, smooth muscle cells and fat cells; and cysts (which can develop in AMLs) are the most common manifestations. By adulthood, up to 70% of patients with TSC have AMLs (62), AMLs differ from SEGAs since they keep growing after the first two decades of life (63). 35% of patients with TSC present only simple cysts (64, 65). Renal cell carcinoma is extremely rare in TSC but can affect children (66-68).

Lesions that are growing and are >30 mm in diameter are most at risk of causing bleeding (35, 69). Percutaneous embolization used to be the first line treatment for acute

bleeding in AMLs (70). Systemic mTOR inhibitor therapy rather than embolization is now the preferred pre-emptive treatment for AMLs. (71). The EXIST-1 trial has shown that everolimus is effective in stabilizing and partially reversing early renal disease in children and provides a durable response (72, 73).

*Skin*

Skin manifestations are the most common features of TSC. Focal hypomelanotic plaques are present in almost every patient. The usual site of presentation is the back. Facial angiofibromas are present in 75% of the patients. Ungueal fibromas are present in 50% of the patients. Fibrous cephalic plaques are present in 25% of patients. Shagreen patches, areas of thickened skin, are present in 50% of the patients. Sun exposure has been implicated in the development of such lesions (35, 72).

Clinical trials have demonstrated consistent partial responses to both systemic and topical (Rapamycin 1% preparation) mTORC1 inhibitor therapy (73, 74). The EXIST-1 and EXIST-2 trials of systemic everolimus therapy for SEGA and AML reported significant partial responses compared with placebo. In addition, oral sirolimus (rapamycin) has been shown to significantly improve the outcome of TSC skin lesions, particularly angiofibromas, during long-term treatment (35, 75).

*Opthalmic Manifestations*

The anterior segment and the retina are frequently involved in TSC. Angiofibromas of the eyelid are present in 40% of the TSC population; hamartomas of the iris and ciliary body are less common. The astrocytic retinal hamartomas are by far the most common lesion, and

sometimes represent the first manifestation of the disease. Typically, the hamartomas are located near the optic nerve head, are frequently bilateral but only rarely cause loss of vision. Chorioretinal hypopigmented lesions are also quite common in TSC patients. They are located in the posterior retina and have been observed in 40% of the patients (76-78).

*Heart*

Cardiac rhabdomyomas (CRs) are the earliest detectable hamartoma in TSC. Curiously they represent the only lesion in TSC that regress spontaneously. Mostly rhabdomyomas are asymptomatic; however, they can lead to arrhythmias or cardiac failure; moreover, they represent the most frequent cause of death among TSC children below 10 years of age. Since postnatal regression of CRs is common, only very large and hemodynamically significant lesions need to be removed. The size is usually between 5-15 mm in diameter; they can be multiple and affect both ventricles and less commonly the atria. Since they represent an exceptional finding in the normal population, the observation of a CR in a child should be followed by genetic evaluation. Conservative approach and strict follow-up of the lesions are the common approach, while excision is considered only in patients with a severe hemodynamic syndrome. Rapamycin has been reported to have no significant benefit in the treatment of RCs (79-82).

## *1.5 The Role of mTORC1 Signaling in Tuberous Sclerosis*

Rapamycin was discovered in 1975, as a product of a strain of bacteria called Streptomyces Hygroscopicus isolated from a soil sample from an island called Rapa Nui (Easter Island) (83). Rapamycin is a molecule with antibiotic and antifungal properties belonging to the class of macrolides.

Rapamycin associates with FKB12, an immunophilin protein. The connection between the two molecules is fundamental for the activity of rapamycin. Studies on mammalian cells identified a single protein directly inhibited by the FKBP12-rapamycin complex; this is universally recognized as mammalian Target of Rapamycin, **mTOR** (fig 8).

The mTOR protein is 2549 amino acids and contains several domains. It assembles into two different complexes called mTORC1 and mTORC2. The mTORC1 complex is formed by: mTOR, mLST8, PRAS40, and RAPTOR. The mTORC2 complex consists of: mTOR, mLST8, SIN1, RICTOR and PROTOR/PRR5. The capability of TOR proteins to form large macromolecular complexes is highly conserved between species (84). MTORC1 is very sensitive to rapamycin, whereas mTORC2 is insensitive to acute rapamycin treatment but sensitive after chronic exposure (85).

Before the discovery of mTOR, rapamycin was already known to be a potent inhibitor of proliferation in T and B cells, because of its effect in blocking the cell cycle in G-1 phase (86). Rapamycin decreases the activation of the 70KD ribosomal S6 Kinase (S6K1) mediated by cytokines and growth factors, as well as the phosphorylation of the eukaryotic translation

factor 4E (elF4) and 4E binding protein 1 (4E-BP1), two proteins involved in the control of mRNA translation (87-89). These effects of rapamycin are dependent on mTORC1 inhibition, since mTORC1 can directly phosphorylate S6K1 and 4E-BP1 (90). The phosphorylation of S6K1 by mTORC1 occurs on T389, in a hydrophobic motif C-terminal to the S6K1 kinase domain, leading to the full activation of S6K1. S6K1 is itself a kinase able to phosphorylate S6 and eIF4B, promoting protein synthesis and cell growth (91). Regarding 4E-BP1, mTORC1 phosphorylates residues S65 and T70. After being phosphorylated, 4E-BP1 is released from the binding protein eIF4E, allowing eIF4G association, ribosome recruitment and translation initiation (92, 93). Both S6K1 and 4EBP1 shared a motif called the Tor signaling motif (TOS) that binds RAPTOR, therefore the two proteins are specifically phosphorylate by mTOR (94).

The activity of mTORC1 is regulated through a protein complex formed by TSC1 and TSC2. Co-overexpression of TSC1 and TSC2 inhibits, while the loss of either protein stimulates mTOR dependent phosphorylation of its substrates (95). Strikingly, S6K1 and 4E-BP1 were found to be highly phosphorylated in cells lacking the TSC1-TSC2 complex, suggesting that constitutive mTORC1 signaling might contribute to TSC pathology (96).

The link between TSC1-2 and mTOR was found in a member of the RAS superfamily called RHEB (Ras-homologue enriched in brain) (97). When the TSC1-TSC2 complex is active, TSC2 stimulates the conversion from the GTP-bound state of RHEB (active) to the GDP-bound state (inactive), the inactive form of RHEB does bind mTORC1, a necessary condition for its activity, consequently mTORC1 is inhibited (98).

In TSC1 or TSC2 deficient cells, in which mTORC1 is constitutively hyperactive, mRNA translation is promoted, due to the increased activity of S6K, whereas the block in cap

dependent translation is withdrawn through phosphorylation and therefore inhibition of 4EBP-1. Therefore, losses of TSC1-TSC2 triggers aberrant mRNA translation and, through increased ribosomal biogenesis, total protein synthesis.

Under normal conditions, mTORC1 can sense signals indicating the presence of nutrients, availability of ATP, hormones (insulin), growth factors and cytokines. Nevertheless, TSC2 deficient cells can proliferate, in an mTORC1 dependent manner, under conditions in which their wild-type counterparts undergo cell cycle arrest (eg. hypoxia or serum starvation). Therefore, the TSC1-TSC2 complex can be considered an oncosuppressor, since its loss results in an uncontrollable hyperactivation of mTORC1, regardless of the environmental status.

The TSC1-TSC2 complex is regulated in turn by many pathways. Insulin, through IRS (insulin receptor substrates) stimulates PI3K/AKT. Phosphorylation by AKT inhibits the GAP domain of TSC2, therefore releasing RHEB and activating mTORC1. TSC2 phosphorylation by AKT also enables the binding of 14-3-3 proteins to TSC2, which further inhibit TSC2 function (99). The ERK-RSK pathway activates mTORC1, since RSK can directly phosphorylate TSC2, disrupting the TSC1-TSC2 complex (100). AMPK, which is activated in low ATP conditions, directly phosphorylates TSC2 on S1271 and S1381. These phosphorylations activate TSC2, therefore inhibiting RHEB and mTORC1 (101). Also, hypoxia can affect mTORC1 through an AMPK dependent mechanism (102); Interestingly, AMPK can also inhibit mTORC1 by directly phosphorylating RAPTOR, reinforcing its effects on TSC1-TSC2 complex. Activity of mTORC1 is also sensitive to amino acid availability through the RAG family of proteins (103, 104).

Several other proteins along the years were discovered to be activated or inhibited by mTORC1, and this kinase complex is a key regulator of cell physiology. For example, mTORC1 can phosphorylate STAT3 at Ser727, and loss of either TSC1 or TSC2 is linked to elevation of STAT3 phosphorylation. STAT3 was found to be necessary to promote the proliferation and survival of cells in which mTORC1 is constitutively active (105). Recently, mTORC1 was recognized as a positive regulator of the expression of many lipogenic genes, including the sterol-regulatory-element-binding proteins (SREBPs). The depletion of SREBPs blocks proliferation in cells with constitutively active mTORC1 (106-107). The positive effect of mTORC1 in lipogenesis is also mediated by the stimulation of peroxisome proliferator-activated receptor γ (PPARγ), a nuclear receptor implicated in the expression of genes that are required for fatty acid synthesis and uptake, through 4E-BP1 (108). MTORC1 controls the transcriptional activity of PPARγ coactivator-1 (PGC1α), a nuclear cofactor that regulates mitochondrial biogenesis and metabolism (110). Furthermore, mTORC1 is a potent inhibitor of autophagy and lysosomal biogenesis through, respectively, inhibition of ULK-1 (a protein involved in the initiation of autophagy) and TFEB (a transcription factor involved in lysosomal biogenesis) (111,112). MTORC1 also increases the expression of ribosomal RNA, transfer RNA and messenger RNA through a positive effect on RNA polymerases (113, 114).

In contrast to mTORC1, mTORC2 is not acutely inhibited by rapamycin. Less is known about the activity of mTORC2 compared to mTORC1, but mTORC2 appears to play a role in the regulation of the actin in cytoskeleton (115, 116). A confirmed target of mTORC2 is the serine/threonine kinase AKT; mTORC2 phosphorylates AKT on S473, a site closely related to the T389 on S6K1 (117). AKT phosphorylation on S473 was found to be severely impaired in TSC deficient cells; therefore, mTORC2 activity is inhibited when mTORC1 is hyperactive

(118). This inhibition of AKT, secondary to inhibition of mTORC2 in TSC deficient cells seems to be responsible for the benign nature of the tumors in TSC, since hyperactivation of AKT is a hallmark of malignant cancers (119).

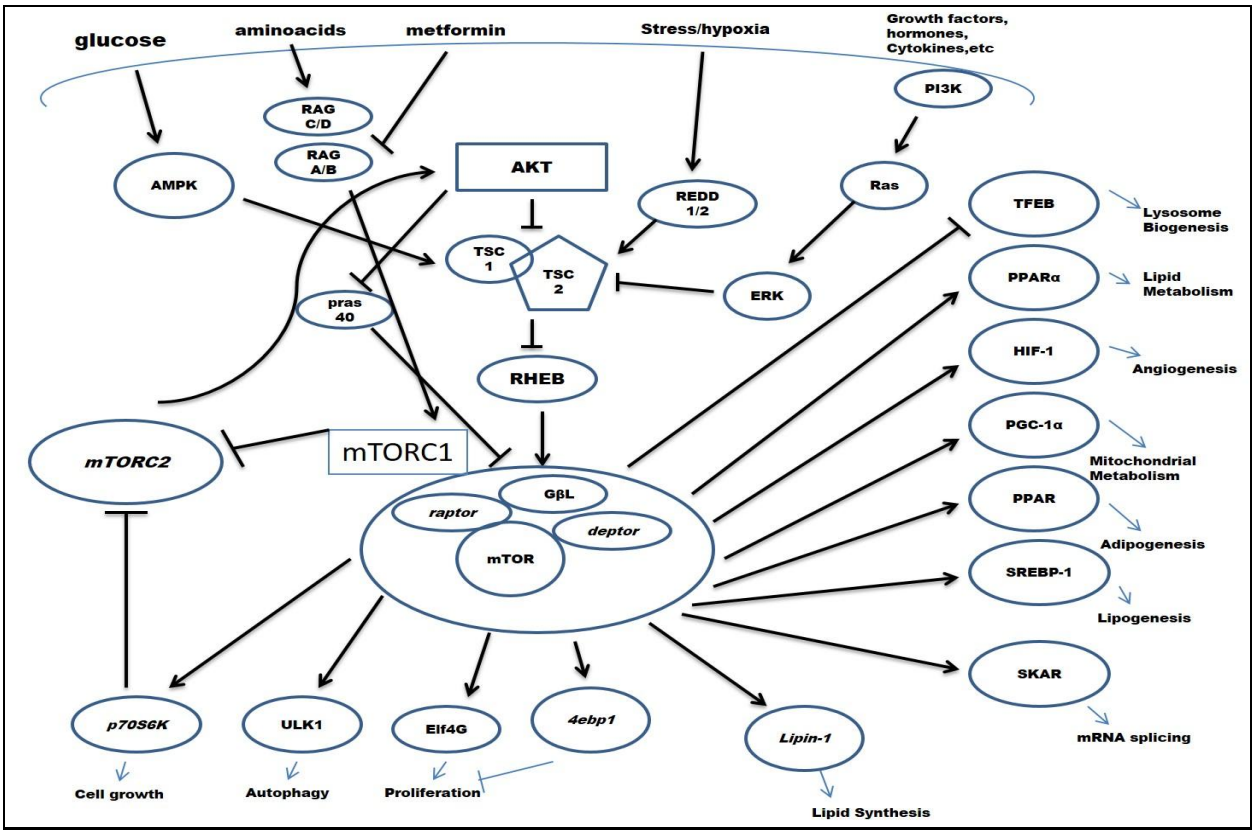


Fig.8. M-TOR signaling pathway.

## *1.6 Elements of Bone Physiology*

Bone is a composite tissue composed of protein and mineral. The three main cell types residing in bone are osteoclasts (OC), which degrade bone, osteoblasts (OB) which create new bone, and osteocytes, specialized cells of the osteoblast lineage that act as mechanosensors. Bone is a highly dynamic tissue, in which degradation and deposition of new bone are continuously active, leading to a complete turnover of the skeleton occurring every 10 years. Bone remodeling is necessary for growth, to repair damage (for example after a fracture) and plays a role in the regulation of the calcium-phosphate metabolism. The remodeling process is executed by the concerted and sequential effort of OC and OB, spatially linked in what is called the bone remodeling unit (120). OC are multinucleated giant cells that differentiate from myeloid osteoclast precursors (OCP) under the influence of the cytokines: macrophage colony stimulating factor (MCSF) and receptor activator of NF-Kappa-B ligand (RANKL). Osteoclasts degrade bone by the secretion of proteolytic enzymes (cathepsin A, B, K), and acid (H+), which hydrolyze and solubilize the organic and inorganic components of bone. Proton and enzyme secretion is directed into the resorption lacunae which is isolated from the rest of the bone microenvironment by the osteoclasts themselfself, forming a spatial barrier (121, 122).

After the resorption phase performed by the osteoclasts, mechanisms, not yet fully understood, promote the recruitment of mesenchymal stem cells to the site of the resorption, with subsequent differentiation into osteoblasts. After acquiring a fully mature phenotype, osteoblasts secrete the organic component of bone (osteoid), which will be later mineralized by the incorporation of hydroxyapatite (123). Secreting osteoid, some osteoblasts become incorporated within the matrix therefore becoming osteocytes. Osteocytes do not produce bone

matrix anymore; their function is to monitor bone quality and coordinate remodeling through the expression of specific membrane ligands and through the secretion of specific factors.

The observation that bone resorbing OC stimulate bone formation by OB was named OC-OB coupling. When coupling is not acting properly, the balance between the activity of OB and OC is lost, resulting in bone diseases: osteoporosis if resorption is higher than formation, Paget like bone diseases if the formation is increased more than the resorption (fig.9, Charles et al, 120, 124, 125).

All the three cell lines, as well as macrophages and T cells, are involved in the coupling (126, 127). The study of the coupling is difficult since osteoclasts do not represent a unique population; for example, trabecular osteoclasts behave differently from cortical ones in both resorption and secretion of enzymes and cytokines (128, 129).

The identification of possible coupling factors has been, in the last few years, a very active field of research. Initially Transforming Grow Factor β1 (TGF β1) and Insulin-like Grow Factor 1 (IGF-1) were considered as possible mediators of the process. TGF β1 released during osteoclasts culture on bone induces the migration of mesenchymal stem cells (MSC) and MSC migration to bone surfaces is reduced in *Tgf β1* deficient mice (130); IGF-1 liberated from bone by osteoclastic resorption promoted osteogenic differentiation (131). It was seen that the secretive function of the osteoclasts is not coupled with their resorbing function (132), in fact, mice globally deficient in cathepsin K (*CtsK*) or with conditional deletion in osteoclast precursors can still show increased osteoblast numbers (133, 134).

Several potential osteoclasts-derived coupling factors sometimes referred to as clastokines, have been identified using in vitro approaches. Among these, the factors with *in*

*vivo* evidence of a role in this process are: collagen triple helix repeat containing 1 (CTHRC1), complement factor 3a (C3a) and sphingosine-1-phosphate (S1P). Global deficiency of *Cthrc1* decreased osteoblast number and bone formation in vivo; Moreover, *Cthrc1* was found to be strongly induced in osteoclasts active in resorption. Deletion of *Cthrc1* in osteoclasts resulted in reduced bone mass, without impairing their function, therefore suggesting a positive role of this factor in coupling (135). The complement cascade component C3a is produced by osteoclasts cultures in vitro, and was observed to stimulate osteoblast differentiation (136). Sphingosine kinase 1 (SPHK1) and its product, S1P, are induced during osteoclasts differentiation and, in vitro, S1P promotes osteoblast differentiation (137). Mice with myeloid-specific deficiency of cathepsin K showed how non-resorbing osteoclasts express higher levels of SPHK1, together with elevated osteoblast number (138).

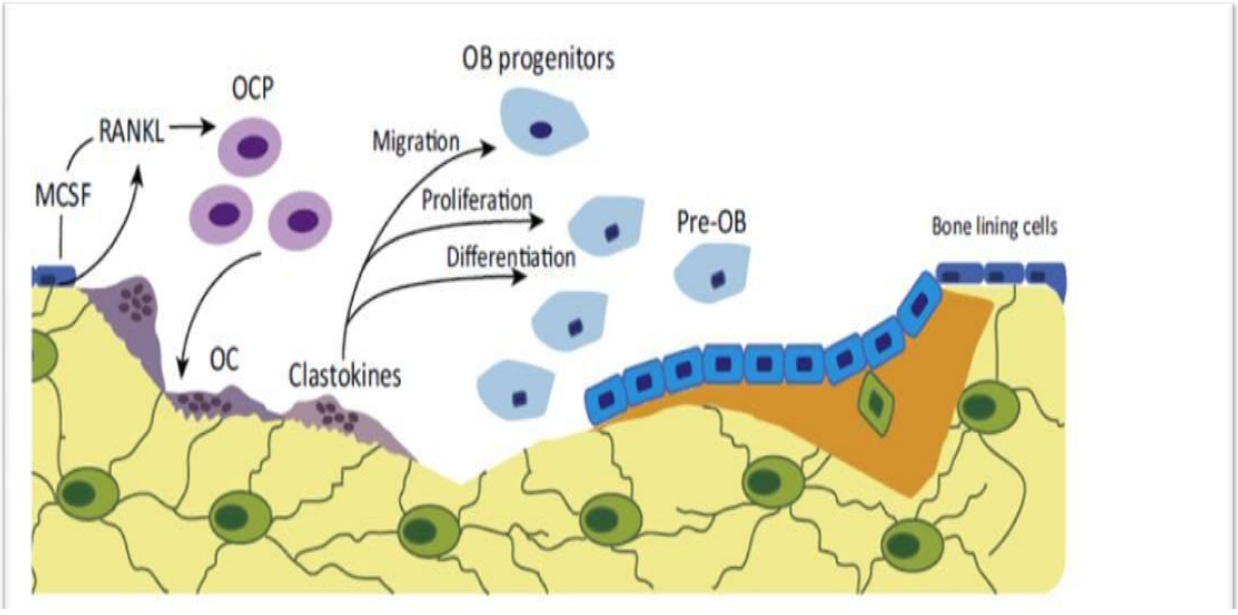


Fig.9. The coupling (Charles et al, 120).

## *1.7 mTORC1 signaling in osteoblasts*

The role of mTOR in osteoblast formation is the subject of several studies. Its effect has been addressed both directly (genetic inhibition) and indirectly (mTOR inhibitors, primarily rapamycin). Osteoblasts are derived from mesenchymal stem cells (MSC), therefore several investigators used MSC as a model to study mTORC1 dependent osteoblast maturation and function.

In an elegant publication, the IGF-1- mTORC1 pathway was recognized to play a role in maintaining proper bone mass, stimulating MSC to differentiate in the osteoblastic lineage; furthermore, rapamycin diminished the number of osteoblast, inhibiting their differentiation from MSC (139). Similarly, in MSC derived osteoblasts, rapamycin was able to reduce ALP (alkaline phosphatase, a marker of osteoblast maturation and activity) and calcium content if used alone, and negatively modulating the positive osteogenic effect of dexamethasone if used in combination (140). MSC differentiated in osteogenic medium and transplanted subcutaneously into rats treated daily with rapamycin, showed a decrease in ALP activity and mineralization of the matrix compared to non-treated mice (141).

Rapamycin is effective in inhibiting proliferation and differentiation of primary mouse bone marrow stromal cells (BMSCs) and the mouse osteoblast cell line MC3T3-E1. Rapamycin dramatically reduces osteoblast-specific osteocalcin (Ocn), bone sialoprotein (Bsp), osterix (Osx) mRNA expression, ALP activity, mineralization capacity and Runx2 expression (master regulator of osteoblast differentiation required for osteoblast-specific gene expression). However, the drug treatment had no effect on osteoblast differentiation parameters when they were completely differentiated (142). Moreover, mTORC1 signaling contributes to WNT7B-

induced bone formation by MSC, since deletion of Raptor (a component of mTORC1) in the osteoblast precursors alleviated the WNT7B-induced high-bone-mass phenotype. The same effect was seen with rapamycin treatment (143).

Similarly, the effect of BEZ235, a newly developed dual PI3K and mTORC1 and mTORC2 inhibitor currently in phase I–II clinical trials for advanced solid tumors, resulted in a dose-dependent decrease in MSC proliferation, showing how mTOR signaling is necessary for proliferation of pre-osteoblast. However, BEZ235 strongly promoted osteogenic differentiation if MSC were induced to mature toward the osteoblast lineage, as evidenced by an increase in mineralized matrix production, an upregulation of genes involved in osteogenesis like: (*BMP2*, *-4*, and *-6*), transforming growth factor β1 (TGF-β1) superfamily members (*TGFB1*, *TGFB2*, and *INHBE*), and increased activation of SMAD signaling molecules. Suppression of mTORC1 with rapamycin or shRNA mTORC1 induced increase in mineral formation, similarly to BEZ235 (144).

This dual effect of mTORC1 along the transition from mesenchymal stem cells to mature osteoblasts has been seen in the work of two other groups. In the first one, activation of mTORC1 in MC3T3-E1 cells, a murine preosteoblast cell line, increases preosteoblasts proliferation but does not favorite the maturation to adult osteoblasts, consistently, in mice, deletion of tuberous sclerosis 1 (Tsc1) in preosteoblasts produces immature woven bone, due to excess proliferation but impaired differentiation and maturation of the preosteoblasts. Rapamycin restored these in vitro and in vivo phenotypic changes. Mechanistically, mTORC1 prevented osteoblast maturation through activation of the STAT3/p63/Jagged/Notch pathway and downregulation of Runx2. Consequently, inhibition of the Notch pathway restored the ability of preosteoblasts with hyperactive mTORC1 to fully differentiate to osteoblasts (145).

In the second, deletion of *Raptor* in primary calvarial osteoblasts resulted in a decrease in matrix synthesis and mineralization under osteogenic culture condition. However, in this report, the deletion of *Raptor*, and therefore loss of mTORC1 activity, reduced the expression of late-stage markers of osteoblast differentiation (Bglap, Ibsp, and Col1a), while slightly increasing early osteoblast lineage markers (Runx2, Sp7, and Alpl). Consistent with these *in vitro* findings, genetic ablation of *Raptor* in osterix-expressing cells led to osteopenia in mice (146). In another paper, rapamycin resulted in a 50% decrease in ALP activity (a marker of mature osteoblast) induced by Osteogenic protein 1 (OP-1) or OP-1 plus IGF-1, suggesting a positive role of mTORC-1 as downstream of OP-1 and IGF-1 in the maturation of pre-osteoblasts (147). Similarly, in fetal rat calvarial cells, bone morphogenetic proteins (BMPs) were shown to promote osteoblast differentiation and bone formation through mTORC1/pS6K signaling. Rapamycin treatment blocked the BMP-7 driven expression of osteogenic markers (AP, Osterix, Osteocalcin). Therefore, BMP-7 acts upstream of m-TORC1/ pS6K. However, BMP2 was seen to be negatively regulated by mTORC1 in another study using human embryonic stem cells as a model. In this work, rapamycin acted as a potent stimulator of osteoblastic differentiation, inducing the up-regulation of the early osteogenic markers BMP2 and Runx2 as well as Smad 1/5/8 (148).

While the body of evidence points towards a positive and benefical role of mTORC1 in the maturation of the osteoblasts, knockout of mTORC1 or rapamycin treatment rescued osteopenia in FBN1-deficient (*Fbn1*+/-) mouse model of systemic sclerosis. *Fbn1*+/- bone marrow mesenchymal stem cells (BMMSC) exhibited IL4-mediated activation of mTORC1 signaling pathway, which leads to down-regulation of RUNX2, an essential transcription factor for osteoblast maturation. At baseline, *Fbn1*+/- BMMSCs have decreased osteogenic and

increased adipogenic differentiation. Inhibition of mTORC1 was shown to improve osteogenic differentiation of BMMSCs (149).

Similarly, the effects of rapamycin on a rat osteoblast-like osteosarcoma cell line (ROS 17/2.8) resulted in a direct inhibition of the proliferation; however, rapamycin caused a significant increase in alkaline phosphatase (ALP) activity and in the expression of osteopontin and osteocalcin mRNAs, indicating that rapamycin induces osteoblastic differentiation (150) in this situation.

In conclusion, the mTORC1 activity is required in the transition from mesenchymal stem cells to osteoblast lineage commitment; however, the effect of mTORC1 in mature osteoblasts seems to be detrimental for the acquisition of a full mature phenotype (145). The different role of mTORC1 in *Fbn* +/- mice or in rat osteosarcoma cell lines is, at the moment unclear; it is possible that additional genetic mutation might be responsible (149, 150).

Notably, two trials in rats were performed in the 1990's to evaluate the effect of rapamycin as a bone sparing immunosuppressant; in the first one, animals were treated with 2.5 mg/kg/day for 14 days. Rapamycin transiently depressed serum osteocalcin levels and elevated blood ionized calcium levels on day 7, also lowered 1, 25(OH) 2D levels on day 14. No morphologic differences (BV/TV) were observed in tibial specimen, therefore the conclusion was that short-term treatment with Rapamycin does not result in excess resorption or loss of bone volume; Nonetheless, they assumed that the alteration in calcium and Vitamin D might have an effect in long term therapy (151). The same group, two years later, published another study comparing rapamycin with cyclosporine and tacrolimus, two widely used immunosuppressants with the side effect of osteopenia. Using the same dose of rapamycin for

28 instead of 14 days, the authors confirmed previous observation of no changes in bone morphology (BV/TV) by rapamycin, whereas cyclosporine and tacrolimus treated animals demonstrated high turnover osteoporosis with serum elevation of 1,25(OH)2 D and osteocalcin. Nevertheless, rapamycin induced a decrease in bone longitudinal growth rate, raising the question if rapamycin might be a problem if used long-term in growing individuals (152).

Lastly, mTORC1 inhibitors effect in bone health have been explored in patients as well, with the phase 3 BOLERO-2 trial demonstrating that everolimus might have a positive effect on bone health in postmenopausal women with HR+ breast cancer progressing despite nonsteroidal aromatase inhibitor (NSAI) therapy. Bone marker data suggest that everolimus suppresses bone turnover and reverses the increases in bone resorption associated with exemestane treatment. Adding everolimus to exemestane therapy also reduced the incidence of bone metastasis as well as the disease progression in bone. Everolimus protected bone health, determining a significant decrease in bone marker levels when added to exemestane at week 6 (26.4% for BSAP, 55.9% for P1NP, and 35.9% for CTX) and at week 12 (20.3% for BSAP, 66.2% for P1NP, and 40.5%for CTX) relative to baseline (exametasane + placebo). Overall, the results of the BOLERO-2 exploratory analyses suggest that everolimus may protect bone health, potentially compensating the negative bone effects associated with exemestane therapy (153).

## *1.8 mTorc2 signaling in osteoblasts*

Little is known about the effect of mTORC2 in bone pathophysiology, with only a few reports mainly focusing on osteoblasts; nothing is known about mTORC2 role in osteoclasts. SiRNA mediated knock down of *Rictor* (a component of mTORC2) in mesenchymal stem cells caused significantly reduced levels of osterix mRNA and osteocalcin mRNA as well as alkaline phosphatase after 4 days of culture in osteogenic medium, indicating that early osteoblast differentiation was reduced in cells where mTORC2 activity was inhibited. Moreover, Rictor deficiency not only prevents the osteoblast lineage maturation but predispose the cells to acquire an adipogenic phenotype (154).

*Prx1Cre+/ Rictor f/f* mice, in which mTORC2 is not functional in early limb mesenchymal cells show low bone formation in both cortical and trabecular compartments. This is the effect of both: decrease osteoblast activity and decrease in osteoclast number since mutated osteoblast produce less RANK-L, a key molecule in osteoclast proliferation (155). It is surprising that osteoblast number was not reduced in these mice given that *Rictor* deficient BMSCs were impaired in osteoblast differentiation in vitro, as seen in the previous paper; most likely *in vivo* a more complex cascade of signals can overcome the absence of mTORC2 activity (154).

Interestingly, WNT3A signals through LRP5 and RAC1 activating mTORC2 and consequently AKT, resulting in upregulation of glycolytic enzymes. Suppressing WNT3A, therefore mTORC2 impairs osteoblast differentiation *in vitro*. Deletion of *Lrp5* in the mouse, which decreases postnatal bone mass, reduces mTORC2 activity and glycolytic enzymes in bone cells. Conversely, mice expressing a mutant hyperactive LRP5 present high bone mass

and increased glycolysis in bone. Thus, WNT-LRP5-mTORC2 signaling promotes bone formation in part through direct reprogramming of glucose metabolism (156).

## *1.9 mTORC1 signaling in Osteoclasts.*

Little is known about the effects of mTORC1 and its inhibitor rapamycin in osteoclast function and osteoclastogenesis, only few studies explored this relationship. Reviewing all the information present in literature, there is clear a negative role of rapamycin in osteoclast function, as well as in osteoclast formation from precursors. Therefore, mTORC1 seems to play a vital role in osteoclasts.

The first study showing the positive effect of mTORC1 in osteoclasts was published in 2004 by Kneissel et al, they reported that: in pit assay osteoclast activity, as well as osteoclast formation by TRAP+ staining, was reduced significantly if cells were treated with everolimus, a derivative of rapamycin. Moreover, mRNA and protein expression of cathepsin K (the main collagen-degrading protease) in mature osteoclasts *in vitro* was decreased by everolimus. Everolimus also prevented the ovariectomy-induced loss of cancellous bone in mice, an effect predominantly associated with decreased osteoclast-mediated bone resorption, showing again its negative effect on osteoclast function (157).

This result was confirmed by other reports showing the negative effect of rapamycin in osteoclastogenesis; curiously, rapamycin was found to have no effect in bone resorbing activity of mature osteoclasts, whereas Torin1, an inhibitor of both mTORC1 and mTORC2, showed a great effect in the inhibition of mature osteoclasts as well as in the prevention of the maturation of the preosteclasts (158).

The positive effect of mTORC1 in osteoclasts was further confirmed in vivo: 24-month-old male rats were injected with Rapamycin daily for 12 weeks. Micro-CT evaluation

demonstrated that rapamycin ameliorates age-related bone loss by decreasing osteoclasts number. Furthermore, rapamycin induced autophagy in osteocytes, therefore decreasing their apoptosis rate (159).

In a mouse model of rheumatoid arthritis, inhibition of mTORC1 by rapamycin or everolimus reduced synovial osteoclast formation, thus, protecting against local bone erosions and cartilage loss. The final effect was an improvement in the clinical signs of arthritis in the mouse and histologic evaluation showed a decrease in synovitis. In vitro, mTORC1 inhibition down-regulated the expression of bone resorption enzymes and led to osteoclast apoptosis. Moreover, in the same paper it was shown how mTORC1 signaling was hyper active in synovial membrane tissue samples of patients with Rheumatoid Arthritis, particularly in synovial osteoclasts (160).

Osteoclasts derived from Giant Cell Tumors of the bone (GCT), a benign tumor in which the presence of hyperactive osteoclasts causes osteolytic lesions, were inhibited by rapamycin *in vitro* (161). Importantly, reduced serum levels of bone resorption markers (CTX-1) were detected in patients treated with sirolimus (rapamycin) after kidney transplantation compared to a control regimen; the authors expanded these observations with in vitro studies showing profoundly reduced osteoclast differentiation and subsequently diminished hydroxyapatite resorption in the presence of sirolimus compared to tacrolimus. Moreover, sirolimus significantly reduced osteoclast precursors proliferation compared to tacrolimus and led to augmented apoptosis in osteoclast precursors (162).

The negative effect of rapamycin in osteoclasts is not only direct, but can act through different cells communicating with osteoclasts: ST2 cells (bone marrow derived stromal cells)

treated with rapamycin have been observed to secrete more osteoprotegerin (OPG), a factor that regulates bone mass by inhibiting osteoclastogenesis. Treatment with bone morphogenetic protein-4 (BMP4) induced OPG protein synthesis in ST2 cells, secondarily to down-regulation of mTORC1. Thus, suitable suppression of mTORC1 phosphorylation is a necessary requirement for OPG production and inhibition of osteoclastogenesis by bone marrow stromal cells (163).

To date, rapamycin has been shown to positively regulate osteoclast function in only one paper: Niziolek et al reported that in mice treated with Rapamycin there was a significant increase in serum Trap5b levels, a marker of bone resorption secreted by osteoclasts. (164).

## *1.10 Mouse models recapitulating bone lesions in TSC.*

To date only three mouse models were generated with a deletion of either *Tsc1* or *Tsc*2 in a specific bone cell population using the *Cre-lox* system. Interestingly in all models, the cells lacking TSC1 or TSC2 were osteoblasts or their precursors.

In the first study, Riddle et al. investigated insulin receptor activation in bone formation and energy metabolism. Since TSC2 is a downstream target of insulin receptor signaling, through the PI3K/AKT pathway, they generated mice in which *Tsc2* was selectively disrupted in osteoblasts. To do this, they crossed a *Tsc2 fl/fl* mouse with an *Osteocalcin-Cre* mouse. Since osteocalcin is a protein only expressed by mature osteoblasts, the loss of *Tsc2* is confined to these cells. Specifically, they provided evidence that *Tsc2* modulates insulin-generated signals to control osteoblast development together with the regulation of the production of the hormone osteocalcin. In fact, they observed an increase in the number of osteoblasts in the mutated mice, due to the increase proliferation secondary to hyperactivation of mTORC1. The bone formation rate was therefore increased; however, the performance of individual osteoblasts in the mutant mice was impaired, leading to poor quality of the newly formed bone. An *in vitro* adeno-Cre based approach was used to confirm the results of the *in vivo* model. *In vitro* differentiation assays revealed impaired expression of genetic markers of osteoblast differentiation and reduced mineralization, together with the reduction in osteoblast apoptosis. These findings together may explain the accumulation of immature osteoblastic cells in the mutant mice. This study suggests that the mechanism responsible for the failure of *Tsc2*-deficient osteoblasts to fully differentiate is due, at least in part, to the overactivation of mTORC1 and impaired insulin signaling that occurs indirectly via the engagement of a negative feedback loop. Rapamycin

treatment rescued the differentiation defect of *Tsc2*-deficient osteoblasts. Moreover, deletion of one allele of mTOR in the mutated mice to reduced bone density to a level comparable to control. Taken together all these data imply that *Tsc2* represents a critical regulator of anabolic signaling necessary for osteoblasts to attain a fully mature phenotype (165).

Huang et al created a mouse model of *Osx-GFP-CreTG/+; Tsc1fl/fl* in order to specifically knock down *Tsc1* in osteoprogenitors committed to the osteoblast lineage. The mice showed square skull and dwarfism at 4 weeks of age, as well as lower body weight. Increased bone mass was evidenent in vertebrae, long bones and skull. BV/ TV (bone volume/ tissue volume) was consistently increased in cancellous bone as well as in the femoral mid shaft; however, the bone resulted was more porous, with less mineral content as evaluated by Masson Trichrome staining. By femur histology, an increased number of osteoblasts were observed, 5-bromo-2'-deoxyuridine BRDU staining showed increased proliferation of the mutated osteoblasts *in vitro*. Decreased osterix and osteocalcin staining was also observed, suggesting that the cells were unable to attain a mature phenotype. Using a dexamethasone induced *Cre* model, the authors were also able to study *Tsc1* loss in mature osteoblasts. They found that mature *Tsc1* deficient osteoblasts were unable to properly mineralize, and markers of mature bone were decreased. Interestingly, even in this mouse model rapamycin was able to fully reverse the phenotype.

Fang et al generated a viable model of the skull bone lesions seen in TSC by deleting *Tsc1* in neural crest derived cells. *Tsc1 fl/fl; P0-Cre* mice (CKO) showed dramatically increased thickness of neural crest derived frontal and sphenoid bones, but not of mesoderm derived parietal bones. Histomorphometric analysis of 1-month-old mutant mice demonstrated enhanced bone formation rate on both extracranial and intracranial surfaces of the frontal bone.

Osteoblast differentiation marker gene expression was normal in the mutant mouse, only Osteocalcin was found slightly increased. Lineage tracing experiments found increased P0-Cre targeted cells in neural crest derived frontal bones in one-week-old skulls of mutant mice compared to heterozygous mice, as well as increased osteoblast density in the periosteum. All these data suggested that *Tsc1* deletion using *P0-Cre* leads to increased commitment of neural crest derived cells to the osteoblast lineage. Interestingly, rapamycin treatment in new born mice completely rescued the calvaria thickness, but the same result was not found if the drug was delivered after 1-month of age, suggesting that the causative change of sclerotic bone phenotype has already occurred at 1-month of age. Therefore, the enlarged osteogenic stem cell pool is responsible for the increased bone mass acquisition (166).

The three studies discussed above, in which the hyperactivation of mTORC1 was obtained at different stages of the osteoblast maturation, are consistent in the finding that mTORC1 is of key importance for bone formation by osteoblasts. Moreover, inhibition of mTORC1 by pharmacological or genetic approaches is shown to be effective in reversing the phenotype. The only importance difference is in the bone quality: in the osteocalcin *Cre* as well as in the *Osx Cre* model, the quality of bone seems poor, with a reduced mineralization; in the P0 *Cre* mouse instead the quality of the calvaria bone appears to be normal.

## *1.11 Bone Lesions in Tuberous Sclerosis Complex*

Bone is frequently involved in Tuberous Sclerosis Complex; the peculiar lesions observed in TSC were documented since the early 1920's (167-175). Dickerson, in 1955, gave an accurate autopsy description of the phalanges of a TSC patient: "The specimens from the phalanges can be described together. They show areas of lack of bone in various stages of fibrous replacement. Dense collagenous connective tissue mingled with adipose tissue is found in these defects. Neighboring cortical and cancellous bone is thickened with added layers of new bone, giving a pattern which is much like that found in Paget's disease. These defects appear to be of long standing and to be undergoing partial repair rather than enlargement." (167).

It was later recognized that many of the areas of apparent intracranial calcification in Tuberous Sclerosis represent sclerotic plaques in the cranial vault, as reported by Dalsgaard Nielsen and Gottlieb and Lavine (175, 176).

Reviews about skeletal involvement in TSC were published in the 1950's, the first by Holt and Dickerson, the second by Berland (177, 178). Holt and Dickerson reported that in a population of TSC patients, 50% presented with skull abnormalities and 66% hands or feet abnormalities consisting of cyst-like foci in the phalanges and a rather distinctive type of periosteal new bone formation along the shafts of the metatarsals and the metacarpals bones. He also observed that the "cystic" foci are not present at birth but may appear relatively early in childhood and gradually increase in size and number over a period of many years (177).

Berland observed that the calcifications of the skull found in Tuberous Sclerosis are multiple and bilateral, notably, he was considering to diagnose TSC just observing the radiographical bone findings: "the diagnosis of tuberous sclerosis should always be considered when the following are present: cyst-like lesions in the phalanges; irregular thickening of the cortex of the metatarsal or metacarpal bones; irregular thickening of the cortex of any of the bones in the hands or feet associated with fragmentation or cyst-like changes. When these findings present themselves with calcifications within the skull, the diagnosis can be clearly established. The percentage of cases in which both these changes are present can be estimated to be between 60 and 65%" (178).

Curiously the early reports were mainly focusing on extremities (the characteristic cystic lesion of the phalanges, and the thickening of the metacarpal and metatarsal bones) and skull. Accordingly, with all these early reports, Roach et al inserted bone cysts in the list of minor diagnostic criteria for the diagnosis of TSC (179). However, they are no longer diagnostic in the current revised clinical diagnostic criteria for tuberous sclerosis complex by Northnup since they are considered nonspecific (180).

Sclerotic bone lesions (SBLs), areas of increased bone density seen on plain radiographs, are described in several reviews regarding the radiological aspects of tuberous sclerosis; they are considered as abnormalities without definite clinical significance (181-184). However, after renal angiomyolipomas (AMLs) and cortical tubers, sclerotic bone lesions are the third most common finding on imaging in TSC patients being detected by computed tomography (CT) in almost 100% (185).

Osteosclerotic lesions can affect the entire axial skeleton; a predilection to the vertebral bodies and posterior elements of the thoracic spine has been noted (186). The sclerotic foci are usually small, multiple and assume variable shapes. Radiographic appearance is commonly associated with patchy areas of increased bone density; skull radiographs may detect calvarial sclerosis due to hyperostosis of the inner table and prominent trabeculae in the diploic spaces. Long bone radiographs can reveal irregular thickening in the bone cortex of the extremities (metacarpals, metatarsals and phalanges). Neural arches and pelvis brim are other common sites of involvement. The hips have been reported to present bone lesions in TSC for the first time in 1957, in a patient with concomitant spine lesions (187). Sacrum and proximal femur can also be involved, together with the classic vertebral and iliac involvement (188).

The anomalous growth of certain bones has also been reported: a patient has been described with a swollen left ring finger, which has become more evident as she grew older, the swelling has been proportionally increasing with her size without limiting manual function, interestingly radiographic imaging showed an increase in size of the metacarpal bone as well as the phalanges (189).

As mentioned, the skull is a frequent site of involvement: the frontal bone can overgrow leading to the characteristic facies of a TSC patient (24); it can be the involved singularly or together with an expansion of the mandible, or a general hyperostosis of the calvaria (190, 191).

Attempting to evaluate the prognosis of such lesions, Smith et al studied a cohort of patients with TSC and musculoskeletal involvement; they concluded that none of the fractures seen in TSC patients appeared to be through regions of sclerotic or lytic lesions in the bone (192).

The bone lesions in TSC has been always considered benign, therefore only incidentally observed at radiological examination, nonetheless, even if rarely, they can cause a clinical syndrome. In one report, Stosic-Opincal et al describe a case of a TSC patient with lower back pain, with multiple focal lesions (up to 2cm in diameter) of the vertebral bodies, pedicles, and laminas, as well as lesions in the iliac bones and femur observed on imaging; all the lesions showed the same MRI features: low signal intensity on both T1-weighted and T2-weighted images, and no contrast enhancement after intravenous administration of gadolinium (193).

Bone lesions in TSC have been shown to be worsened by concomitant factors, like massive renal involvement (tubular acidosis) and anticonvulsant therapy. The patients back pain in the above case was resolved by Vitamin D therapy. Curiously, in this patient radiography revealed discrete, uneven thickening of the cortices in the proximal two-thirds of the tibia and fibula, two sites rarely involved (194).

Rarely, the bone lesions can be massive and therefore leading to pancytopenia. Tashiro et al observed a patient with TSC and severe anemia, extraordinary thickening of the cortex of long bones of the extremities as well as patchy osteosclerotic findings in vertebrae, suggesting that hematopoietic space was significantly reduced; bone marrow scintigraphy with 111InCl3 demonstrated that peripheral marrows in long bones and skull did not show any uptake, which suggests significantly decreased hematopoiesis in peripheral bone marrow (195).

The presence of bone lesions in a patient with TSC and a concomitant malignant cancer syndrome has been reported in literature. In these cases, was important to recognize the benign feature of the bone lesions to exclude a metastatic bone involvement. In this report by Song et al, the TSC patient had coexisting pulmonary adenocarcinoma and multiple sclerotic lesions in

the vertebrae and ribs, recognized as skeletal manifestation of TSC rather than metastases because they remained stable during 5-year follow-up. Likewise, none of these lesions showed abnormal Tc- 99m methylene diphosphonate (MDP) uptake (196). The finding coincided with the report of Pui et al. in which the sclerotic bone lesions of a TSC patient with concomitant bronchogenic carcinoma had normal radionuclide uptake on bone scintigraphy (197).

Increased radionuclide uptake was instead shown in other two reports of patient with Tuberous Sclerosis (198, 199). The difference in patients age: 64-year-old, and 72-year-old in the studies in which the scintigraphy was negative, 25-year-old and 15-year-old in the ones in which the scintigraphy was positive, might be the cause of this discrepancy. The bone lesions in elderly patients with TSC might be metabolically inactive compared to those in younger patients.

Curiously, ossification was reported inside a cortical tuber resected from a patient with *TSC1* mutation. Surgery was necessary because anticonvulsant therapy was unable to control seizures. The area of mineralization corresponded to a fragment of mature cortical-like bone with lamellar architecture, Haversian like canals and small osteocytes with delicate canaliculi. The bone surface was sharply demarcated from adjacent gliotic white matter by a rim of flattened osteoblasts (200). The presence of lamellar bone in the current case raises interesting questions regarding the cell of origin of the cortical tubers, as well as regarding the mechanisms of increased ossification in patients with *TSC1-2* mutations.

Recently, two clinical studies with a large cohort of patients were published aiming to elucidate the real incidence of sclerotic bone lesions in patients with Tuberous Sclerosis. In the first study, Avila et al focused on sclerotic bone lesions as a possible marker to differentiate

patients with TSC and Lymphangioleiomyomatosis (LAM), from patients with sporadic Lymphangioleiomyomatosis. Four or more sclerotic bone lesions were detected in 88% of the patients with TSC/LAM, 3% in the group with sporadic LAM and 100% in patients with only TSC. They also never observed more than 4 lesions in patients with LAM whereas patients with TSC and TSC/LAM could reach frequently more than 10 lesions, in exceptional cases 100. Therefore, this study concludes that in the context of distinguishing patients with sporadic LAM from patients with TSC/LAM, the absence of four or more lesions have a sensitivity of 1.0, specificity of 0.97 and a positive predictive value of 0.87. Regarding the site, SBLs were found in the spine and commonly in the pelvis, each patient had at least one lesion in the thoracic or lumbar spine or in the sacrum; within the spine SBLs were seen in all anatomic components: vertebral bodies, pedicles and posterior elements. SBLs were also found in ribs, sternum, proximal femora, and humerus (185).

A second important clinical study aimed to evaluate the presence of sclerotic bone lesions in patients with TSC undergoing abdominal CT scan or MRI for a concomitant renal involvement. 51 children out of 70 had sclerotic bone lesions, however in no cases the patients report symptoms. 51% of the children showed 1 or 2 lesions, 23 children showed 3 to 9 lesions and 2 girls (10 and 14 years old) had 10 or more lesions. In a total of 173 lesions, 160 were in the vertebrae and 13 in the sacrum, iliac bone and ribs. Distribution in the vertebrae was: 88 in pedicles, 3 in laminas, 18 in spinous processes, 13 in transverse processes and 10 in vertebral bodies. 7 lesions were in the sacrum, 3 in the iliac bones and 3 in the ribs. The follow up studies revealed an active nature of the lesions: 50% of the patients showed new lesion or enlargement of the preexisting one. Interestingly, they observed that renal involvement was more frequent in children with sclerotic bone lesions compared to those without; moreover they excluded any

significant differences in patients with *TSC1* mutation compared to patients with *TSC2* mutations (201).

Although less common than sclerotic bone lesions, fibrous dysplasia has been reported as a possible bone malformation associated with Tuberous Sclerosis. Fibrous dysplasia is a benign skeletal disorder, typically seen in adolescents and young adults, in which normal bone marrow is replaced by fibro-osseous tissue. There have been two cases in the literature of concurrent TSC and cranial fibrous dysplasia. In the report by Gasparetto et al, the authors presented the case of an 11-year-old female patient with a right nasal mass. CT examination revealed fibrous dysplasia involving the frontal, ethmoid, sphenoid, and vomer bones (202). The second report described a patient with superior displacement of the orbit and proptosis due to sphenoid sclerosis characteristic of fibrous dysplasia. A pelvic osteosclerotic lesion suggested polyostotic involvement (203).

Fibrous dysplasia was also observed outside the skull in TSC, in a 2-year-old patient who developed a right chest wall deformity that, after imaging, was discovered to be a focus of fibrous dysplasia. At 8 years, chest radiography and MR showed progression of the bone dysplasia to include the sixth cervical and thoracic vertebrae (C6 and T6 vertebrae) and fifth and seventh right ribs. The patient started rapamycin at the age of 8 and a consequent magnetic resonance imaging (MRI) showed no significant changes in the rib and vertebral lesions from a previous observation, therefore rapamycin treatment was efficacious in blocking the progression (204).

In conclusion, bone lesions in TSC should not always be considered benign, as they may be more clinically significant than currently assumed. Further studies should be conducted

to classify the different kinds of bone manifestations in TSC, their prevalence, and whether rapamycin is effective in blocking their progression.

## *2. Rationale of the project*

The increased activity of the mTOR pathway, responsible for the manifestations of TSC, has been widely explored in osteoblast maturation and function but less is known about its effect in osteoclast physiology. Despite the fact that the vast majority (88-100%) of patients with TSC present with dense bone lesions, only few mouse models with a deletion of *Tsc1-2* in bone cells have been generated. Importantly, these models presented a *Tsc1-2* deficiency at various stage of maturation of osteoblasts yet, nothing is known about *Tsc1-2* deficiency in osteoclasts.

For all these reasons we generated mouse models with deletion of *Raptor* and *Tsc2* specifically in osteoclasts as well as in their precursors.

Our aim is to investigate the role of osteoclasts in the development of the bone lesions in TSC and, possibly, elucidate the role of TSC complex and mTORC1 in these cells, whose function in bone physiology, beyond the role as simple “bone eaters” is just beginning to be understood.

# 3. Results:

In order to evaluate the role of mTORC1 in osteoclast maturation and function, we first examined mice with post-natal deletion of *Raptor* (a key component of mTORC1). Therefore, we generated a mouse in which the *Cre* recombinase is under the control of the *Mx1* promoter. This promoter is silent normally, but can be induced to high levels of transcription by administration of interferon alpha, interferon beta, or synthetic double-stranded RNA (such as polyinosinicpolycytidylic acid, polyI:C). *Mx1* encodes a guanosine triphosphate (GTP)-metabolizing protein that participates in the cellular antiviral response, and is expressed in myeloid precursors. When combined with a mutant carrying a gene that has been flanked by *lox* recognition sites (in this case *Raptor*), the expression of *Cre* recombinase causes the flanked gene to be removed.

*Mx1-Cre; Raptorfl/fl* mice were treated with polyI:C, which induces *Cre* expression in all interferon responsive cells, including the myeloid precursors of osteoclasts. Bone marrow cells were harvested and cultured in MCSF for 3 days, then re-plated in MCSF and RANKL for 5 days in order to have mature osteoclasts. Osteoclast formation was detected by TRAP (tartrate resistant acid phosphatase, an osteoclast marker) staining, with TRAP+ cells with 3 or more nuclei identified as osteoclasts. Loss of *Raptor* inhibited osteoclast formation *in vitro* (fig. 1).

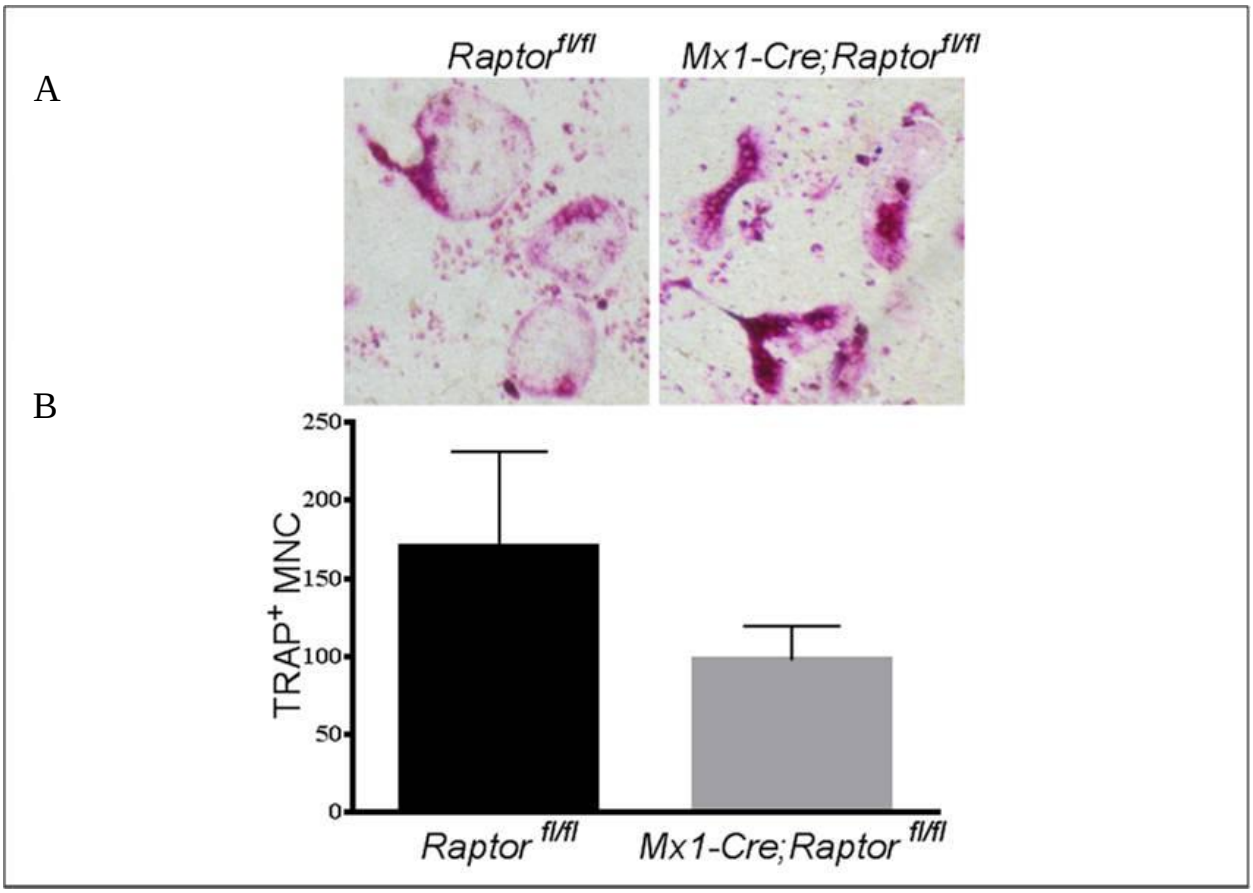


**Fig.1. Raptor loss is detrimental for osteoclast formation *in vitro* A.** total bone marrow cells from *Mx1-Cre; Raptorfl/fl* and *Raptorfl/fl* mice were differentiated in the presence of RANKL. Multi-nucleated osteoclast formation was assessed by TRAP staining, representative images **B.** osteoclast differentiation from *Tsc2ΔOC* splenic monocytes as assessed by TRAP+ multinucleated cells (MNC), columns represent the number of TRAP+ multinucleated osteoclasts in the considered field.

Next, we hypothesized that increased mTORC1 activity would promote osteoclast differentiation; therefore, we generated a mouse model of hyperactive mTORC1 in myeloid precursors, crossing the *Mx1-Cre* mouse with a *TSC2fl/fl* mouse. *Mx1-Cre; Tsc2fl/fl* and *Tsc2fl/fl* littermates were treated with polyI:C, and flow cytometric analysis of bone marrow

monocytes was performed 4 weeks later. Consistent with *Tsc2* deletion increasing mTORC1 activity, phosphorylated S6K (a downstream of mTORC1) was increased in *Mx1-Cre; Tsc2fl/fl* monocytes compared to *Tsc2fl/fl* controls (Fig. 2A).

Unexpectedly, bone marrow from polyI: C treated *Mx1-Cre; Tsc2fl/fl* mice completely failed to form osteoclasts *in vitro* after culturing them in the same maturation protocol we used before (Fig. 2B) and it is likely that osteoclast formation *in vivo* is also decreased in these animals, since trabecular bone mass was significantly increased in the femurs of *Mx1-Cre; Tsc2fl/fl* mice compared with polyI:C treated *Tsc2fl/fl* controls within 4 weeks after *Tsc2* deletion (Fig. 2C). Unfortunately, myelopoiesis is altered in *Mx1-Cre; Tsc2fl/fl* mice, leading to an altered pool of osteoclast precursors (OCP), which indirectly decreases osteoclast formation. Therefore, to determine the effect of increased mTORC1 activity specifically in OCP, we used fluorescence activated cell sorting (FACS) to purify bone marrow OCP, which are defined as *CD11b lo/neg, Ly6C hi*. Culturing OCP with MCSF and RANKL following the same established protocol, we found that *Tsc2*-deficiency does not prevent osteoclast differentiation from OCP as assessed by TRAP staining (Fig. 2D). Thus, investigating the cellular consequences of *Tsc2*-deficiency in osteoclasts in *Mx1-Cre; Tsc2fl/fl* is confounded by altered myelopoiesis, and a model of *Tsc2* deletion more specific to osteoclasts was required.

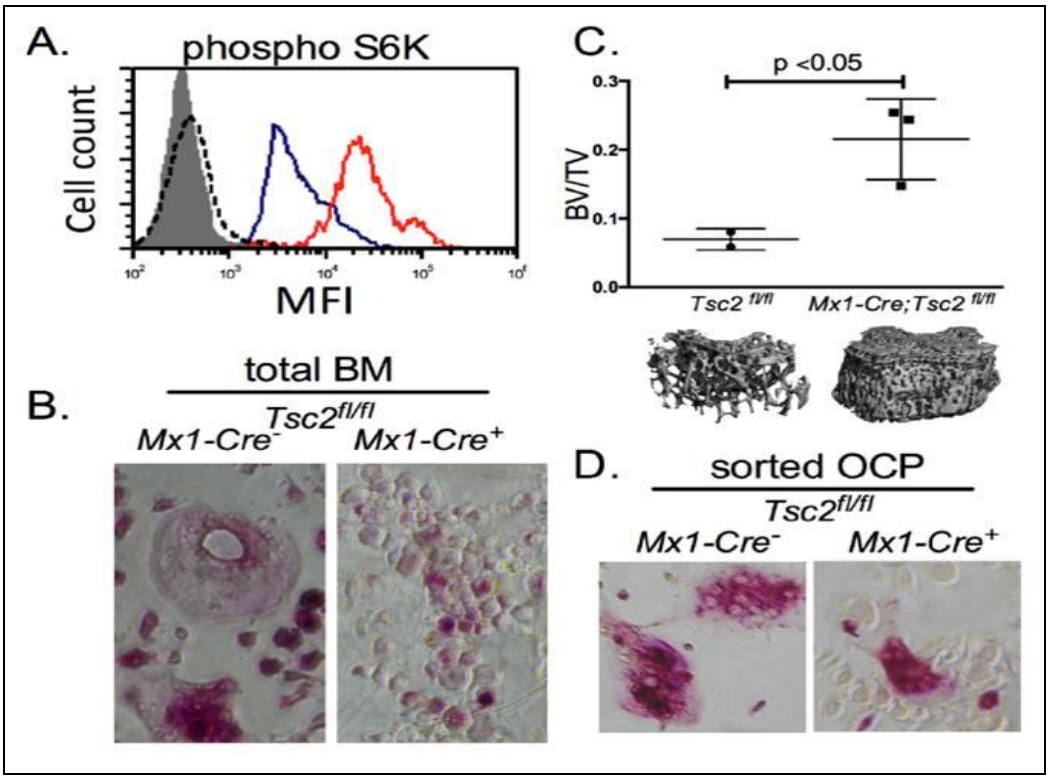


**Fig. 2.** ***Tsc2*** **deficiency in myeloid precursors increases bone mass. A.** Intracellular staining for phospho-S6K in monocytes shows increased pS6K phosphorylation in *Mx1-Cre; Tsc2fl/fl* mice (red line) compared to *Cre*-littermates (blue line) treated with polyI:C; isotype control staining on mutant and WT cells is indicated by gray fill and dotted line, respectively. **B.** 4 weeks after polyI:C treatment, total bone marrow cells from *Mx1-Cre; Tsc2fl/fl* and *Tsc2fl/fl* mice were differentiated in the presence of RANKL. Multi-nucleated osteoclast formation was assessed by TRAP staining. **C.** 4 weeks after *Cre* induction with polyI:C, bone mass (BV/TV, bone volume/tissue volume) was measured by micro-CT. Each symbol represents one animal; significance determined by Student's t-test. Representative 3D micro-CT images of trabecular bone are shown. below the graph. **D.** FACS purified osteoclast precursors (OCP) from *Mx1-Cre; Tsc2fl/fl* are capable of forming multinucleated osteoclasts in the presence of RANKL.

To generate mice with conditional deletion of *Tsc2* in mature osteoclasts, we made use of the *Cathepsin K-Cre* (*Ctsk-Cre*) mouse strain. Cathepsin K is a lysosomal enzyme secreted by mature, resorbing osteoclasts; thus, *Ctsk-Cre* drives deletion in mature osteoclasts. We crossed *Ctsk-Cre* mice with *Tsc2fl/fl* mice to generate *CtskCre; Tsc2fl/fl* mice, hereafter denoted as *Tsc2ΔOC*.

Splenocytes were harvested and cultured in the presence of M-CSF for 6 days to expand myeloid precursors. Splenic myeloid precursors were then replated in the presence of MCSF and RANK-L in order to achieve maturation into osteoclasts. We confirmed, by western blot analysis, that spleen derived osteoclasts generated from *Tsc2ΔOC* mice showed the expected increase in mTORC1 activity assessed by the increase in S6K phosphorylation (2 fold) compare to a littermate control. Cathepsin K, a marker of osteoclast maturation was also evaluated and demonstrates similar degrees of commitment of the spleen precursors to the osteoclast lineage (Fig. 3A, B).

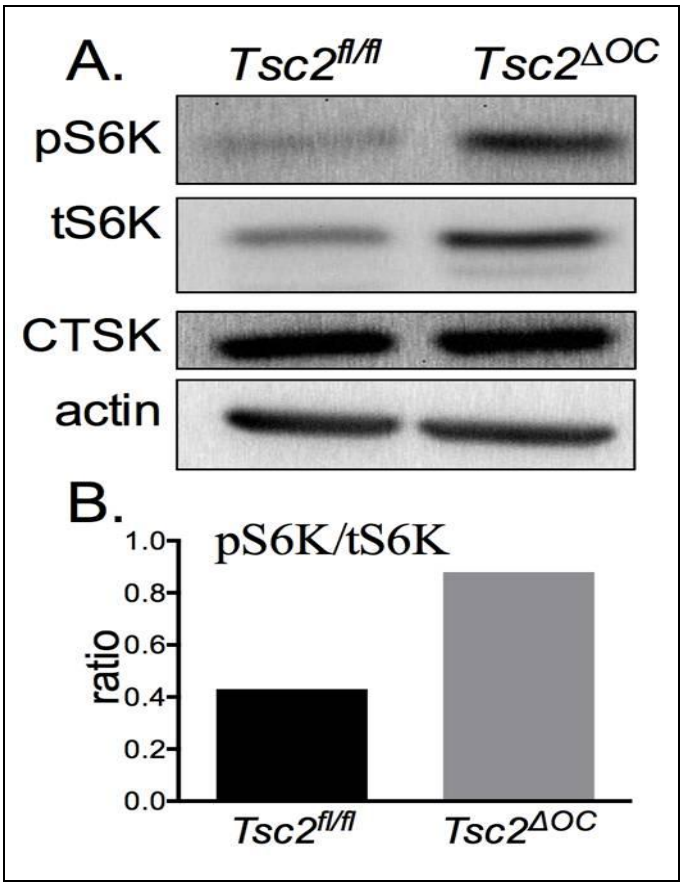


**Fig. 3**. **mTORC1 hyperactivation in TSC deficient spleen derived osteoclasts A.** Western blot showing increased phosphorylated S6K (pS6K) and total S6K (tS6K) in spleen monocyte derived osteoclasts in *Tsc2ΔOC* and *Tsc2fl/fl* controls. Cathepsin K expression confirmed the osteoclast lineage commitment in both genotypes; actin loading control. **B.** Increased pS6K /tS6K ratio is consistent with increased mTORC1 activity in *Tsc2ΔOC* osteoclasts. Densitometry of the immunoblot bands was evaluated with ImageJ.

Loss of *Tsc2* in osteoclasts had no effect on differentiation *ex vivo*, since the splenocytes were able to fully differentiate into mature osteoclasts as assessed by TRAP+ (marker of mature osteoclast) staining (Fig 4 A, B). Moreover, the number of *Tsc2ΔOC* derived osteoclasts was comparable to control derived osteoclasts; therefore, loss of TSC2 does not impair the survival of mature osteoclasts. Similar results were obtained from cultures of bone marrow derived osteoclasts (data not shown).

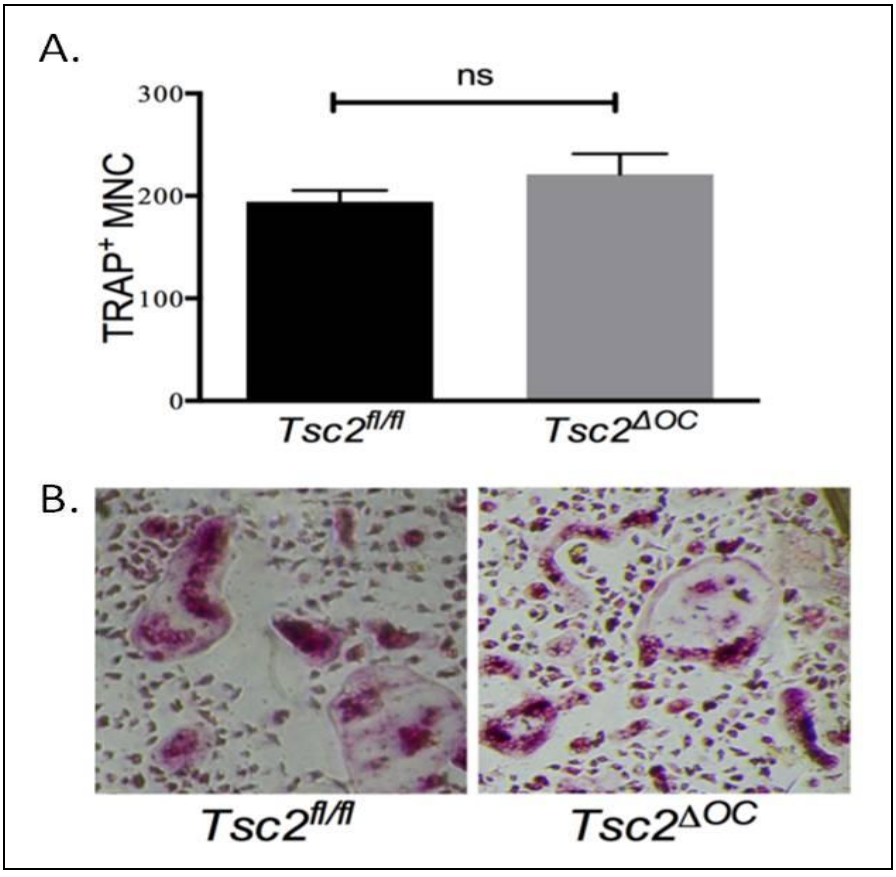


**Fig. 4. Osteoclast-specific deletion of *Tsc2* does not alter osteoclast number and differentiation. A.** osteoclast differentiation from *Tsc2ΔOC* splenic monocytes as assessed by TRAP+ multinucleated cells (MNC), significance determined by Student's t-test, columns represent the number of TRAP+ multinucleated osteoclasts in the considered field. **B.** Representative Images of TRAP+ stained osteoclast cultures from WT and *Tsc2ΔOC* littermates.

To further evaluate the function of the *TSC2* deficient osteoclasts in vitro, we measured the secretion of TRAP in the cultured media by bone marrow derived osteoclasts and spleen derived osteoclasts from both Wild Type and Tsc2ΔOC mice. The media was stained for TRAP and the absorbance was measured at 405nm. No differences were observed between the absorbance of culture media of Tsc2ΔOC bone marrow derived osteoclasts and control (2.906 ± 0.4061 vs 3.108 ± 0.7515, p= 0.8095), as well as in Tsc2ΔOC spleen derived osteoclasts and control (1.851 ± 0.4970 vs 2.441 ± 0.4525, p= 0.4756) (fig 5).

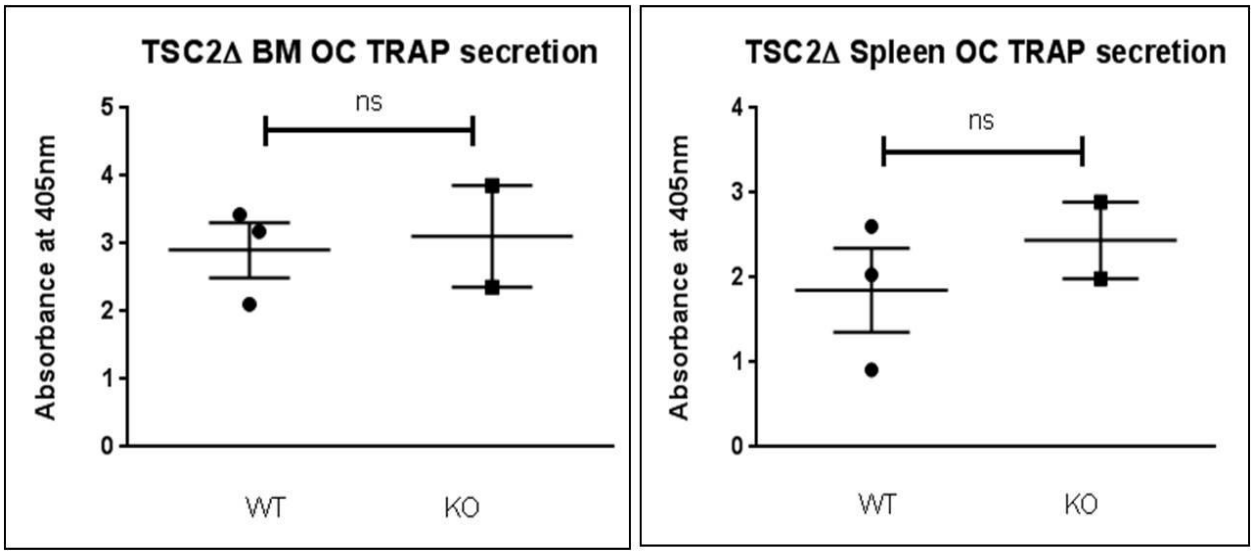


**Fig.5. TRAP secretion in bone marrow and spleen derived osteoclasts.** To measure TRAP activity, p-NPP was added to cell culture supernatant and absorbance was measured at 405nm. WT group n=3 vs *Tsc2Δosteoclasts n=2*. Each symbol represents the assay absorbance value of cells derived from one animal; significance was determined by Student's t-test. Mean and Standard Deviation for each group are represented in the graphs.

*In vivo* osteoclast differentiation was consequently assessed in femur histological sections. 9-month-old male *Tsc2ΔOC* mice appear to have normal osteoclasts, despite the *TSC2* deletion, as assessed by TRAP + staining. Despite the normality of the osteoclasts, in the femur histology of *Tsc2ΔOC* mice, an increase in bone deposition it is clearly visible, with a decrease in bone marrow space, in both epiphysis and diaphysis (Fig. 6A). Moreover, relative mRNA expression of Cathepsin K (marker of mature osteoclast) in whole bone was found to be slightly but significantly increased (2 fold) in 3-month-old *Tsc2ΔOC* male mice. This is consistent with the *in vivo* and *in vitro* TRAP+ staining showing the formation of mature osteoclasts, and further confirms that *TSC2* loss in mature osteoclasts does not inhibit osteoclast formation or ability of synthesize at least some of the lysosomal enzymes necessary for the bone resorption activity (fig 6B).

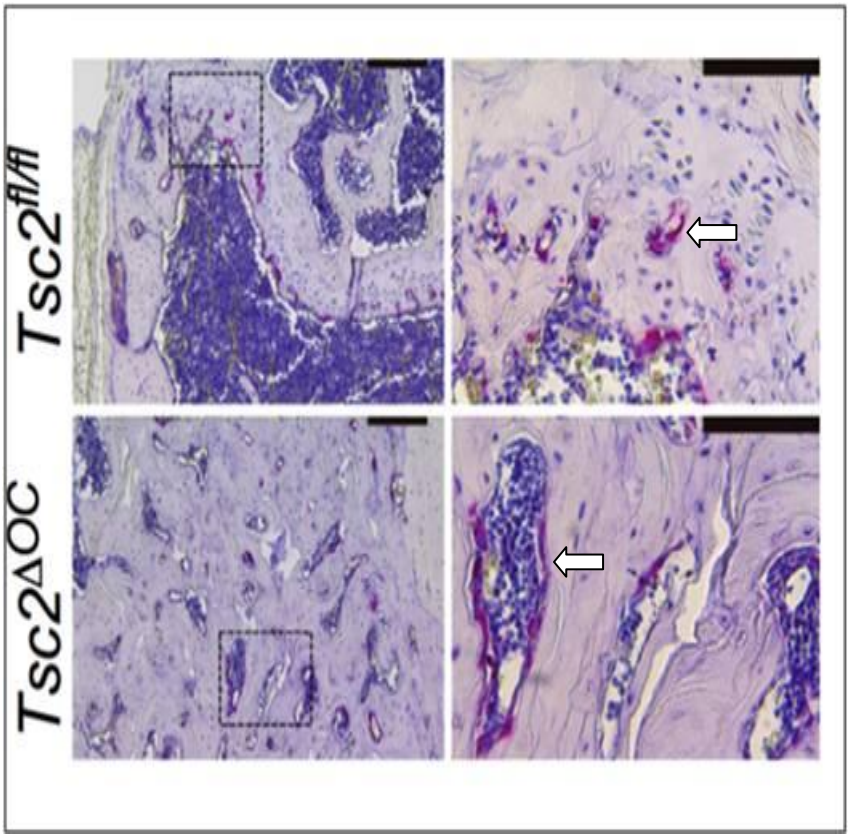


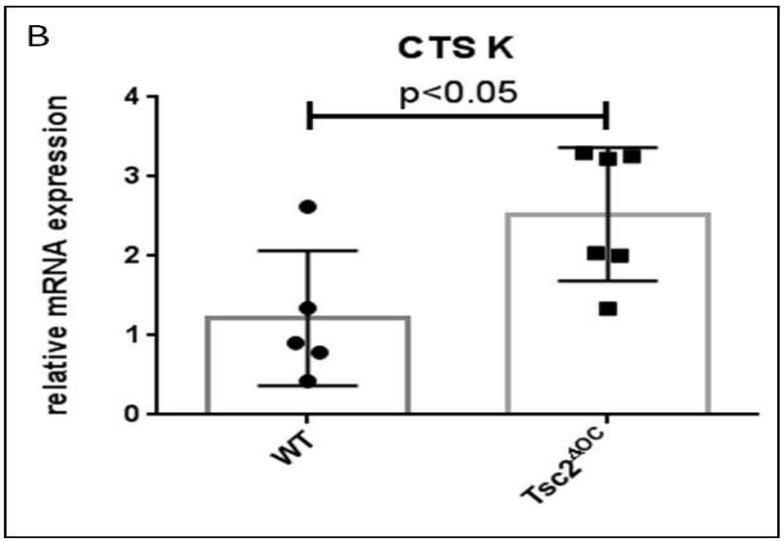


**Fig. 6. A. Increased trabecular bone in 9 moth old *Tsc2$^{\Delta OC}$* mice with normal osteoclasts.** Staining of femur sections from 9-month-old mice for tartrate resistant acid phosphatase (TRAP+) activity shows the presence of active osteoclasts in *Tsc2ΔOC* mice (low panel) and WT littermates (top panel). Arrows identifies TRAP + osteoclasts (digital enlargement of boxed area on left panel). **B. mRNA relative expression of Cathepsin K in 3-month-old male *Tsc2ΔOC* mice.** WT n=5 vs *Tsc2ΔOC* n=6. HPRT was used as housekeeping gene. RNA was extracted from right femur. Each symbol represents one animal; significance was determined by Student's t-test. Mean and Standard Deviation for each group are represented in the graphs.

The increased trabecular bone mass seen in the femur histology sections stained with TRAP+ was also observed in femur histology stained with Safranin O (a cartilage marker); in this section the strikingly diminished bone marrow space is also visibile. Moreover, femur histology demonstrates an increase in cartilage deposition in *Tsc2ΔOC* mice therefore the cartilage is not only present in the epiphyseal plate, as would normally occur in mice of these age, but also in the trabecular bone area just adjacent to the growth plate (Fig 7).

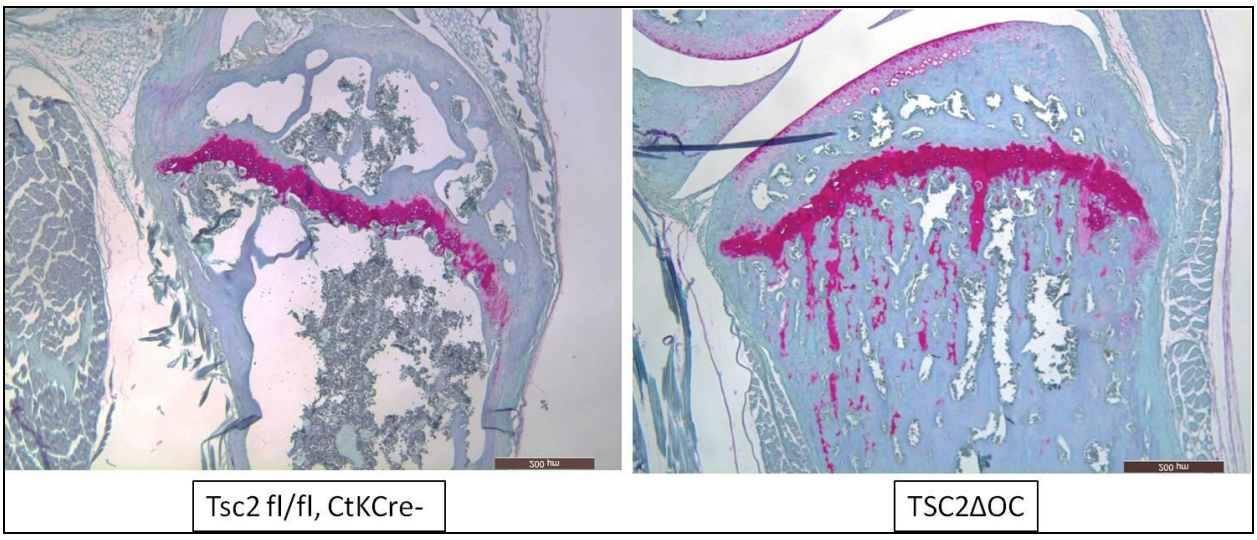


**Fig. 7. Increased Cartilage Deposition in Tsc2ΔOC mice.** Safranin O staining (red) for cartilage shows an increase in cartilage deposition, together with a decrease in the bone marrow space in both epiphysis and diaphysis in deficient mice compared to wild type littermates.

Given the massive loss of bone marrow space, we examined *Tsc2ΔOC* mice for defect in platelet, white and red blood cell numbers. White blood cells were similar in female wild-type and heterozygous (*CtsK Cre; TSC2 fl/+*) vs T*sc2ΔOC* (7.870 ± 2.872 K/ul, n=6 vs 6.140 ± 2.740 K/ul, n=2; p= 0.7596), as well as in male wild-type and heterozygous vs *Tsc2ΔOC* (9.197 ± 2.619 K/ul, n=7 vs 7.895 ± 1.726 K/ul, n=4; p= 0.7371). No differences were detected in red blood cell count in female *Tsc2ΔOC* (8.597 ± 0.8768 M/ul, n=6 vs 8.460 ± 0.02000 M/ul, n=2; p= 0.9347) or male *Tsc2ΔOC* (8.469 ± 0.6718 M/ul, n=7 vs 9.225 ± 0.4036, n=4; p= 0.4489). Moreover, platelets number was not altered in female *Tsc2ΔOC* (484.0 ± 165.5, n=6 vs 442.5 ± 58.50, n=2; p= 0.8957) or male *Tsc2ΔOC* (723.1 ± 143.4, n=7 vs 831.0 ± 180.3, n=4; p= 0.6557) (fig 8). Mouse necroscopy showed massive spleen enlargement in *Tsc2ΔOC* mice (data not shown), therefore it is reasonable to think that spleen hematopoiesis is increased consequent to loss of bone marrow space leading to normal CBC counts.

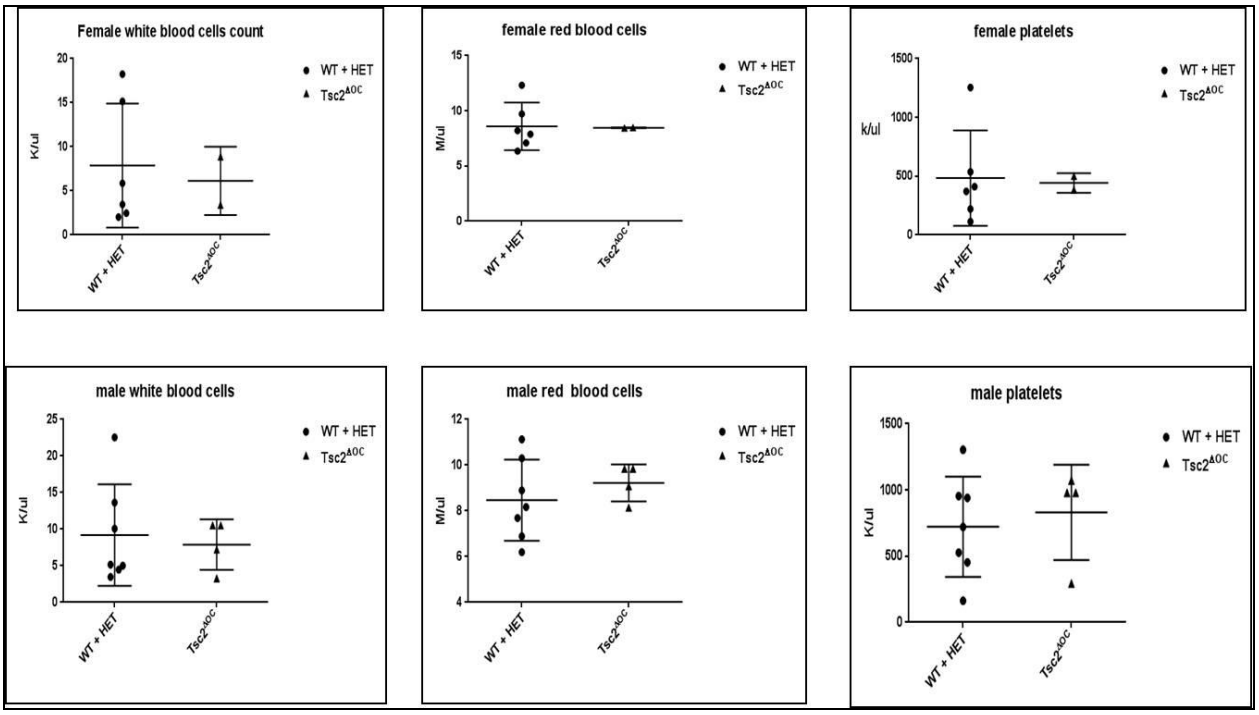


**Fig. 8. Complete Blood Count in *Tsc2ΔOC* female and male mice.** CBC counts of white, red blood cells and platelets. In both female and males, WT and Het were considered in one group vs *Tsc2ΔOC (*n=6 WT+ HET female vs n=2 *Tsc2ΔOC* female) (n=7 WT+ HET male vs n=4 *Tsc2ΔOC*). Each symbol represents one animal; no significance was determined by Student's t-test. Mean and Standard Deviation for each group are represented in the graphs.

In order to understand the paradoxical increase in bone mass in our mutant mice despite the presence of normal osteoclasts, we evaluated trabecular and cortical bone parameters of the right femur of 9-month-old mice using micro-computed tomographic imaging (micro-CT). All parameters were significantly increased in *Tsc2ΔOC* mice compared to wild type (*Tsc2 fl/fl*). Examining cortical bone, we found that at 9 months of age *Tsc2ΔOC* mice have increased cortical thickness (0.2702 ± 0.01125mm vs 0.2130 ± 0.01277mm; $p<0.02$), periosteal circumference (15.40 ± 0.8008 mm vs 9.430 ± 0.2006 mm; $p<0.01$), and periosteal area (2.843 ± 0.1219 $mm^2$ vs 2.151 ± 0.03554 $mm^2$; $p<0.01$) (fig. 9). Cortical porosity was unchanged

(0.07769 ± 0.005264 vs 0.07928 ± 0.005511; p= 0.8696), however. Trabecular bone is also dramatically increased in *Tsc2ΔOC* mice, as measured by BV/TV (bone volume/ tissue volume) (0.4981 ± 0.04740 $mm^2$ vs 0.1397 ± 0.01306 $mm^2$; p=0.0007) and by trabecular BMD (bone mineral density) (961.9 ± 9.300 vs 892.9 ± 6.340; p=0.007). Other trabecular parameters were altered consistent with the observed increase in BV/TV like: increase in trabecular number (7.675 ± 0.8254 vs 3.930 ± 0.1093, p=0.01) and trabecular thickness (0.09413 ± 0.004678 vs 0.05095 ± 0.0008694 mm, p<0.0001) and decrease in trabecular spacing (0.1541 ± 0.01738 vs 0.2417 ± 0.007311 mm; p=0.01) (fig 9).

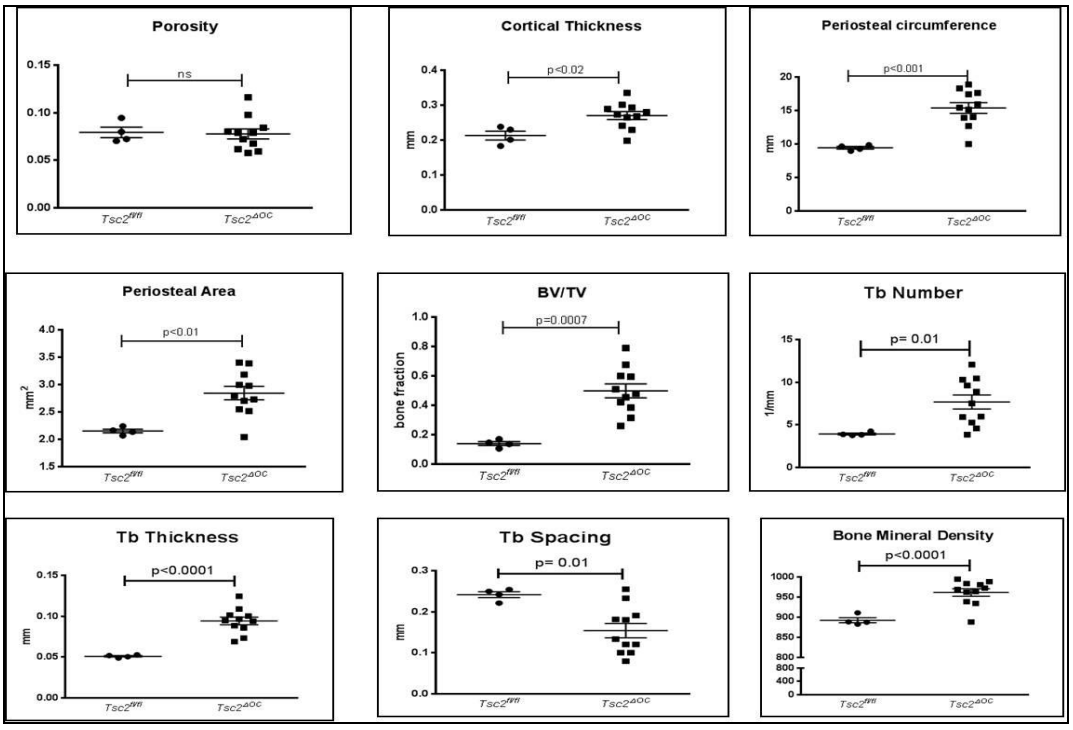


**Fig. 9. Micro CT analysis of femoral bones from 9-month-old male mice.** *Tsc2fl/fl* control (n=4) vs *Tsc2ΔOC* (n=11). Each symbol represents one animal; significance was determined by Student's t-test. Mean and Standard Deviation for each group are represented in the graphs.

Images obtained by 3D reconstruction of of the femoral epiphysis and midshaft femur are consistent with what previously seen in histology sections: an increase in the thickness of the cortical bone, together with an almost complete fusion of the trabeculae of the epiphysis of the femur (fig 10).

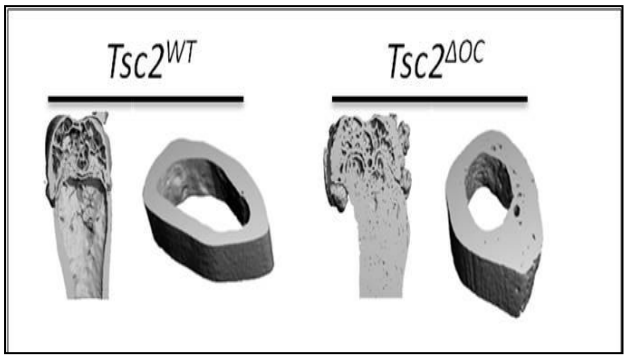


**Fig. 10.** 3D reconstruction of right femur of 9-month-old male mice, Wild Type (Cathepsink *CRE– TSC2* fl/fl) versus Tsc2ΔOC. Representative images.

Although osteoclasts form in vivo in *Tsc2ΔOC* mice and express the degradative enzymes TRAP and Cathepsin K, it is possible that *Tsc2ΔOC* osteoclasts do not resorb normally, thus explaining the high bone mass phenotype in the mutants. To evaluate the *in vivo* activity of the osteoclasts in *Tsc2ΔOC* mice, CTX-1 level were measured as a proxy for osteoclast activity. CTX-1 is the C-terminal telopeptide sequence of type I collagen, the predominant form of collagen found in bone. This telopeptide is cleaved by the activity of osteoclasts during bone resorption and released into the serum. Its serum levels are proportional to osteoclast activity at the time blood sample is drawn.

Unexpectedtly, CTX-1 was increased in male $Tsc2^{\Delta OC}$ mice (30.05 ± 11.10 ng/ml vs 74.83 ± 40.39 ng/ml, $p<0.0001$) compared to WT + Heterozygous and normal in $Tsc2^{\Delta OC}$

females compared to WT + Heterozygous (33.04 ± 7.591 ng/ml vs 25.29 ± 2.242 ng/ml, p=0.23). Therefore, defective osteoclast resorptive function is unlikely to explain the high bone mass phenotype in *Tsc2*$^{\Delta OC}$ mice (fig 11).

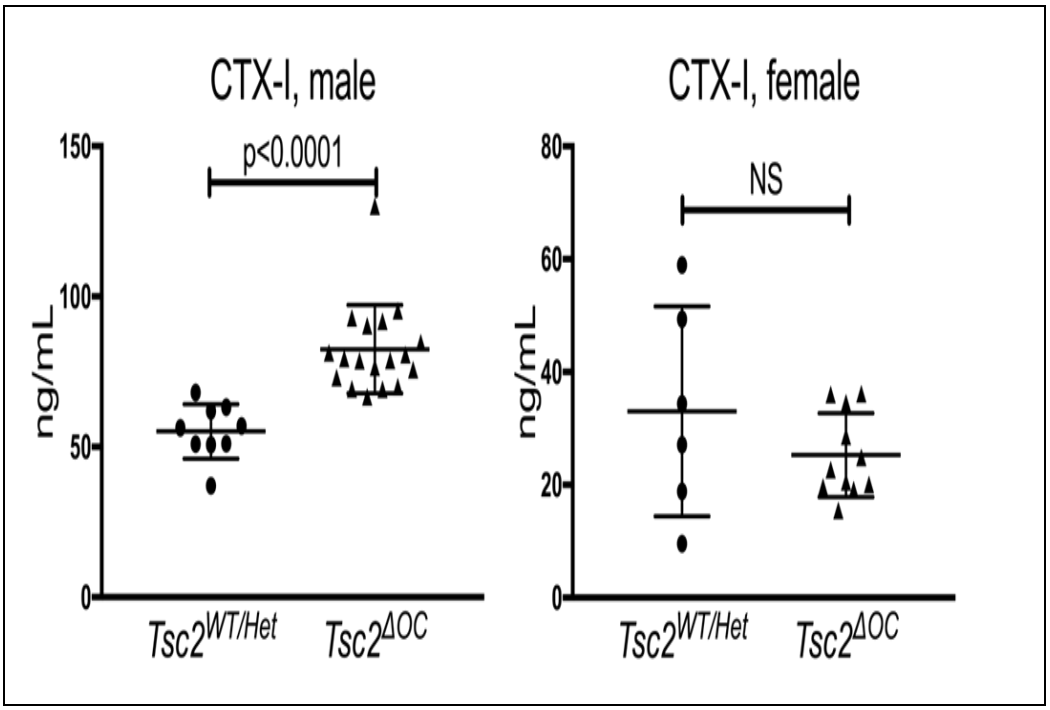


**Fig. 11. CTX-I levels in 9-month-old male and female mice.** Serum CTX-I measured with competitive ELISA in 9-month-old male *Tsc2*$^{\Delta OC}$ ( WT + HET n=9 vs *Tsc2*$^{\Delta OC}$ n= 18) and 9-month-old female. (WT + HET n=6 vs *Tsc2*$^{\Delta OC}$ n=11). Each symbol represents one animal; significance was determined by Student's t-test. Mean and Standard Deviation for each group are represented in the graphs.

We next decided to evaluate the function of osteoblasts, the cells responsible for the deposition of bone matrix. P1NP is the N-terminal propeptide of procollagen 1. In bone, collagen is synthesized by osteoblasts in the form of procollagen, and the propeptide is removed by specific proteinases before the individual collagen molecules can assemble into the triple helix that forms the collagen fibril. The propeptide can be found in the circulation and its

concentration in the serum reflects the synthesis rate of collagen type I and consequently osteoblast activity. Therefore, we measured the concentration of P1NP in both 9-month-old male and female mice. The serum concentration of procollagen type I N propeptide (P1NP), a measure of osteoblast activity, was elevated in $Tsc2^{\Delta OC}$ male (55.61 ± 10.31 ng/ml vs 82.48 ± 21.83 ng/ml, $p<0.0001$) and female (57.24 ± 16.38 ng/ml vs 100.74 ± 10.81 ng/ml, $p=0.04$) mice compared to WT + HET, suggesting that loss of *Tsc2* in osteoclasts stimulates bone formation by osteoblasts (fig 12).

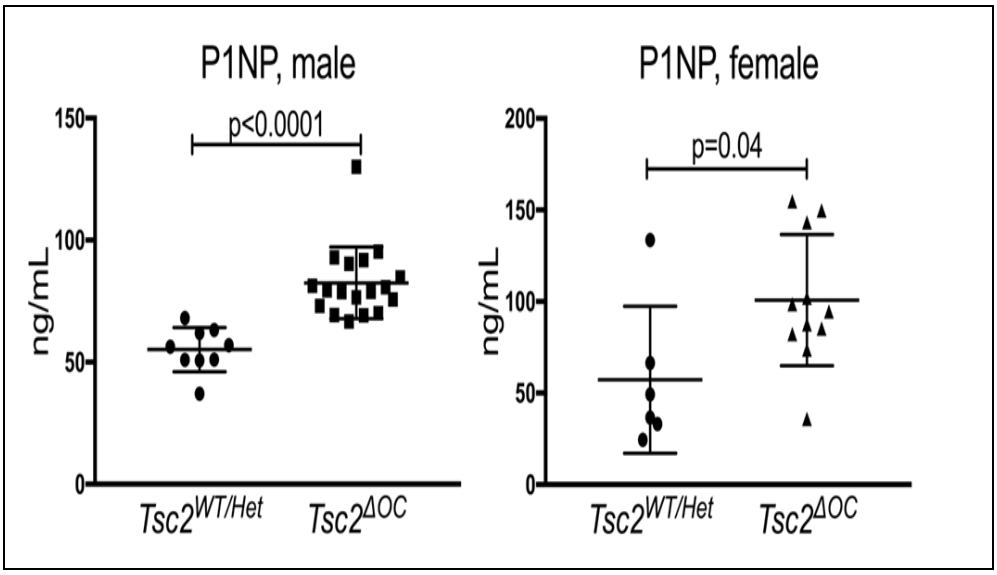


**Fig. 12. P1NP levels in 9-month-old male and female mice.** Serum CTX-I measured with competitive ELISA in 9-month-old male $Tsc2^{\Delta OC}$ ( WT + HET n=9 vs $Tsc2^{\Delta OC}$ n= 18) and 9-month-old female. (WT + HET n=6 vs $Tsc2^{\Delta OC}$ n= 11). Each symbol represents one animal; significance was determined by Student's t-test. Mean and Standard Deviation for each group are represented in the graphs.

We next wanted to evaluate if the phenotype observed is age dependent or if it is already present earlier in life; therefore femoral bone from a cohort of 3 month old male mice was analyzed by micro-CT (fig 13). All the bone parameters examined by micro-CT are

significantly increased in 3-month-old male *Tsc2*$^{\Delta OC}$ mice compared to a pooled control group of wild type and heterozygous mice. In the trabecular compartment, BV/TV (0.3732 ± 0.03488 vs 0.1100 ± 0.01001 vs; p< 0.0001) and trabecular BMD (969.6 ± 8.077 mg of HA/ cm3 vs 896.4 ± 5.492 mg of HA/ $cm^3$; p < 0.0001) are significantly increased. Consistent with this, we observed increased trabecular number (5.687 ± 0.3008/mm vs 4.377 ± 0.2036/mm; p= 0.0009), trabecular thickness (0.08575 ± 0.004971mm vs 0.04244 ± 0.001003 mm; p < 0.0001) and decreased trabecular spacing (0.1681 ± 0.008263/ mm vs 0.2320 ± 0.01158/ mm; p= 0.0003). In the cortical compartment, cortical thickness (0.2418 ± 0.006798 mm vs 0.1944 ± 0.003965 mm; p < 0.0001), and periosteal area (1.344 ± 0.05185 $mm^2$ vs 1.041 ± 0.02862 $mm^2$; p < 0.0001) were both significantly increased. Cortical porosity (0.09158 ± 0.003486 vs 0.1032 ± 0.001873; p= 0.0043) and cortical BMD (1182 ± 3.540 mg of HA/ $cm^3$ vs 1207 ± 4.208 mg of HA/ $cm^3$; p= 0.0001) were decreased, notably cortical BMD didn't show any difference at 9 months old. Therefore, the increase in mass is established by the time of sexual maturity in the mouse (fig 13, 14). Furthermore, as the difference in bone mass and cortical thickness are more prominent in the 9-month-old cohort, we surmise that the increase in bone formation and accretion of bone mass is progressive over the life of the animal.

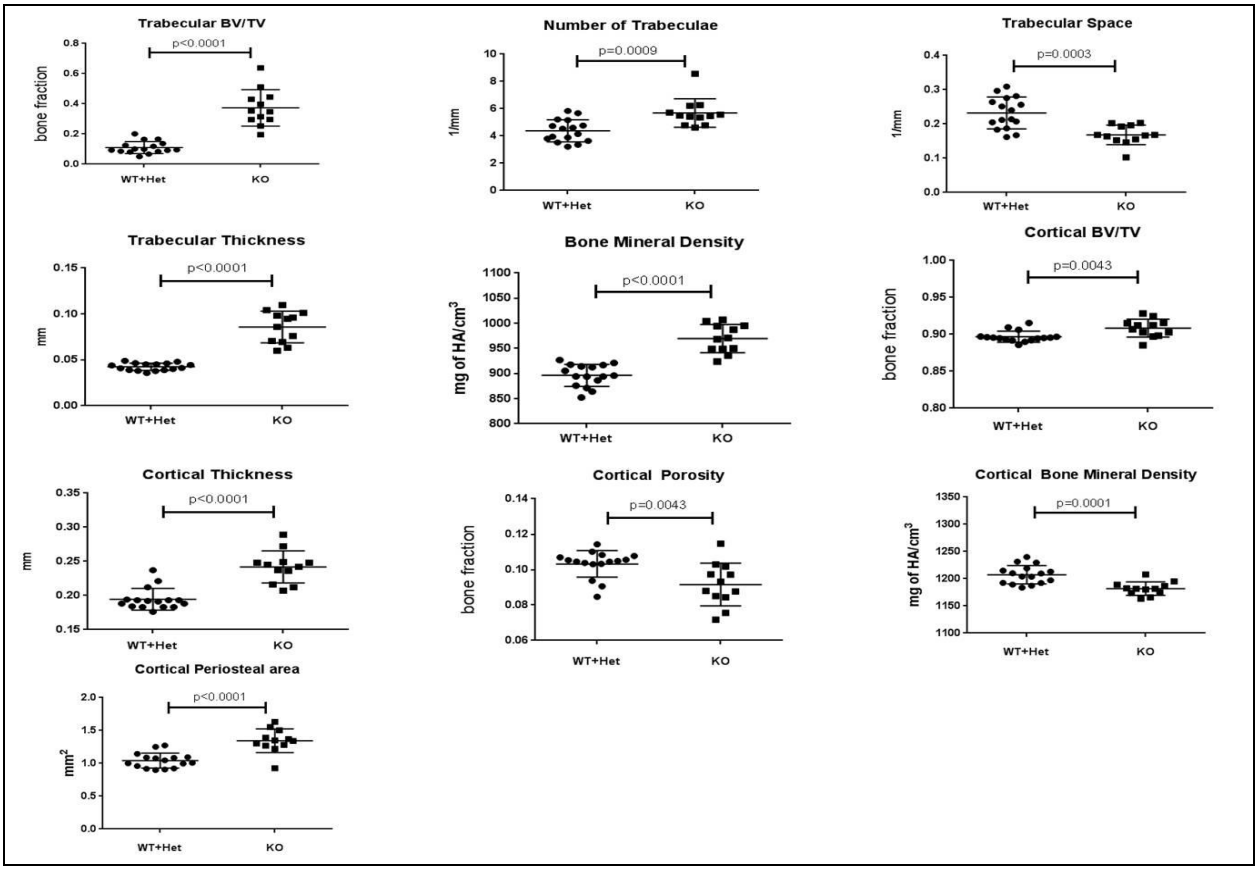


**Fig. 13. Micro CT parameters of 3-month-old male mice.** n=16 in WT+ HET mice group, n=12 in *Tsc2ΔOC.* t-student test was utilized for statistical analysis. Each symbol represents one animal; significance was determined by Student's t-test. Mean and Standard Deviation for each group are represented in the graphs.

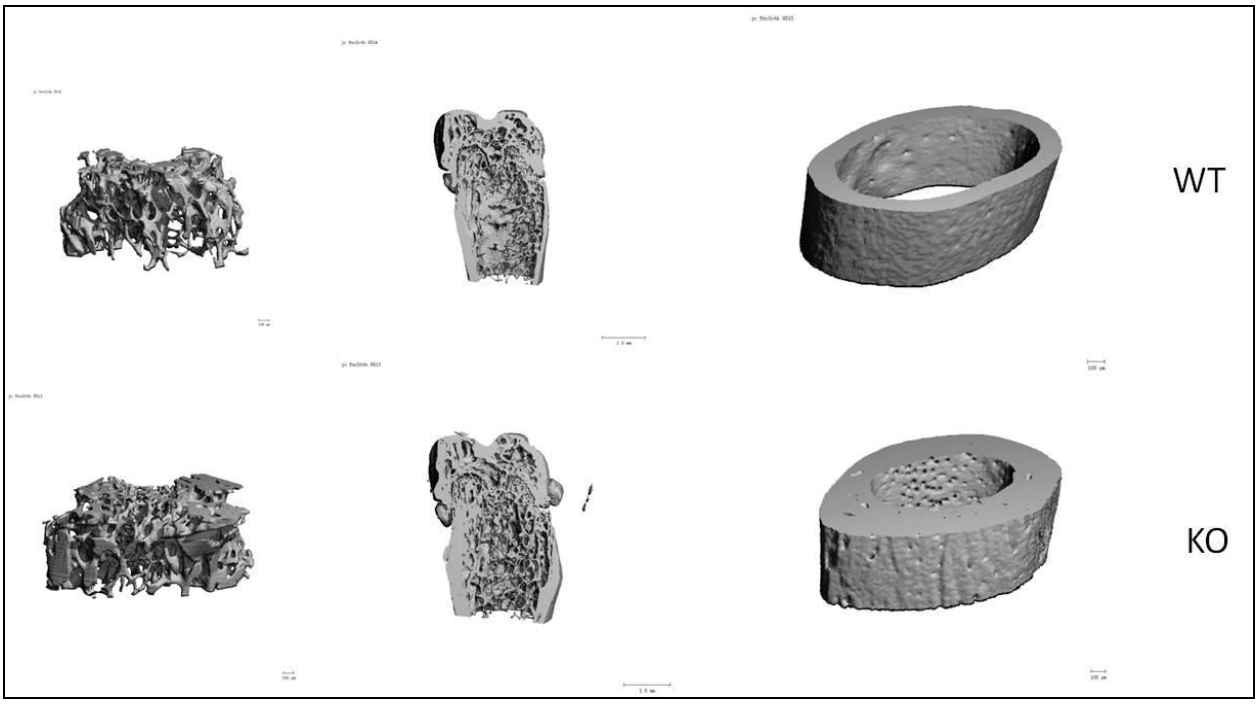


**Fig 14. Epiphysis and Diaphysis of 3mo male mice.** An increased trabecular mass is clearly seen in epiphysis as well as increased thickness of the cortical bone in diaphisys**.**

The serum levels of the degradation products of C-terminal telopeptide of type I collagen (CTXI) was measured in serum of 3-month-old mice; as seen for the 9-month-old female cohort, serum CTX-I was found comparable between *Tsc2*$^{\Delta OC}$ mice and the control group in both females (15.35 ng/ml vs 22.86 ng/ml, p= 0.3504) and males (14.9 ng/ml vs 14.49 ng/ml, p= 0.9226). This again suggests that defective osteoclast resorptive function is unlikely to explain the high bone mass phenotype in *Tsc2*$^{\Delta OC}$ mice even at earlier stage of life (fig 15).

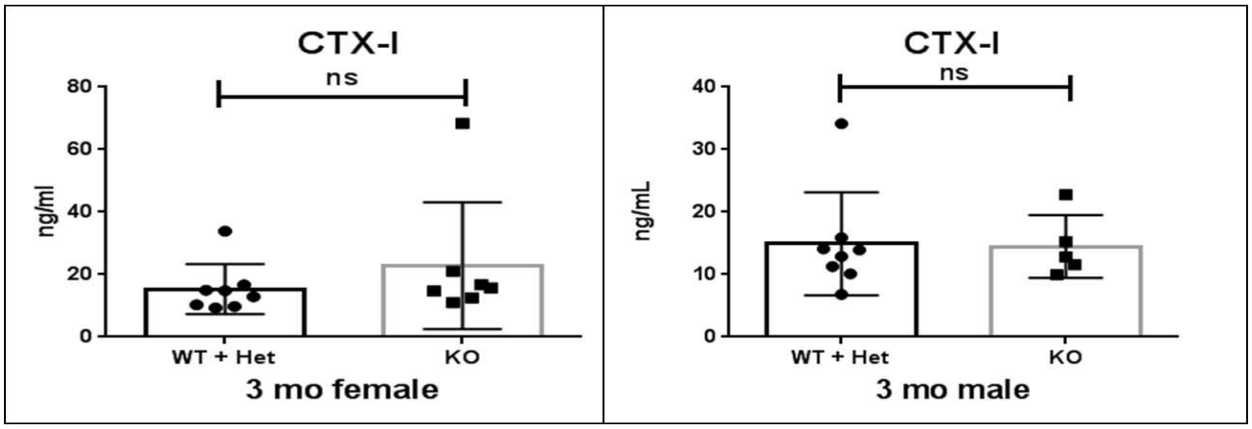


**Fig. 15. CTX-1 levels in plasma of 3-month-old females and males.** Female (WT + HET n=8 vs *Tsc2*$^{\Delta OC}$ n=7) mice. male (WT + HET n=8, *Tsc2*$^{\Delta OC}$ n=5). Each symbol represents one animal; significance was determined by Student's t-test. Mean and Standard Deviation for each group are represented in the graphs.

Importantly, serum P1NP levels in the 3-month-old cohort is also highly elevated in mutant compared to control mice, similar to what was seen in the 9-month-old cohort. We observed increased bone formation as measured by P1NP in both females (66.64 ng/ml vs 165.5 ng/ml, p= 0.002) and males (71.83 ng/ml vs 192.9 ng/ml, p= 0.004). Therefore, it is now clear that even at earlier stage of life the phenotype is the result of a hyper-activation of the osteoblasts, even though the mutation is only present in Cathepsin K expressing osteoclasts (fig 16).

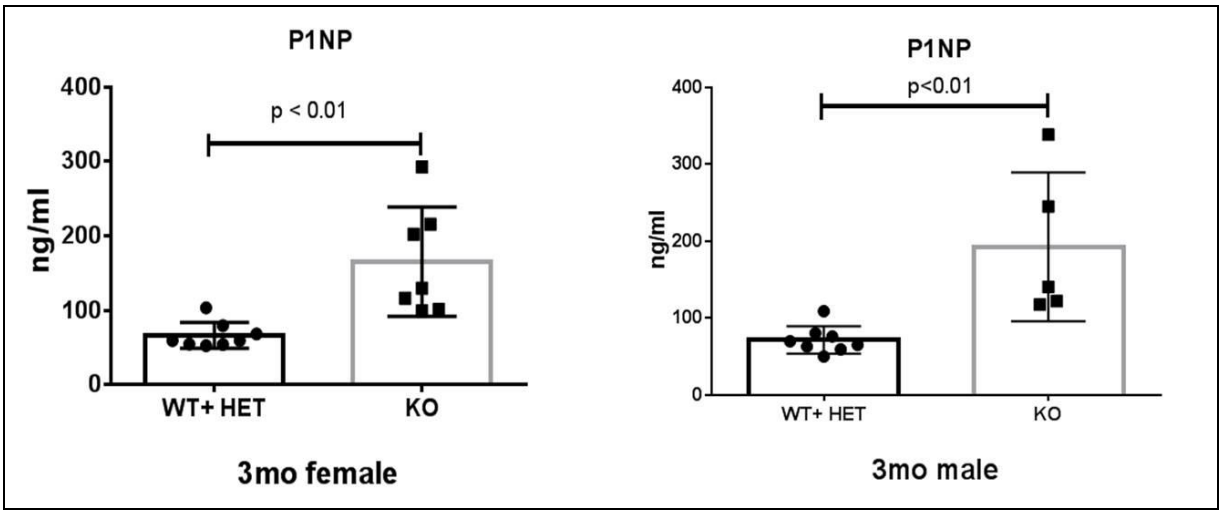


**Fig. 16. CTX-1 levels in plasma of 3-month-old females and males.** Female (WT + HET n=8 vs *Tsc2*$^{\Delta OC}$ n=7) mice. Male (WT + HET n=8, *Tsc2*$^{\Delta OC}$ n=5). Each symbol represents one animal; significance was determined by Student's t-test. Mean and Standard Deviation for each group are represented in the graphs.

How to explain and OC mutant causing an OB phenotype? We looked for alterations in OC –OB communication; osteoclasts are known to produce secreted factors called coupling factors or clastokines, which are able to promote the bone deposition activity of osteoblasts. Some clastokines were identified *in vivo*, therefore we decided to test if their presence is increased in our mouse model. We focused on CTHRC1 (Collagen Triple Helix Repeat Containing 1), SPHK1 and SPHK2 (Sphingosine Kinase 1 and 2, respectively). We extracted mRNA from femurs of a small cohort of *Tsc2*$^{\Delta OC}$ male mice and littermate controls. Surprisingly, in 9-month-old *Tsc2*$^{\Delta OC}$ the level of *Cthrc1* mRNA extracted from femurs is 37 times higher than WT control (WT relative mRNA expression =1, *Tsc2*$^{\Delta OC}$ n1=52.438500, n2 =22.094140). Whereas mRNA levels of *Sphk1* and *Sphk2* were not significantly altered in the mutants (*Sphk1* 1.37-fold increase, *Sphk2* 0.42-fold increase) (fig 17).

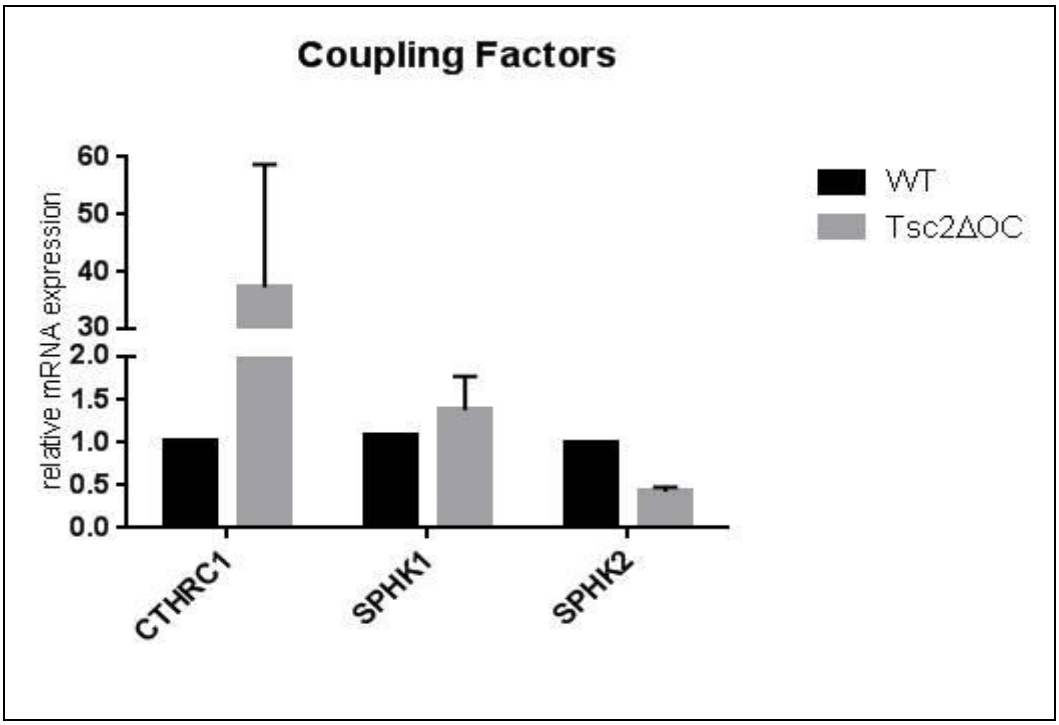


**Fig. 17. Relative mRNA expression of clastokines in WT and *Tsc2$^{\Delta OC}$* mice**. RNA extracted from right femur of 9mo mice. WT n=1, *Tsc2$^{\Delta OC}$* n=2. HPRT was used as housekeeping gene. t- student test was utilized for statistical analysis. Mean and Standard Deviation for the ***Tsc2$^{\Delta OC}$*** group is represented in the graphs.

Due to this preliminary result, we next focused on the increase of *Cthrc1* expression as a possible factor explaining the increase in bone formation in our mice. Therefore, we repeated the experiment in a cohort of 3-month-old male mice in order to show the same increase in *Cthrc1* seen in 9-months-old mice. Importantly, the level of *Cthrc1* mRNA was found increased 9.6 times (WT relative mRNA expression 1.101 ± 0.2127 n=5 and *Tsc2$^{\Delta OC}$* 9.646 ± 1.731 n=6, p= 0.0016) even in 3-month-old *Tsc2$^{\Delta OC}$* mice compared to wild type mice (fig 18).

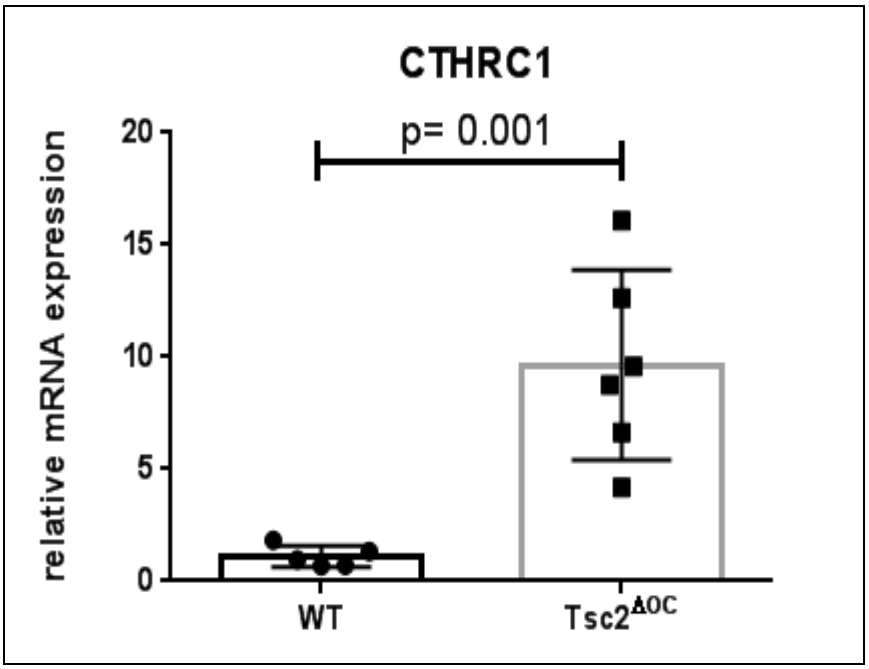


**Fig. 18. mRNA relative expression of CTHRC1 in 3-month-old male *Tsc2*$^{\Delta OC}$ mice.** HPRT was used as housekeeping gene. RNA extracted from right femur. Each symbol represents one animal; significance was determined by Student's t-test. Mean and Standard Deviation for each group are represented in the graphs.

After establishing the phenotype of the *Tsc2*$^{\Delta OC}$ mice, in which the loss of *Tsc2* is only present in osteoclasts, we tried to evaluate the bone morphology also in TSC2 heterozygous mice (*Tsc2* +/-), which are genetically analogous to patients with the disease Tuberous Sclerosis Complex. Mice were sacrificed at 10-12 months of age and the right femur was harvested for micro-CT evaluation. *Tsc2* +/+ littermates were used as control. All the bone parameters considered were not significantly changed by loss of a single allele of *Tsc2*: BV/TV (0.009050 ± 0.00305 vs 0.009225 ± 0.002065, p= 0.9637), trabecular number (1.626 ± 0.08950 /mm vs 1.969 ± 0.1050/ mm, p= 0.1090), trabecular thickness (0.0350 ± 0.0008000 mm vs 0.03015 ± 0.001953 mm, p= 0.1778), trabecular spacing (0.6245 ± 0.02380 mm vs 0.5129 ± 0.02788 mm, p= 0.0653), bone mineral density (974.2 ± 3.332 vs 940.9 ± 7.962, p= 0.07),

cortical thickness (0.2310 ± 0.0110 mm vs 0.2265 ± 0.009819 mm, p= 0.7949), cortical porosity (0.0701 ± 0.002700 vs 0.07215 ± 0.003139, p= 0.7022), periosteal area (1.457 ± 0.02658 $mm^2$ vs 1.383 ± 0.02470 $mm^2$, p= 0.1391) (fig 19).

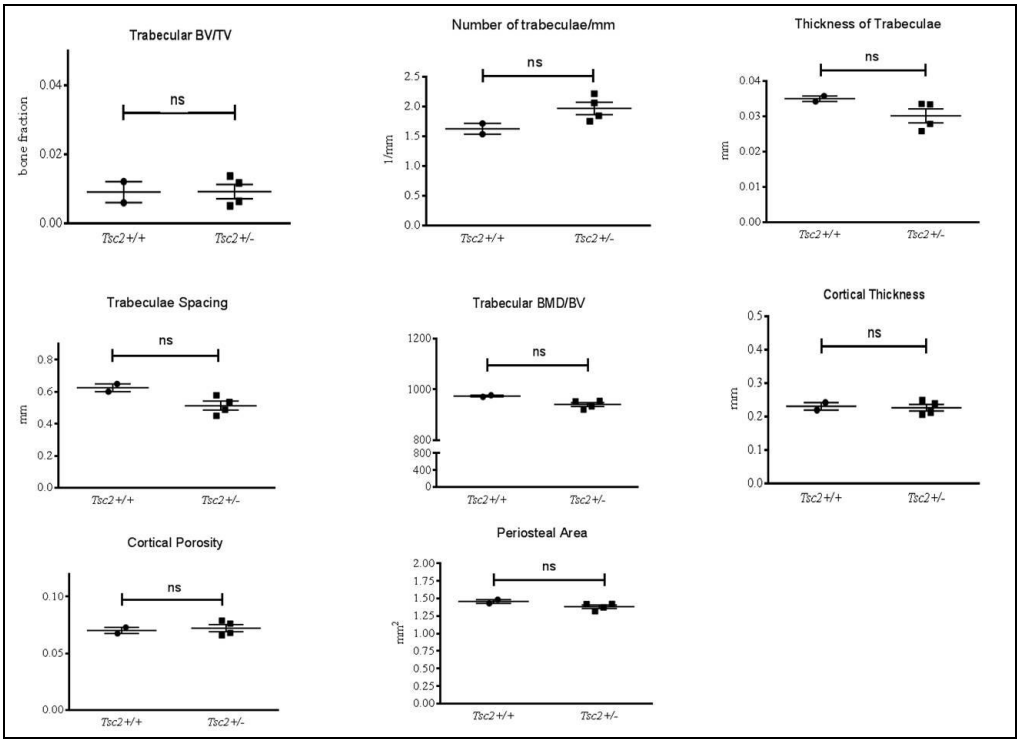


**Fig. 19. Micro-CT scan measurement of right femur of Tsc*2* +/+ and *Tsc2* +/- 10-month-old female mice.** Mice femur was harvested and used for micro CT scan measurement. *Tsc2* +/+ n=2, Tsc2 +/- n=4. Each symbol represents one animal; significance was determined by Student's t-test. Mean and Standard Deviation for each group are represented in the graphs.

Since we have access to plasma samples of patients with Tuberous Sclerosis Complex (TSC), we decided to test bone formation and resorption markers also in human serum. We identified a cohort of 7 female TSC patients (ages 27-48 years), and 7 age matched healthy controls (ages 30-50 years), in which we tested serum CTX-1 as well as P1NP. CTX-1 did not show any difference in control vs TSC patients (0.353441 ± 0.23131 ng/ml vs 0.412267 ± 0.245462 ng/ml, p=0.65) as expected. P1NP did not show any difference between controls and

TSC patients as well (76.074 ng/ml ± 16321.42 vs 85.71 ± 7934.725 ng/ml, p=0.18). Unfortunately, no clinical information about the presence of bone lesions in these patients was available (fig 20).

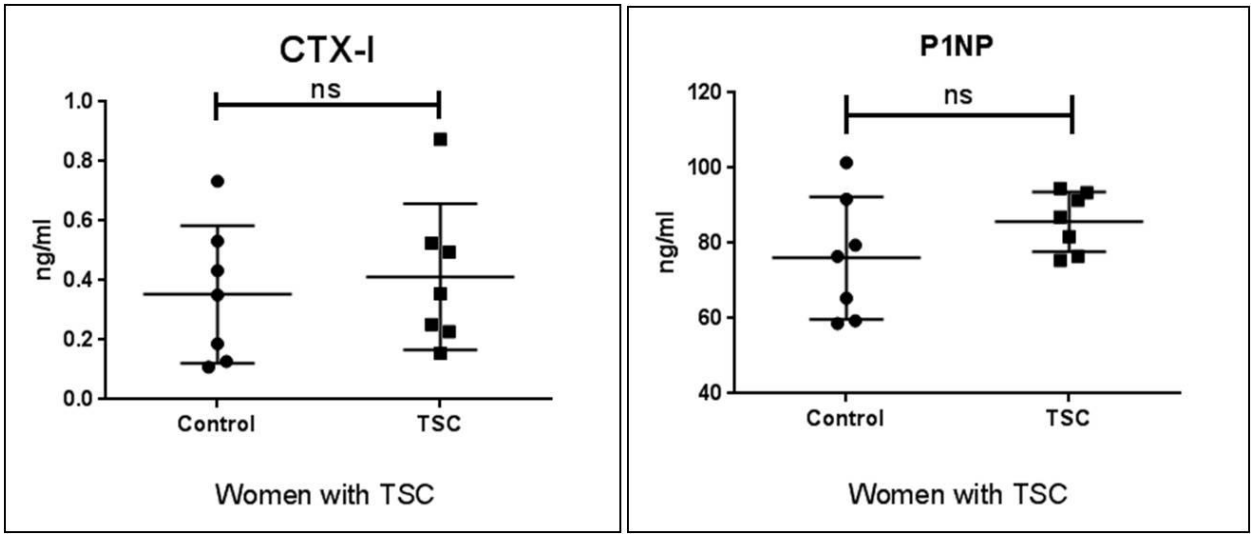


**Fig. 20. CTX-1 and P1NP levels in plasma of women with TSC and age matched control.** Serum levels of CTX-1 and P1NP measured by ELISA in a cohort of 7 patients with Tuberous Sclerosis and 7 age matched healty individuals. Each symbol represents one individual. t-student test was utilized for statistical analysis. Mean and Standard Deviation for each group are represented in the graphs.

# *4. Discussion*

The skeleton is frequently involved in TSC; the most common finding is the presence of multiple sclerotic bone lesions, seen in 88-100% of TSC patients (185). The sclerotic bone lesions are seen mostly in: vertebral bodies, pedicles and posterior elements, as well as in ribs, sternum, proximal femora, and humerus (201). Other skeletal findings can include: cystic lesions of the phalanges, hyperostosis of the calvaria, periosteal apposition of new bone and cortical thickening (198), and rarely fibrous dysplasia (202-204). Early reports of skeletal abnormalities in patients with TSC can be dated back in the early 1900' (167-175). Although frequently asymptomatic and poorly documented, sometimes these lesions can cause symptoms such as back pain, or in dramatic cases, pancytopenia (193-195). Preliminary observations suggest a worsening of the sclerotic lesions with time (204). Curiously, ossification was also observed within a cortical tuber raising the question if mTORC1 hyperactivity in specific unknown cells can stimulate ossification through the secretion of specific factors, even outside the normal bone tissue (200). The role of rapamycin has been poorly explored; rapamycin treatment was able to stabilize a previously active lesion in only one patient with a progressive form of fibrous dysplasia (204). Little is known about bone diseases in TSC, including whether patients with TSC are more or less likely to develop common bone diseases such as osteoporosis and fragility fractures.

Genetic manipulation of the TSC complex-mTORC1, in mice using conditional deletion of *Tsc1*, *Tsc2* or components of mTORC1 has revealed essential functions of these proteins in bone health. A variety of *Cre* drivers have been used to genetically manipulate the pathway at various stages of osteoblast differentiation. Achievement of normal bone mineralization requires mTORC1 activity in osteoprogenitor cells that give rise to osteoblasts. Deletion of

either *mTor* or *Raptor* in these cells leads to diminished ossification, but also to short limbs (143). The short limb phenotype is explained by a requirement for exquisite temporal control of mTORC1 activity in longitudinal bone growth, with high mTORC1 activity required for proliferation of early osteoblasts; whereas low mTORC1 activity is necessary for a fully differentiation of pre-osteoblasts (146). Increased mTORC1 activity can also be detrimental in more mature osteoblasts, since a specific deletion of either *Tsc1* or *Tsc2* results in high bone mass due to increased bone formation; however, the bone formed is of poor quality, with impaired mineralization (146, 165). The cellular mechanism for the poor quality/high bone mass phenotype seen with osteoblast-specific *Tsc1* or *Tsc2* deletion is reduced maturation of mutant osteoblasts. The evidence suggests that this is due to increased mTORC1 activity as the phenotype can be rescued by osteoblast-specific deletion of one *mTor* allele (165) or rapamycin treatment (146).

While the effect of mTORC1 activity modulation in osteoblasts has been examined in some detail, little is known about the role of mTORC1 in osteoclasts *in vivo*. Osteoclasts have been reported to express mTOR, RAPTOR, and RAG A. In one report, osteoclast formation was inhibited by deletion of either *mTor* or *Raptor* in hematopoietic precursors or *ex vivo* by rapamycin treatment, suggesting that mTORC1 activity is required for osteoclast differentiation (158). Consistent with this, rapamycin treatment of aged rats decreased osteoclast number and bone resorption as measured by serum TRAP5b (159). Moreover, everolimus was shown to decrease the osteoclast maturation in pit assay by TRAP staining, as well as decrease in the resorptive activity of the mature osteoclasts. Rapamycin was also seen to decrease the CTX-1 levels in plasma of patients in immunosuppressive therapy after kidney transplant. In contrast,

others have reported that rapamycin treatment of adult mice increased serum TRAP5b, suggesting that rapamycin enhanced osteoclastic bone resorption (164).

To address whether osteoclasts require *Tsc2* or mTORC1 components for normal differentiation and function *in vivo*, we utilized both induced and conditional deletion strategies to specifically target *Tsc2* and *Raptor* in osteoclasts or their progenitors. Bone marrow cells harvested from *Mx1-Cre; Raptor fl/fl* had decreased osteoclast formation when cultured in vitro with M-CSF and RANKL, therefore confirming the previous published results.

In order to test if osteoclast precursors maturation in positively enhanced by mTORC1 signaling as for osteoblast precursors, we generated an *Mx-1 Cre; Tsc2 fl/fl* mouse. Unexpectedly, bone marrow cells lacking TSC2 were unable to form osteoclasts, not because of a direct effect in osteoclasts precursors but because myelopoiesis in total was altered. Therefore, FACS sorting was used to purify bone marrow osteoclast precursors, then cultured in an M-CSF, RANKL enriched media in order to stimulate osteoclast maturation; using this approach cells were perfectly able to differentiate into mature osteoclasts.

Our aim was to investigate the effect of TSC2 loss and consequent mTORC1 activation in mature osteoclasts; therefore we choose to delete *Tsc2* only in cells expressing Cathepsin K, a marker of mature osteoclasts that are able to produce degradative enzymes. Spleen derived osteoclasts from 9-month-old *Tsc2ΔOC* mice looked similar to control as assessed by TRAP+ staining. TRAP secretion in culture media was not altered in either *Tsc2ΔOC* bone marrow derived osteoclasts or spleen derived osteoclasts; moreover, femur histology sections from *Tsc2ΔOC* mice showed the presence of normal appearing osteoclasts compared to littermate

control. Taken together, these data show how losing TSC2 does not decrease the generation of osteoclasts in vivo.

Curiously, mRNA expression of Cathepsin K was increased in femurs harvested from 3 -month-old male *Tsc2ΔOC* mice compared to control. This increase, although significant, is hard to explain since the expression of resorption enzymes and the number of osteoclasts is comparable between TSC2 deficient and TSC2 expressing osteoclasts; on the other hand, it confirms that TSC2 deficient osteoclasts are perfectly able to attain a mature phenotype. To assess osteoclast activity *in vivo*, we measured CTX-I, a marker of bone resorption and found that in 9-month-old male *Tsc2ΔOC* mice, CTX-1 levels were increased compared to controls, whereas no difference was found in females. Therefore, we concluded that the activity of TSC2 deleted osteoclasts is normal not only *in vitro* as previously shown, but also *in vivo.* Thus, the increase in bone and cartilage deposition, assessed by both femur histology and micro-CT scan at 9 months of age, was quite surprising given the normality of osteoclast number and function *in vitro* and *in vivo*.

This surprising result drove us to evaluate the activity of the second cell type involved in bone re-modeling: the osteoblast. Surprisingly, measuring P1NP (marker of bone deposition therefore osteoblast activity) in the same plasma samples in which we measured CTX-I, we found it increased in both males and females *Tsc2ΔOC* mice at 9 months of age; Therefore, the surprising phenotype aroused in our mouse model is explained by an increase in the activity of osteoblasts.

We next investigated if the phenotype is acquired at a late stage of life or can be observed even at earlier time points. We repeated the micro-CT scan at 3-month-old male

mice; importantly, all the parameters evaluated were consistent with an increase in bone formation of both cancellous and cortical bone in *Tsc2ΔOC* mice. Bone resorption as measured by CTX-1 levels in serum was similar to that of control mice. However, bone formation as measured by P1NP levels were higher, pointing towards the direction that, in our mouse model, the bone phenotype is already established at early stage of life and it is due to hyperactivity of the osteoblasts.

The increase of osteoblast activity in a mouse model in which *Tsc2* is deleted in osteoclasts, can be explained by a mechanism called osteoclast-osteoblast coupling consisting of the production of soluble factors (clastokines) by osteoclasts in order to stimulate osteoblast function. Several clastokines have been identified based on *in vitro* studies; with the clastokine function of a few of them confirmed in vivo (205). We decided to focus on *Sphk1*, *Sphk2* and *Cthrc1* to start. Interestingly, in mRNA extracted from femurs of 9-month-old male *Tsc2ΔOC* mice we found a huge increase in the expression of *Cthrc1* compared to control, whereas the level of *Sphk1* and *Sphk2* didn't change. This exciting result was confirmed in mRNA extracted from 3-month-old femurs, although in this case the increase of *Cthrc1* in *Tsc2ΔOC* mice compared to controls was more modest, yet significant in a large cohort of animals.

As previously reported, the bone lesions in TSC consists of focal areas of dense bone formation, therefore our model recapitulates the lesions observed in TSC patients. Notably, also the three mouse model with deletion of either *Tsc1* or *Tsc2* in various stage of osteoblast maturation expressed a phenotype consistent with ours (146, 165, 166). We can speculate that the dense bone lesions in TSC patients emerge from a second hit mutation in osteoblasts and/or in osteoclasts, at various stage of development.

*Tsc2* +/- mice are the best model to study TSC, since they have only one gene mutated as in humans. Therefore, we evaluated if a bone phenotype was present in these mice. However, micro-CT analysis of 10-12-month-old female heterozygous mice did not show any significant differences compared to wild type *Tsc2* +/+ mice. This result was not unexpected, since in human patients the bone lesions are circumscribed to a small portion of the skeleton and rarely can affect a conspicuous segment of a long bone, suggesting that a second hit mutation is needed for a bone lesion to form.

Lastly, we tried to evaluate if the serum bone markers were changed in a cohort of female patients with TSC compared to a control group of age matched females: no differences were found in CTX-1 and P1NP levels. Even if, as reported by Avila et al (185), almost 100% of the patients have 4 or more bone dense lesions, and frequently the number can rise to more than 10, this is likely insufficient to increase circulating P1NP levels to an extent detectable by ELISA. Moreover, in humans the values of both P1NP and CTX-1 fluctuates enormously, and can change during life.

In conclusion, we established the first *in vivo* mouse model of *Tsc2* loss in mature osteoclasts; this model, generated to study the bone lesions of TSC, helped us to unmask a function of mTORC1 as a regulator of osteoclast-osteoblast coupling. We hypothesize that this may be due to mTORC1 regulation of CTHRC1. Further experiments will be needed to clarify the nature of this regulation. This is the first observation for a role for mTORC1 in regulating the coupling between osteoclasts and osteoblasts, and indeed one of the only models in which coupling is deregulated.

These observations will have several implications for the advancement of the knowledge of TSC, in which the extraordinary presence of bone lesions has just begun to be recognized by the scientific community. Moreover, the recognition of mTORC1 as one of the actors involved in the induction of bone formation by osteoclasts may suggest potential new avenues of therapy of bone diseases such as osteoporosis.

# *5. Material and Methods*

## Mice

Tsc2 fl/fl mice generated by Dr Gambello (207), were crossed to Cathepsin K Cre mice (gift of Dr. Kato) to generate Tsc2ff Ctk Cre mice (hereafter referred to as Tsc2DeltaOC) and controls. Both strains were backcrossed to C57BL/6 for 20 generations. Alternatively, Tsc2 ff was crossed to Mx1 Cre (Jackson Lab, catalog # 003556). At 4 weeks Mx1Cre+ and Cre- offspring were treated with 500ug of poly I: C IP every other day x 3 doses to induce Cre expression and Tsc2 deletion. Raptor fl/fl (Jackson Lab, catalog # 013188) were purchased from Jackson Laboratory and crossed to the previously described Mx1 Cre mice in order to create a Mx1 Cre+ Raptor fl/fl mouse. All experiments were performed in accordance with AALAS (American Associaton for Laboratory Animal Science) guidelines and under the supervision of the Harvard Center for comparative medicine IACUC (Institutional Animal Care and Use Committee). Tsc2 +/- mice were generated in Dr Kwiatkowski laboratory (205).

## ELISA for Serum CTX-I, and P1NP.

Serum was derived from blood samples collected by cardiac puncture, using serum separation tubes (Becton Dickinson). Serum C-terminal telopeptides (CTX-I) and Procollagen type 1 propeptides (PINP) were quantified using EIA assays (Immunodiagnostics Systems). All ELISAs were read with Synergy H1 Hybrid Reader (Biotek).

***Isolation and culture of osteoclast precursors (OCP).***

Bone marrow isolated by flushing long bones was subjected to RBC lysis and resuspended in sorting media (alpha-MEM media containing 20% FBS). Cells were stained for lineage markers with antibodies to Ter119, CD20, CD3, CD11b and Ly6C (all from BioLegend) according to published methods (206). Cells were analyzed on a FACSAria II (BD Biosciences) and the population negative for Ter119, CD20, and CD3 was further examined for CD11b and Ly6C staining. The CD11b lo/negative Ly6Chi population, which is known to contain the bone marrow OCP, was then isolated by flow cytometric cell sorting. Purified OCP were cultured in MCSF and RANK-L at a density of 5000 cells per well on a 96 well plate. After 4-5 days of culture, cells were fixed and stained for TRAP activity to detect the formation of multinucleated TRAP+ osteoclasts.

**RNA Isolation and Real-Time PCR.**

Bones were homogenized in ice-cold TRIzol, using bullet blender beads (Next Advance), and RNA was isolated using a standard TRIzol protocol. Samples obtained after TRIzol extractions were further purified using the RNeasy Plus Micro Kit with on-column genomic DNA-digest (Qiagen). Affinity Script quantitative PCR (qPCR) cDNA Synthesis Kit (Agilent Technologies) and was used to generate cDNA. Real-time PCR was performed on StepOne Plus Realtime PCR Machine (Applied Biosystems), using Fast SYBR Green Master Mix (Thermo Fisher Scientific). Gene expression was determined relative to the housekeeping gene HPRT (Hypoxantine Phosphorybosiltransferase). Fold change of experiment groups compared with control group was calculated by the delta-delta-Ct method. Real-time PCR primer sequences are listed in Table 1.

**Micro-CT**

After serial fixation in 4% (g/100 mL) paraformaldehyde and 70% (vol/vol) ethanol, femurs were scanned using a μCT 35 (Scanco Medical AG). Scans were conducted in 70% ethanol using a voxel size of 7 μm, X-ray tube potential of 55 kVp, intensity of 0.145 Ma, and integration time of 600 ms. A region beginning 0.35 mm proximal to the growth plate and extending 1 mm proximally was selected for trabecular bone analysis. A second region 0.6 mm in length and centered at the midpoint of the femur was used to calculate diaphysis parameters. The region of interest was thresholded using a global threshold that set the bone/marrow cutoff at 352.3 mg HA/ cm3 for trabecular bone and 589.4 mg HA/cm3 for cortical bone. 3D microstructural properties of bone were calculated using software supplied by the manufacturer. Bone length was measured using the scout view feature.

**Cell lysates and Immunoblot**

For immunoblot analyses cells were washed with ice-cold PBS and lysed on ice in 1x RIPA buffer (CST) with phosphatase and protease inhibitors (Sigma). Lysates normalized to protein concentration, denatured with loading buffer and resolved by electrophoresis on a 4-12% Bis-Tris gel (Invitrogen). Proteins were transferred to PVDF membranes, blocked in 5% BSA or nonfat milk for 1h probed with primary antibodies (1:1000) in 1x TBST buffer (CST) overnight at 4°C. Membranes were washed with TBST and incubated with secondary antibody (1:10000) for 1h at room temperature and chemiluminescence was visualized using Super Signal (Pierce) and the SynGene G-BOX gel documenting system. The following antibodies were used: phospho-p70S6K (Thr 389) (Cell Signaling Technology),

Actin (Cell Signaling Technology), TS6K (Cell Signaling Technology), Cathepsin K (abcam).

**Preparation and analysis of murine osteoclast in vitro**

Cell culture experiments were performed in α-MEM (Cellgro) containing 10% fetal calf serum (Hyclone), 100 U penicillin and 100 μg/ml streptomycin (Cellgro) at 37 °C with 5% $CO_2$. Mouse bone marrow cells were cultured for 3 days in the presence of 40 ng/ml murine recombinant M-CSF (R&D Systems) in a suspension culture dish (Corning Costar Ins) to which stromal and lymphoid cells cannot adhere. Alternatively, total splenocytes were cultured for 6 days in the presence of 40 ng/ml murine recombinant M-CSF (R&D Systems) in a bacteriologic plate. Thereafter, cells were washed with PBS once to remove nonadherent cells, harvested by pipetting with 10 mM EDTA in phosphate-buffered saline (PBS) and seeded on plastic with 20 ng/ml M-CSF and 10 ng/ml RANKL (R&D Systems) at a density of $3x10^4/cm^2$. After 3 days, the cytokines were replenished every other day. To evaluate osteoclast formation, we either 1) stained for tartrate resistant acid phosphatase (TRAP) as previously described (206) 2) assayed for TRAP activity in the tissue culture supernatants performed as following: Transfer 50ul of the supernatant from cell plate to 96 NUNC plate, prepare a mixture of: H20, acetate buffer (2.5M, pH 5.2 from sigma #3863-50mL), 1M tartrate and 760mM pNPP (sigma cat # P4744). Add 150 ul of the mixture to each well. After 1-hour incubation at 37 C, stop reaction with 50 uL of 3N NaOH. Absorbance was measured at 405 nm with Synergy H1 Hybrid Reader (Biotek).

**Resorption assays**

Osteoclast were seeded in Corning Osteologic wells. Cultured for 10 days. Wells are stained with 1% silver nitrate followed by 1% pyrogallol. Resorption area was calculated using Image J.

**Histology**

Femurs were fixed in 4% PFA at 4deg C x 24hr, then decalcified in 14% EDTA, pH 7.2 for 14-21 days. Paraffin embedded. 5u sections were stained with H&E or for TRAP activity using a Leukocyte Acid Phosphatase kit (Sigma). Safranin O staining was performed to examine cartilage remnants and growth plate cartilage with 0.1% Safranin O with 0.05% Fast Green counterstain.

| | | |
|---|---|---|
| Hprt-2R | AGGGCATATCCAACAACAAACTT | Designed with Primer 3 program. |
| Hprt-2F | GTTAAGCAGTACAGCCCCAAA | Designed with Primer 3 program. |
| Ctsk F | GGGCTCAAGGTTCTGCTGC | Designed with Primer 3 program. |
| Ctsk R | GTTAAGCAGTACAGCCCCAAA | Designed with Primer 3 program. |
| Sphk1 F | TGAGGTGGTGAATGGGCTAATGGA | Lotinun et al JCI 2013 (138) |
| Sphk1 R | AACAGCAGTGTGCAGTTGATGAGC | Lotinun et al JCI 2013 (138) |
| Sphk2 F | TGGGCTGTCCTTCAACCTCATACA | Lotinun et al JCI 2013 (138) |
| Sphk2 R | AGTGACAATGCCTTCCCACTCACT | Lotinun et al JCI 2013 (138) |
| Cthrc1 F | AAGCAAAAAGCGCTGATCC | Takeshita et al (135) |
| Cthrc1 R | CCTGCTGGTCCTTGTAGACAC | Takeshita et al (135) |

Table 1. qPCR primers used.

# *6. Bibliography*


1- Gomez, MR, Sampson JR, Whittemore VH. Tuberous sclerosis complex. *3rd edn. New York: Oxford University Press.* (1999).

2- Curatolo, P. Tuberous sclerosis complex: from basic science to clinical phenotypes. *London: Mac Keith Press for the International Child Neurology Association*. (2003).

3- Curatolo, P. Bombardieri, R. Jozwiak, S. Tuberous sclerosis. *Lancet.* 372, 657-68 (2008).

4- Moolten, S.E. Hamartial nature of the tuberous sclerosis complex and its bearing on the tumour problem: report of one case with tumour anomaly of the kidney and adenoma sebaceum. *Arch Intern Med*. 69, 589–623 (*1942).*

5- Jay, V. Historical contributions to paediatric pathology: tuberous sclerosis. *Pediatr Dev Pathol.* 2, 197–98 (*2004*).

6- Bourneville, D.M. Sclérose tubéreuse des circonvolutions cérébrales. *Arch Neurol.* (1880) 1, 81–91 (1880).

7- Bourneville, DM., Brissaud E. Ence´phalite ou scle´rose tube´reuse descirconvolutions ce´re´brales. *Arch Neurol* (Paris). 1, 390–410 (1881).

8- Jansen, F.E., Van Nieuwenhuizen O., Van Huffelen AC. Tuberous sclerosis complex and its founders. *J Neurol Neurosurg Psychiatry.* 75, 770 (2004).

9- Pringle, J.J. A case of congenital adenoma sebaceum. *Br J Dermatol*. 2, 1–14 (1890).

10-Van Der Haeve, J. Eye Symptoms in Tuberous Sclerosis of the brain. *Trans.Opthalmol.Soc.U.K.* 40, 329-334 (1920).

11- Vogt, H. Zur diagnostic der tuberosen Sklerose.Z.Erforsch.Behandl.Jugendl Schwachsinos. 2,1-12 (1908).

12- Goodrick, S. The road to Vogt's triad. *The Lancet Neurology*, Volume 14, Issue 7, 690.

13- Schuster, P. Beitrage Zur Klink der tuberosen Sklerose des Gehirns. *Z. Nervenheilk*. 50, 96-133 (1914).

14- Gomez, M.R. Tuberous Sclerosis Complex. *New York: Oxford University Press*, 1999.

15- Gomez, M.R. Phenotypes of the Tuberous Sclerosis Complex with a Revision of Diagnostic Criteria. *Annals New York Academy of Sciences*. (1991).

16- Jannsen, B., Sampson, J., Van Der Est, M., Deelen, W., Verhoef, S., Daniels, I., Hesseling, A., Brook, C.P., Nellist, M., Lindhout, D., Sandkuijl, L., Halley, D. Refined localization of

TSC1 by combined analysis of 9q34 and 16p13 data in 14 tuberous sclerosis families. *Hum Genet*. 94, 437-440 (1994).

17- Povey, S., Burley, M.W., Attwood, J., Benham, F.., Hunt, D., Jeremiah, S.J., Franklin, D., Gillett, G., Malas, S., Robson, E.B., Tippett, P., Edwards, J.H., Kwiatkowski, D.J., Super, M., Mueller, R., Fryer, A., Clarke, A., Webb, D., Osborne, J. Two loci for tuberous sclerosis: one on 9q34 and one on 16p13. *Ann. Hum. Genet*. 58, 107-127 (1994).

18- Kandt, R., Haines, J., Smith, M., Northrup, H., Gardner, R., Short, M., Dumars, K., Roach, E., Steingold, S., Wall, S., Blanton, S., Flodman, P., Kwiatkowski, D., Jewell, A., Weber, J., Roses, A., Pericak-Vance, M. Linkage of a major gene locus for tuberous sclerosis to a chromosome-16 marker for polycystic kidney disease. *Nat. Genet*. 2, 37-41 (1992).

19- European Chromosome 16 Tuberous Sclerosis Consortium. Identification and characterization of the tuberous sclerosis gene on chromosome 16. *Cell*. 75, 1305-1315 (1993).

20-Van Slegtenhorst, M., Nellist, M., Nagelkeren, B., Cheadle, J., Snell, R., van den Ouweland, A., Reuser, A., Sampson, J., Halley, D., van der Sluijs, P. Interaction between hamartin and tuberin, the TSC1 and TSC2 gene products. Hum Mol Genet. 7, 1053-1058. (1998).

21- Sampson, J.R., Maheshwar, M.M., Aspinwall, R., Thompson, P., Cheadle, J.P., Ravine, D., Roy, S., Haan, E., Bernstein, J., Harris, P.C. Renal Cystic disease in tuberous sclerosis: role of the polycystic kidney disease 1 gene. *Am. J. Hum. Genet*. 61, 843-851 (1997).

22- Kozlowski, P., Roberts, P., Dabora, S., Franz, D., Bissler, J., Northrup, H., Au, K.S., Lazarus, R., Domanska-Pakiela, D., Kotulska, K, Jozwiak, S., Kwiatkowski, D.J. Identification of 54 large deletions/ duplications in TSC1 and TSC2 using MLPA, and genotype-phenotype correlations. *Hum. Genet*. 121, 389-400 (2007).

23- Emmerson, P., Maynard, J., Jones, S., Butler, R., Sampson, J.R., Cheadle, J.P. Characterizing mutations in samples with low level mosaicism by collection and analysis of DHPLC fractioned heteroduplexes. *Hum. Mutat*. 21, 112-115 (2003).

24- Verhoef, S., Bakker, L., Tempelaars, A.M., Hesseling-Janssen, A.L., Mazurczak, T., Jozwiak, S., Fois, A., Bartalini, G., Zonnenberg, B.A., van Essen, A.J., Lindhout, D., Halley, D.J., van den Ouweland, A.M. High rate of mosaicism in tuberous sclerosis complex. *Am. J. Hum. Genet*. 64, 1362-1367 (1999).

25- Kwiatkowska, J., Wigowska-Sowinska, J., Napierala, D., Slomski, R., Kwiatkowski, D.J. Mosaicism in tuberous sclerosis as a potential cause of the failure of molecular diagnosis. *N. Engl. J. Med*. 340, 703-707 (1999).

26- Yates, J. R., van Bakel, I., Sepp, T., Payne, S.J., Webb, D.W., Nevin, N.C., Green, A.J. Female germline mosaicism in tuberous sclerosis confirmed by molecular genetic analysis. *Hum. Mol. Genet*. 6, 2265-2269 (1997).

27- Rose, V.M., Au, K.S., Pollom, G., Roach, E.S., Prashner, H.R., Northrup, H. Germ-line mosaicism in tuberous sclerosis: how common? *Am. J. Hum. Genet*. 64, 986-992 (1999).

28- Dabora, S.L., Jozwiak, S., Franz, D.N., Roberts, P.S., Nieto, A., Chung, J., Choy, Y.S., Reeve, M.P., Thiele, E., Egelhoff, J.C., Kasprzyk-Obara, J., Domanska-Pakiela, D., Kwiatkowski, D.J. Mutational analysis in a cohort of 224 tuberous sclerosis patients indicates increased severity of TSC2, compared with TSC1, disease in multiple organs. *Am. J. Hum. Genet*. 68, 64-80 (2001).

29- Au, K.S. Williams, A.T., Roach, E.S., Batchelor, L., Sparagana, S.P., Delgado, M.R., Wheless, J.W., Baumgartner, J.E., Roa, B.B., Wilson, C.M., Smith-Knuppel, T.K., Cheung, M.Y., Whittemore, V.H., King, T.M., Northrup, H. Genotype/phenotype correlation in 325 individuals referred for a diagnosis of tuberous sclerosis complex in the United States. *Genet. Med*. 9, 88-100 (2007).

30- Sancak, O. Nellist, M., Goedbloed, M., Elfferich, P., Wouters, C., Maat-Kievit, A., Zonnenberg, B., Verhoef, S., Halley, D., van den Ouweland, A. Mutational analysis of the TSC1 and TSC2 genes in a diagnostic setting: genotype-phenotype correlations and comparison of diagnostic DNA techniques in tuberous sclerosis complex. *Eur. J. Hum. Genet*. 13, 731-741 (2005).

31- van Eeghen, A. M., Black, M. E., Pulsifer, M. B., Kwiatkowski, D. J. & Thiele, E. A. Genotype and cognitive phenotype of patients with tuberous sclerosis complex. *Eur. J. Hum. Genet.* 20, 510–515 (2012).

32- van Eeghen, A. M., Nellist, M., van Eeghen, E. E., Thiele, E. A. Central *TSC2* missense mutations are associated with a reduced risk of infantile spasms. *Epilepsy Res.* 103, 83–87 (2013).

33- Wong, H. T. McCartney, D.L., Lewis, J.C., Sampson, J.R., Howe, C.J., de Vries, P.J. Intellectual ability in tuberous sclerosis complex correlates with predicted effects of mutations on TSC1 and TSC2 proteins. *J. Med. Genet.* 52, 815–822 (2015).

34- Switon, K., Kotulska, K., Janusz-Kaminska, A., Zmorzynska, J., Jaworski, J., Tuberous sclerosis complex: From molecular biology to novel therapeutic approaches. *IUBMB Life*. 68, 955–962 (2016).

35- Henske, E. P., Józwiak, S., Kingswood, J. C., Sampson, J. R., Thiele, E. A. Tuberous sclerosis complex. Nat. Rev. Dis. Primers 2, 16035. (2016).

36- O' Callaghan, F.J., Shiell, A.W., Osborne, J.P., Martyn, C.N. Prevalence of tuberous sclerosis estimated by capture-recapture analysis. *Lancet*. 351,490. (1998).

37- Schwartz, R. A., Fernandez, G., Kotulska, K., Józwiak, S. Tuberous sclerosis complex: advances in diagnosis, genetics, and management. *J. Am. Acad. Dermatol.* 57, 189–202 (2007).

38- Northrup, H., Krueger, D. A. & International Tuberous Sclerosis Complex Consensus Group. Tuberous sclerosis complex diagnostic criteria update: recommendations of the 2012

International Tuberous Sclerosis Complex Consensus Conference. *Pediatr. Neurol.* 49, 243–254 (2013).

39- Holmes, G. L., Stafstrom, C. E. & Tuberous Sclerosis Study Goup. Tuberous sclerosis complex and epilepsy: recent developments and future challenges. *Epilepsia.* 48, 617–630 (2007).

40- Kotulska, K., Jurkiewicz, E., Domańska-Pakieła, D., Grajkowska, W., Mandera M., Borkowska, J., Jóźwiak S. Epilepsy in newborns with tuberous sclerosis complex. *Eur. J. Paediatr. Neurol.* 18, 714–721 (2014).

41- Józ´wiak, S., Kotulska, K. Prevention of epileptogenesis — a new goal for epilepsy therapy. *Pediatr. Neurol*. 51, 758–759 (2014).

42- Overwater, I. E., Bindels-de Heus, K., Rietman, A.B., Ten Hoopen, L.W., Vergouwe, Y., Moll, H.A., de Wit, M.C. Epilepsy in children with tuberous sclerosis complex: chance of remission and response to antiepileptic drugs. *Epilepsia.* 56, 1239–1245 (2015).

43- Chu-Shore, C. J., Major, P., Camposano, S., Muzykewicz, D., Thiele, E. A. The natural history of epilepsy in tuberous sclerosis complex. *Epilepsia*. 51, 1236–1241 (2010).

44- Curatolo, P. Jóźwiak, S., Nabbout, R. TSC Consensus Meeting for SEGA and Epilepsy Management. Management of epilepsy associated with tuberous sclerosis complex (TSC): clinical recommendations. *Eur. J. Paediatr. Neurol.* 16, 582–586 (2012).

45- Rogawski, M. A., Loscher, W. The neurobiology of antiepileptic drugs. *Nat. Rev. Neurosci*. 5, 553–564 (2004).

46- Kotulska, K., Chmielewski, D., Borkowska, J., Jurkiewicz, E., Kuczyński, D., Kmieć, T., Łojszczyk, B., Dunin-Wąsowicz, D., Jóźwiak, S. Long-term effect of everolimus on epilepsy and growth in children under 3 years of age treated for subependymal giant cell astrocytoma associated with tuberous sclerosis complex. *Eur. J. Paediatr. Neurol*. 17, 479–485 (2013).

47- Perek-Polnik, M., Józ´wiak, S., Jurkiewicz, E., Perek, D. & Kotulska, K. Effective everolimus treatment of inoperable, life-threatening subependymal giant cell astrocytoma and intractable epilepsy in a patient with tuberous sclerosis complex. *Eur. J. Paediatr. Neurol*. 16, 83–85 (2012).

48- Kossoff, E. H., Thiele, E. A., Pfeifer, H. H., McGrogan, J. R., Freeman, J. M. Tuberous sclerosis complex and the ketogenic diet. *Epilepsia*. 46, 1684–1686 (2005).

49- Larson, A. M., Pfeifer, H. H., Thiele, E. A. Low glycemic index treatment for epilepsy in tuberous sclerosis complex. *Epilepsy Res*. 99, 180–182 (2012).

50- Parain, D., Penniello, M.J., Berquen, P., Delangre, T., Billard, C., Murphy JV. Vagal nerve stimulation in tuberous sclerosis complex patients. *Pediatr. Neurol*. 25, 213–216 (2001).

51- Liang, S. Li, A., Zhao, M., Jiang, H., Yu, S., Meng, X., Sun, Y. Epilepsy surgery in tuberous sclerosis complex: emphasis on surgical candidate and neuropsychology. *Epilepsia* 51, 2316–2321 (2010).

52- Kotulska, K., Borkowska, J., Mandera, M., Roszkowski, M., Jurkiewicz, E., Grajkowska, W., Bilska, M., Jóźwiak, S. Congenital subependymal giant cell astrocytomas in patients with tuberous sclerosis complex. *Childs Nerv. Syst*. 30, 2037–2042 (2014).

53- Franz, D. N., Belousova, E., Sparagana, S., Bebin, E.M., Frost, M., Kuperman, R., Witt, O., Kohrman, M.H., Flamini, J.R., Wu, J.Y., Curatolo, P., de Vries, P.J., Whittemore, V.H., Thiele, E.A., Ford, J.P., Shah, G., Cauwel, H., Lebwohl. D., Sahmoud, T., Jozwiak, S. Efficacy and safety of everolimus for subependymal giant cell astrocytomas associated with tuberous sclerosis complex (EXIST-1): a multicentre, randomised, placebo-controlled Phase 3 trial. *Lancet.* 381, 125–132 (2013).

54- de Vries, P. J., Whittemore, V.H., Leclezio, L., Byars, A.W., Dunn, D., Ess, K.C., Hook, D., King, B.H., Sahin, M., Jansen, A. Tuberous sclerosis associated neuropsychiatric disorders (TAND) and the TAND Checklist. *Pediatr. Neurol*. 52, 25–35 (2015).

55- Numis, A. L., Major, P., Montenegro, M.A., Muzykewicz, D.A., Pulsifer, M.B., Thiele EA. Identification of risk factors for autism spectrum disorders in tuberous sclerosis complex. *Neurology*. 76, 981–987 (2011).

56- Cudzilo, C. J., Szczesniak, R.D., Brody, A.S.,Rattan, M.S., Krueger, D.A., Bissler, J.J., Franz, D.N., McCormack, F.X., Young, L.R.. Lymphangioleiomyomatosis screening in women with tuberous sclerosis. *Chest* 144, 578–585 (2013).

57- Aubry, M. C., Myers, J.L., Ryu, J.H., Henske, E.P., Logginidou, H., Jalal S.M., Tazelaar, H.D.. Pulmonary lymphangioleiomyomatosis in a man. *Am. J. Respir. Crit. Care Med*. 162, 749–752 (2000).

58- McCormack, F. X., Inoue, Y., Moss, J., Singer, L.G., Strange, C., Nakata, K, Barker, A.F., Chapman, J.T., Brantly, M.L., Stocks, J.M., Brown, K.K., Lynch, JP. 3rd, Goldberg, H.J., Young, L.R., Kinder, B.W., Downey, G.P., Sullivan, E.J., Colby, T.V., McKay, R.T., Cohen, M.M., Korbee, L., Taveira-DaSilva, A.M., Lee, H.S., Krischer, J.P., Trapnell C. National Institutes of Health Rare Lung Diseases Consortium. MILES Trial Group. Efficacy and safety of sirolimus in lymphangioleiomyomatosis. *N. Engl. J. Med*. 364, 1595–1606 (2011).

59- Muzykewicz, D. A., Sharma, A., Muse, V., Numis, A.L., Rajagopal, J., Thiele, E.A. TSC1 and TSC2 mutations in patients with lymphangioleiomyomatosis and tuberous sclerosis complex. *J. Med. Genet*. 46, 465–468 (2009).

60- Bjornsson, J., Short, M. P., Kwiatkowski, D. J., Henske, E. P. Tuberous sclerosis-associated renal cell carcinoma. Clinical, pathological, and genetic features. *Am. J. Pathol*. 149, 1201–1208 (1996).

61- Bissler, J.J., McCormack, F.X., Young, L.R., Elwing, J.M., Chuck, G., Leonard, J.M., Schmithorst, V.J., Laor, T., Brody, A.S., Bean, J., Salisbury, S., Franz, D.N. Sirolimus for angiomyolipoma in tuberous sclerosis complex or lymphangioleiomyomatosis. *N. Engl. J. Med*. 358, 140-145 (2008).

62- Bernstein, J., Robbins, T. O. Renal involvement in tuberous sclerosis. *Ann. NY Acad. Sci.* 615, 36–49 (1991).

63- Dixon, B. P., Hulbert, J. C., Bissler, J. J. Tuberous sclerosis complex renal disease. *Nephron Exp. Nephrol*. 118, e15–e20 (2011).

64- Bissler, J. J., Kingswood, J. C. Renal angiomyolipomata. *Kidney Int*. 66, 924–934 (2004).

65-Rakowski, S. K., Winterkorn, E.B., Paul, E., Steele, D.J., Halpern, E.F., Thiele, E.A.. Renal manifestations of tuberous sclerosis complex: incidence, prognosis, and predictive factors. *Kidney Int*. 70, 1777–1782 (2006).

66- Guo, J., Tretiakova, M.S., Troxell, M.L., Osunkoya, A.O., Fadare, O., Sangoi, A.R., Shen S.S., Lopez-Beltran, A., Mehra, R., Heider, A., Higgins, J.P., Harik, L.R., Leroy, X., Gill, A.J., Trpkov, K., Campbell, S.C., Przybycin, C., Magi-Galluzzi, C., McKenney JK.. Tuberous sclerosis-associated renal cell carcinoma: a clinicopathologic study of 57 separate carcinomas in 18 patients. *Am. J. Surg. Pathol*. 38, 1457–1467 (2014).

67- De Waele, L., Lagae, L., Mekahli, D. Tuberous sclerosis complex: the past and the future. *Pediatr. Nephrol*. 30, 1771–1780 (2015).

68- Bhatt, J.R., Richard, P.O., Kim, N.S., Finelli, A., Manickavachagam, K., Legere, L., Evans, A., Pei, Y., Sykes, J., Jhaveri, K., Jewett, M.A.Natural history of renal angiomyolipoma (AML): most patients with large AMLs >4 cm can be offered active surveillance as an initial management strategy. *Eur Urol*. 70, 85–90 (2016).

69- Kingswood, J. C., Jozwiak, S., Belousova, E.D., Frost, M.D., Kuperman, R.A., Bebin, E.M., Korf, B.R., Flamini, J.R., Kohrman, M.H., Sparagana, S.P., Wu, J.Y., Brechenmacher, T., Stein, K., Berkowitz, N., Bissler, J.J., Franz DN. The effect of everolimus on renal angiomyolipoma in patients with tuberous sclerosis complex being treated for subependymal giant cell astrocytoma: subgroup results from the randomized, placebo-controlled, Phase 3 trial EXIST-1. *Nephrol. Dial. Transplant*. 29, 1203–1210 (2014).

70- Franz, D. N., Belousova, E., Sparagana, S., Bebin, E.M., Frost, M., Kuperman, R., Witt, O., Kohrman, M.H., Flamini, J.R., Wu, J.Y., Curatolo, P., de Vries, P.J., Berkowitz, N., Anak, O., Niolat, J., Jozwiak, S. Everolimus for subependymal giant cell astrocytoma in patients with tuberous sclerosis complex: 2-year open-label extension of the randomised EXIST-1 study. *Lancet Oncol*. 15, 1513–1520 (2014).

71- Teng, J. M., Cowen, E.W., Wataya-Kaneda, M., Gosnell, E.S., Witman, P.M., Hebert, A.A., Mlynarczyk, G., Soltani, K., Darling, T.N. Dermatologic and dental aspects of the 2012 International Tuberous Sclerosis Complex Consensus Statements. *JAMA Dermatol*. 150, 1095–1101 (2014).

72- Tyburczy, M. E., Wang, J.A., Li, S., Thangapazham, R., Chekaluk, Y., Moss, J., Kwiatkowski, D.J., Darling, T.N. Sun exposure causes somatic second-hit mutations and angiofibroma development in tuberous sclerosis complex. *Hum. Mol. Genet*. 23, 2023–2029 (2014).

73- DeKlotz, C. M., Ogram, A. E., Singh, S., Dronavalli, S., MacGregor, J. L. Dramatic improvement of facial angiofibromas in tuberous sclerosis with topical rapamycin: optimizing a treatment protocol. *Arch. Dermatol*. 147, 1116–1117 (2011).

74- Tanaka, M., Wataya-Kaneda, M., Nakamura, A., Matsumoto, S. Katayama, I. First left-right comparative study of topical rapamycin versus vehicle for facial angiofibromas in patients with tuberous sclerosis complex. *Br. J. Dermatol*. 169, 1314–1318 (2013).

75- Nathan, N., Wang, J,A., Li, S., Cowen, E.W., Haughey, M., Moss. J., Darling, T.N. Improvement of tuberous sclerosis complex (TSC) skin tumors during long-term treatment with oral sirolimus. *J. Am. Acad. Dermatol*. 73, 802–808 (2015).

76- Rowley, S.A., O' Callaghan, F.J., Osborne J.P. Ophtalmic manifestations of tuberous sclerosis: a population based study. *Br. J. Opthalmol*. 85, 420-423 (2001).

77- Mencia-Gutierrez, E. Eyelid and cutaneous lesions as the sole indicators of tuberous sclerosis. *Arch. Soc. Esp. Oftalmol*. 79, 401-404 (2004).

78- Nyboer, J.H, Robertson, D.M., Gomez, M.R. Retinal lesions in tuberous sclerosis. *Arch. Ophtalmol*. 94, 1277-1280 (1976).

79- Rosser, T., Panigrahy, A., Mc Clintock, W. The diverse clinical manifestations of tuberous sclerosis complex: a review. *Semin. Pediatr. Neurol*. 13, 27-36 (2006).

80- Franz, D.N. Non-neurologic manifestations of tuberous sclerosis complex. *J. Child. Neurol*. 19, 690-698 (2004).

81- Ibrahim, C.P.H., Thakker, P., Miller, P.A., Barron, D. Cardiac rhabdomyomas presenting as left ventricular outflow tract obstruction in a neonate. *Interact. Cardiovasc. Thorac. Surg*. 2, 572-574 (2003).

82-Tworetzky, W., McElhinney, D.B., Margossian, R., Moon-Grady, A.J., Sallee, D., Goldmuntz, E., Van Der Velde, M.E., Silverman, N.H., Allan, L.D. Association between cardiac tumors and tuberous sclerosis in the fetus and neonate. *Am. J. Cardiol*. 92, 487-489 (2003).

83- Vezina, C., Kudelski, A., Sehgal, S.N. Rapamycin (AY-22,989), a new antifungal antibiotic.I. Taxonomy of the producing streptomycete and isolation of the active principle. *J. Antibiot. (Tokio)*. 28, 721-726 (1975).

84- Loewith, R., Jacinto, E., Wullschleger, S., Lorberg, A., Crespo, J.L., Bonenfant, D., Oppliger, W., Jenoe, P., Hall, M.N. Two TOR complexes, only one of which is rapamycin sensitive, have distinct role in cell growth control. *Mol. Cell*. 10, 475-468 (2002).

85- Sarbassov, D.D., Ali, S.M., Sengupta, S., Sheen, J.H., Hsu, P.P., Bagley, A.F., Markhard, A.L., Sabatini, D.M. Prolonged Rapamycin treatment inhibits mTORC2 assembly and Akt/ PKB. *Mol. Cell*. 22, 159-168 (2006).

86- Kay, J.E., Kromwel, L., Doe, S.E., Denyer, M. Inhibition of T and B lymphocyte proliferation by Rapamycin. *Immunology*. 72, 544-549 (1991).

87- Price, D.J., Grove, J.R., Calvo, V., Avruch, J., Bierer, B.E. Rapamycin-induced inhibition of the 70-Kilodalton S6 protein kinase. *Science*. 257, 973-977 (1992).

88- Chung, J., Kuo, C.J., Crabtree, G.R., Blenis J. Rapamycin-FKBP specifically blocks growth-dependent activation of and signaling by the 70 KD S6 protein kinases. *Cell*. 69, 1227-1337 (1992).

89- Beretta, L., Gingras, A.C., Svitkin, Y.V., Hall, M.N., Sonenberg, N. Rapamycin blocks the phosphorylation of 4E-BP1 and inhibits cap-dependent initiation of translation. *Embo J*. 15, 658-664 (1996).

90- Burnett, P.E., Barrow, R.K., Cohen, N.A., Snyder, S.H., Sabatini D.M. RAFT1 phosphorylation of the translational regulators p70 S6 Kinase and 4E-BP1. *Proc. Natl. Acad. Sci. USA*. 96, 1432-1437 (1998).

91- Holz, M.K., Ballif, B.A., Gygi, S.P., Blenis, J. mTOR and S6K1 mediate assembly of the translation preinitiation complex through dynamic protein interchange and ordered phosphorylation events. *Cell*. 123, 569-580 (2005).

92- Gingras, A.C., Raught, B., Gygi, S.P., Niedzwiecka, A, Miron, M., Burley, S.K., Polakiewicz, R.D., Wyslouch-Cieszynska, A., Aebersold, R., Sonenberg, N. Hierarchical phosphorylation of the translation inhibitor 4E-BP1. *Genes Dev*. 15, 2852-2864 (2001).

93- Richter, J.D., Sonenberg, N. Regulation of cap-dependent translation by eIF4E inhibitory proteins. *Nature*. 433, 477-480 (2005).

94- Schalm, S.S., Fingar, D.C., Sabatini, D.M., Blenis, J. TOS motif-mediated raptor binding regulates 4E-BP1 multisite phosphorylation and function. *Curr. Biol*. 13, 797-806 (2003).

95- Gao, X., Zhang, Y., Arrazola, P., Hino, O., Kobayashi, T., Yeung, R.S., Ru, B., Pan, D. Tsc tumor suppressor protein antagonize amino acid-TOR signaling. *Nat. Cell. Biol*. 4, 699-704 (2002).

96- Jaeschke, A., Hartkamp, J., Saitoh, M., Roworth, W., Nobukuni, T., Hodges, A., Sampson, J., Thomas, G., Lamb, R. Tuberous sclerosis complex tumor suppressor-mediated S6 Kinase inhibition by phosphatidylinositide-3- OH kinase is mTOR independent. *J. Cell. Biol*. 159, 217-224 (2002).

97- Manning, B.D., Cantley, L.C. Rheb fills a GAP between TSC and TOR. *Trends Biochem. Sci.* 28, 573-576 (2003).

98- Tee, A.R., Manning, B.D., Roux, P.P., Cantley, L.C., Blenis, J. Tuberous sclerosis complex gene products, tuberin and hamartin, control mTOR signaling by acting as a GTPase-activating protein complex toward Rheb. *Curr. Biol*. 13, 1259-1268 (2003).

99- Huang, J., Dibble, C.C., Matsuzaki, M., Manning, B.D. The TSC1-TSC2 complex is required for proper activation of mTOR complex 2. *Mol. Cell. Biol*. 28, 4104- 4115 (2008).

100- Ma, L., Chen, Z., Erdjument-Bromage, H., Tempst, P., Pandolfi, P.P. Phosphorylation and functional inactivation of *TSC2* by Erk implications for tuberous sclerosis and cancer pathogenesis. *Cell*. 121, 179-193 (2005).

101- Gwinn, D.M., Shackelford, D.B., Egan, D.F., Mihaylova, M.M., Mery, A., Vasquez, D.S., Turk, B.E., Shaw, R.J. AMPK phosphorylation of raptor mediates a metabolic checkpoint. *Mol. Cell*. 30, 214-226 (2008).

102- Liu, L., Cash, T.P., Jones, R.G., Keith, B., Thompson, C.B., Simon, M.C. Hypoxia-induced energy stress regulates mRNA translation and cell growth. *Mol. Cell*. 21, 521-531 (2006).

103- Sancak, Y., Peterson, T.R., Shaul, Y.D., Lindquist, R.A., Thoreen, C.C., Bar-Peled, L., Sabatini, D.M. The Rag GTPases bind raptor and mediate amino acid signaling to mTORC1. *Science*. 320, 1496-1501 (2008).

104- Kim, E., Goraksha-Hicks, P., Li, L., Neufeld, T.P., Guan, K.L. Regulation of TORC1 by Rag GTPases in nutrient response. *Nat Cell Biol*. 10, 935-945 (2008).

105- Goncharova, E. A., Goncharov, D. A., Damera, G., Tliba, O., Amrani, Y., Panettieri, R. A., Krymskaya, V. P. Signal transducer and activator of transcription 3 is required for abnormal proliferation and survival of TSC2-deficient cells: relevance to pulmonary lymphangioleiomyomatosis. *Mol. Pharmacol*. 76, 766-777 (2009).

106- Bakan, I., Laplante, M. Connecting mTORC1 signaling to SREBP-1 activation. *Curr. Opin. Lipidol*. 23, 226-234 (2012).

107- Duvel, K., Yecies, J. L., Menon, S., Raman, P., Lipovsky, A. I., Souza, A. L., Triantafellow, E., Ma, Q., Gorski, R., Cleaver, S., Vander Heiden, M.G., MacKeigan, J.P., Finan, P.M., Clish, C.B., Murphy, L.O., Manning, B.D. Activation of a metabolic gene regulatory network downstream of mTOR complex 1. *Mol. Cell*. 39, 171-183 (2010).

108- Kim, J.E., Chen, J. Regulation of peroxisome proliferator-activated receptor-gamma activity by mammalian target of rapamycin and amino acids in adipogenesis. *Diabetes*. 53, 2748–2756 (2004).

109- Hudson, C.C., Liu, M., Chiang, G.G., Otterness, D. M., Loomis, D. C., Kaper, F., Giaccia, A. J., Abraham, R. T. Regulation of hypoxia-inducible factor 1alpha expression and function by the mammalian target of rapamycin. *Mol. Cell. Biol*. 22, 7004-7014 (2002).

110- Cunningham, J. T., Rodgers, J. T., Arlow, D. H., Vazquez, F., Mootha, V. K., Puigserver, P. mTOR controls mitochondrial oxidative function through a YY1-PGC-1alpha transcriptional complex. *Nature.* 450, 736-740 (2007).

111- Roczniak-Ferguson, A., Petit, C. S., Froehlich, F., Qian, S., Ky, J., Angarola, B., Walther, T. C., Ferguson, S. M. The transcription factor TFEB links mTORC1 signaling to transcriptional control of lysosome homeostasis. *Sci. Signal*. 5(228): ra42 (2012).

112- Settembre, C., Di Malta, C., Polito, V. A., Garcia Arencibia, M., Vetrini, F., Erdin, S., Erdin, S. U., Huynh, T., Medina, D., Colella, P. et al. TFEB links autophagy to lysosomal biogenesis. *Science* 332, 1429-1433 (2011).

113- Mayer, C., Zhao, J., Yuan, X., Grummt, I. mTOR-dependent activation of the transcription factor TIF-IA links rRNA synthesis to nutrient availability. *Genes Dev*. 18, 423-434 (2004).

114- Shor, B., Wu, J., Shakey, Q., Toral-Barza, L., Shi, C., Follettie, M., Yu, K. Requirement of the mTOR kinase for the regulation of Maf1 phosphorylation and control of RNA polymerase III-dependent transcription in cancer cells. *J. Biol. Chem*. 285, 15380-15392 (2010).

115- Sarbassov, D.D., Ali, S.M., Kim, D.H., Guertin, D.A., Latek, R.R., Erdjument-Bromage, H., Tempst, P., Sabatini, D.M. Rictor, a novel binding partner of mTOR, defines a rapamycin-insensitive and raptor- independent pathway that regulates the cytoskeleton. *Curr. Biol*. 14, 1296-1302 (2004).

116- Jacinto, E., Loewith, R., Schmidt, A., Lin, S., Ruegg, M.A., Hall, A., Hall, M.N. Mammalian TOR complex 2 controls the actin cytoskeleton and is rapamycin insensitive. *Nat. Cell Biol*. 6, 1122- 1128 (2004).

117- Guertin, D.A., Stevens, D.M., Thoreen, C.C., Burds, A.A., Kalaany, N.Y., Moffat, J., Brown, M., Fitzgerald, K.J., Sabatini, D.M. Ablation in mice of the mTORC components raptor, rictor, or mLST8 reveals that mTORC2 is required for signaling to Akt-FOXO and PKCalpha, but not S6K1. *Dev. Cell*. 11, 859-871 (2006).

118- Huang, J., Manning, B.D. A complex interplay between Akt, TSC2, and the two mTOR complexes. *Biochemical Society Transactions*. *37*, 217–222 (2009).

119- Manning, B.D., Logsdon, M.N., Lipovsky, A.I., Abbott, D., Kwiatkowski, D.J., Cantley, L.C. Feedback inhibition of Akt signaling limits the growths of tumors lacking TSC2. *Genes. Dev*. 19, 1773-1778 (2005).

120- Charles J.F., Aliprantis A.O. Osteoclasts: More than 'bone eaters'. *Trend Mol Med.* 20, 449–459 (2014).

121- Sims, N.A., Martin, T.J. Coupling the activities of bone formation and resorption: a multitude of signals within the basic multicellular unit. *Bonekey Rep*. 3, 481 (2014).

122- Teti, A. Mechanisms of osteoclast-dependent bone formation. *Bonekey Rep*. 2, 449 (2013).

123- Boyle, W.J., Simonet, W.S., Lacey, D.L. Osteoclast differentiation and activation. *Nature*. 423, 337–342 (2003).

124- Lacey, D.L., Boyle, W.J., Simonet, W.S., Kostenuik, P.J., Dougall, W.C., Sullivan, J.K., San Martin, J., Dansey, R. Bench to bedside: elucidation of the OPG– RANK–RANKL pathway and the development of denosumab. *Nat. Rev. Drug Discov*. 11, 401–419 (2012).

125- Boyce, B.F. Advances in the regulation of osteoclasts and osteoclast functions. *J. Dent. Res*. 92, 860–867 (2013).

126- Baron, R., Kneissel, M. WNT signaling in bone homeostasis and disease: from human mutations to treatments. *Nat. Med*. 19, 179– 192 (2013).

127-Tawfeek, H. Bedi, B., Li, J.Y., Adams, J., Kobayashi, T., Weitzmann, M.N., Kronenberg, H.M., Pacifici R. Disruption of PTH receptor 1 in T cells protects against PTH-induced bone loss. *PLoS ONE* 5, e12290 (2010).

128- Henriksen, K., Bollerslev, J., Everts, V., Karsdal, M.A. Osteoclast activity and subtypes as a function of physiology and pathology implications for future treatments of osteoporosis. *Endocr. Rev*. 32, 31–63 (2011).

129- Everts, V. de Vries, T.J., Helfrich, M.H. Osteoclast heterogeneity: lessons from osteopetrosis and inflammatory conditions. *Biochim. Biophys. Acta* 1792, 757–765 (2009).

130- Tang, Y. Wu, X., Lei, W., Pang, L., Wan, C., Shi, Z., Zhao, L., Nagy, T.R., Peng, X., Hu, J., Feng, X., Van Hul, W., Wan, M., Cao, X. TGF-beta1-induced migration of bone mesenchymal stem cells couples bone resorption with formation. *Nat. Med*. 15, 757–765 (2009).

131- Xian, L. Wu, X., Pang, L., Lou, M., Rosen, C.J., Qiu, T., Crane, J., Frassica, F., Zhang, L., Rodriguez, J.P., Xiaofeng, J., Shoshana, Y., Shouhong, X., Argiris, E., Mei W., Xu C. Matrix IGF-1 maintains bone mass by activation of mTOR in mesenchymal stem cells. *Nat. Med*. 18, 1095–1101 (2012).

132- Karsdal, M.A. Martin, T.J., Bollerslev, J., Christiansen, C., Henriksen, K. Are nonresorbing osteoclasts sources of bone anabolic activity? *J. Bone Mineral Res*. 22, 487–494 (2007).

133- Pennypacker, B., Shea, M., Liu, Q., Masarachia, P., Saftig, P., Rodan, S., Rodan, G., Kimmel, D. Bone density, strength, and formation in adult cathepsin K/ mice. *Bone* 44, 199–207 (2009).

134- Li, C.Y. Jepsen, K.J., Majeska, R.J., Zhang, J., Ni, R., Gelb, B.D., Schaffler, M.B. Mice lacking cathepsin K maintain bone remodeling but develop bone fragility despite high bone mass. *J. Bone Miner. Res*. 21, 865–875 (2006).

135- Takeshita, S. Fumoto, T., Matsuoka, K., Park, K.A., Aburatani, H., Kato, S., Ito, M., Ikeda, K. Osteoclast-secreted CTHRC1 in the coupling of bone resorption to formation. *J. Clin. Invest*. 123, 3914– 3924 (2013).

136- Matsuoka, K. Park, K.A., Ito, M., Ikeda, K., Takeshita, S. Osteoclast-derived complement component 3a stimulates osteoblast differentiation. *J. Bone Miner. Res*. 29, 1522-1530 (2014).

137- Ryu, J. Kim, H.J., Chang, E.J., Huang, H., Banno, Y., Kim, H.H. Sphingosine 1-phosphate as a regulator of osteoclast differentiation and osteoclast-osteoblast coupling. *EMBO J*. 25, 5840–5851 (2006).

138- Lotinun, S. Kiviranta, R., Matsubara, T., Alzate, J.A., Neff, L., Lüth, A., Koskivirta, I., Kleuser, B., Vacher, J., Vuorio, E., Horne, W.C., Baron, R.. Osteoclast-specific cathepsin K deletion stimulates S1P-dependent bone formation. *J. Clin. Invest*. 123, 666–681 (2013).

139- Xian, L, Wu, X, Pang, L, Lou, M., Rosen, C.J., Qiu, T., Crane, J., Frassica, F., Zhang, L., Rodriguez, J.P., Xiaofeng, J., Shoshana, Y., Shouhong, X., Argiris, E., Mei, W., Xu, C. Matrix IGF-1 regulates bone mass by activation of mTOR in mesenchymal stem cells. *Nature medicine*. 18, 1095-1101 (2012).

140- Isomoto, S., Hattori, K., Ohgushi, H., Nakajima, H., Tanaka, Y., Takakura, Y. Rapamycin as an inhibitor of osteogenic differentiation in bone marrow-derived mesenchymal stem cells. *J Orthop Sci*. 12, 83-88 (2007).

141- Faghihi, F., Baghaban Eslaminejad, M., Nekookar, A., Najar, M., Salekdeh, G.H. The effect of purmorphamine and sirolimus on osteogenic differentiation of human bone marrow-derived mesenchymal stem cells. *Biomedicine & Pharmacotherapy*. 67, 31-38 (2013).

142- Singha, U. K., Jiang, Y., Yu, S., Luo, M., Lu, Y., Zhang, J., Xiao, G. Rapamycin inhibits osteoblast proliferation and differentiation in MC3T3-E1 cells and primary mouse bone marrow stromal cells. *J. Cell. Biochem*. 103, 434–446 (2008).

143- Chen J, Tu X, Esen E, Joeng KS, Lin C, Arbeit JM, Rüegg, M.A., Hall, M.N., Ma, L., Long, F. WNT7B Promotes Bone Formation in part through mTORC1. *PLoS Genet.* 10, e1004145 (2014).

144- Martin, S. K., Fitter, S., Bong, L. F., Drew, J. J., Gronthos, S., Shepherd, P. R., Zannettino, A. C. NVP-BEZ235, a dual pan class I PI3 kinase and mTOR inhibitor, promotes osteogenic differentiation in human mesenchymal stromal cells. *J Bone Miner Res*. 25, 2126–2137 (2010).

145- Huang, B., Wang, Y., Wang, W., Chen, J., Lai, P., Liu, Z., Yan, B., Xu, S., Zhang, Z., Zeng, C., Rong, L., Liu, B., Cai, D., Jin, D., Bai, X. mTORC1 Prevents Preosteoblast Differentiation through the Notch Signaling Pathway. *PLoS Genetics*.11, e1005426 (2015).

146- Chen, J, Long, F. mTORC1 Signaling Promotes Osteoblast Differentiation from Preosteoblasts. *PLoS ONE* 10, e0130627 (2015).

147- Shoba, L. N. N., Lee, J. C. Inhibition of Phosphatidylinositol 3-Kinase and p70S6 Kinase Blocks Osteogenic Protein-1 Induction of Alkaline Phosphatase Activity in Fetal Rat Calvaria Cells. *J. Cell. Biochem*. 88, 1247–1255 (2003).

148- Yeh, L.C., Ma, X., Ford, J. J., Adamo, M. L. Lee, J. C., Rapamycin inhibits BMP-7-induced osteogenic and lipogenic marker expressions in fetal rat calvarial cells. *J. Cell. Biochem*. 114, 1760–1771 (2013).

149- Chen, C., Akiyama, K., Wang, D., Xu, X., Li, B., Moshaverinia, A., Brombacher, F., Sun, L., Shi S. mTOR inhibition rescues osteopenia in mice with systemic sclerosis. *The Journal of Experimental Medicine*. 212, 73-91 (2015).

150- Lee, KW., Yook, JY. , Son M-Y., Kim,MJ., Koo, DB., Han, YM., Cho, YS. Rapamycin Promotes the Osteoblastic Differentiation of Human Embryonic Stem Cells by Blocking the mTOR Pathway and Stimulating the BMP/Smad Pathway**.** *Stem Cells and Development*. 19, 557-568 (2010).

151- Joffe, I., Katz, I., Sehgal, S., Bex, F., Kharode, Y., Tamasi, J., Epstein, S. Lack of Change of Cancellous Bone Volume with Short-Term Use of the New Immunosuppressant Rapamycin in Rats. *Calcif Tissue Int*. 53, 45-52 (1993).

152- Romero, D. F., Buchinsky, F. J., Rucinski, B., Cvetkovic, M., Bryer, H. P., Liang, X. G., Ma, Y. F., Jee, W. S. S., Epstein, S. Rapamycin: A bone sparing immunosuppressant? *J Bone Miner Res*. 10, 760–768 (1995).

153- Peyman Hadjia, P., Coleman, R., Gnantd, M. Bone effects of mammalian target of rapamycin (mTOR) inhibition with everolimus. *Critical Reviews in Oncology/Hematology*. 87, 101–111 (2013).

154- Sen, B., Xie, Z., Case, N., Thompson, W. R., Uzer, G., Styner, M., Rubin, J. mTORC2 Regulates Mechanically Induced Cytoskeletal Reorganization and Lineage Selection in Marrow-Derived Mesenchymal Stem Cells. *J Bone Miner Res*. 29, 78–89 (2014).

155- Chen, J., Holguin, N., Shi, Y., Silva, M. J., Long, F. mTORC2 Signaling Promotes Skeletal Growth and Bone Formation in Mice. *J Bone Miner Res*. 30, 369–378 (2015).

156- Esen, E., Chen, J., Karner, C.M., Okunade, A.L., Patterson, B.W., Long F. WNT-LRP5 Signaling Induces Warburg Effect through mTORC2 Activation during Osteoblast Differentiation. *Cell Metab*. 17, 745–755 (2013).

157- Kneissel, M., Luong-Nguyen, N.H., Baptist, M., Cortesi, R., Zumstein.Mecker, S., Kossida, S., O'Reilly, T., Lane, H., Susa, M. Everolimus suppresses cancellous bone loss, bone resorption, and cathepsin K expression by osteoclasts. *Bone*. 35, 1144–1156 (2004).

158- Indo, Y., Takeshita, S., Ishii, K.-A., Hoshii, T., Aburatani, H., Hirao, A., Ikeda, K. Metabolic regulation of osteoclast differentiation and function. *J Bone Miner Res*. 28, 2392–2399 (2013).

159- Luo, D., Ren, H., Li, T., Lian, K., Lin, D. Rapamycin reduces severity of senile osteoporosis by activating osteocyte autophagy. *Osteoporos Int* 27, 1093 (2016).

160- Cejka, D., Hayer, S., Niederreiter, B., Sieghart, W., Fuereder, T., Zwerina, J., Schett, G. Mammalian target of rapamycin signaling is crucial for joint destruction in experimental arthritis and is activated in osteoclasts from patients with rheumatoid arthritis. *Arthritis Rheum* 62, 2294–2302 (2010).

161- Smink, J.J., Tunn, P.U., Leutz, A. Rapamycin inhibits osteoclast formation in giant cell tumor of bone through the C/EBPbeta - MafB axis. *J Mol Med.* 90, 25–30 (2012).

162- Westenfeld, R., Schlieper, G., Woltje, M., Gawlik, A., Brandenburg, V., Rutkowski, P., Floege, J., Jahnen-Dechent, W., Ketteler, M. Impact of sirolimus, tacrolimus and mycophenolate mofetil on osteoclastogenesis—implications for post-transplantation bone disease. *Nephrol Dial Transplant*. 26, 4115–4123 (2011).

163- Mogi, M., Kondo, A. Down-regulation of mTOR leads to up-regulation of osteoprotegerin in bone marrow cells. *Biochemical and Biophysical Research Communications.* 384, 82–86 (2009).

164- Niziolek, P.J., Murthy, S., Ellis, S.N., Sukhija, K.B., Hornberger, T.A., Turner, C.H. Robling, A.G. Rapamycin impairs trabecular bone acquisition from high-dose but not low-dose intermittent parathyroid hormone treatment. *J. Cell. Physiol*. 221, 579–585 (2009).

165- Riddle, R.C., Frey, J.L., Tomlinson, R.E., Ferron, M., Li, Y., DiGirolamo, D.J., Faugere, M.C. Hussain, M.A. Karsenty, G. Clemens, T.L. Tsc2 is a molecular checkpoint controlling osteoblast development and glucose homeostasis. *Mol Cell Biol*. 34, 1850–1862 (2014).

166- Fang, F., Sun, S., Wang, L., Guan, J.-L., Giovannini, M., Zhu, Y., Liu, F. Neural Crest-Specific TSC1 Deletion in Mice Leads to Sclerotic Craniofacial Bone Lesion. *J Bone Miner Res*. 30, 1195–1205 (2015).

167- Dickerson, W.W. Nature of Certain Osseous Lesions in Tuberous Sclerosis. *AMA Arch NeurPsych.* 73, 525-529 *(*1955).

168- Brooks, B., Lehman, E. P. Bone Changes in Recklinghausen's Neurofibromatosis. *Surg. Gynec. & Obst*. 38, 587-595 (1924).

169- Yakovlev, P.I., Corwin, W. A Roentgenographic Sign in Cases of Tuberous Sclerosis of Brain (Multiple "Brain Stones"). *Arch. Neurol. & Psychiat*. 42, 1030-1037 (1939).

170- Holt, J. F., Wright, E. M. Radiologic Features of Neurofibromatosis, *Radiology.* 51, 647-664 (1948).

171- Kveim, A. Uber Adenoma Sebaceum (Morbus Pringle), und seinen Platz im Neurokutanen Syndrom-v-tuberose Gehirnsklerose-und dessen Beziehung zur v. Recklinghausenschen Krankheit. *Acta dermatovenereol*. 18, 637-683 (1937).

172- Hall, G. S. Tuberose Sclerosis, Rheostosis and Neurofibromatosis. *Quart. J. Med*. 9, 1-10 (1940).

173- Bryan, W. L., Watters, T. A. Tuberous Sclerosis, with a Case Study. *New Orleans M. & S.J.* 94, 592-596 (1942).

174- Ackermann, A. J. Pulmonary and Osseous Manifestations of Tuberous Sclerosis, with Some Remarks on Their Pathogenesis. *Am. J. Roentgenol*. 51, 315-325 (1944).

175- Dalsgaard-Nielsen, T. Tuberous Sclerosis with Unusual Roentgen Picture. *Nord. med. Tidskr*. 10, 1541-1548 (1935).

176- Gottlieb, J. S., Lavine, G. R. Tuberous Sclerosis with Unusual Lesions of the Bones. *Arch. Neurol. & Psychiat*. 33, 379-388 (1935).

177- Holt, J.F., Dickerson, W.W. The osseous lesions of tuberous sclerosis. *Radiology*. 58, 1-8 (1952).

178- Berland, H. I. Roentgenological Findings in Tuberous Sclerosis. A. M. A. *Arch. Neurol. & Psychiat*. 69,669-683 (1953).

179- Roach, E.S., Gomez, M.R., Northrup, H.Tuberous sclerosis complex consensus conference: revised clinical diagnostic criteria. *J Child Neurol*. 13, 624–628 (1998).

180- Umeoka, S., Koyama, T., Miki, Y., Akai, M., Tsutsui, K., Togashi, K. Pictorial review of tuberous sclerosis in various organs. *Radiographics.* 28, e32 (2008).

181- Ajlan, A.J., Bilawich, AM., Müller, N.L. Thoracic Computed Tomographic Manifestations of Tuberous Sclerosis in Adults. *Canadian Association of Radiologists Journal*. 63, 61-68 (2012).

182- Timothy, A. Bernauer Ginat, W. Mirowski, K., Caldemeyer S., Tuberous sclerosis. Part II. Musculoskeletal and visceral findings, Journal of the American Academy of Dermatology. 45, 450-452 (2001).

183- Manoukian, S.B., Kowal, D.J. Comprehensive Imaging Manifestations of Tuberous Sclerosis. *American Journal of Roentgenology*. 204, 933-943 (2015).

184- Hoffmann, A. D. Imaging of Tuberous Sclerosis Lesions Outside of the Central Nervous System. *Annals of the New York Academy of Sciences*. 615, 94–111 (1991).

185- Avila, N.A., Dwyer A.J., Rabel. A., Darling. T., Hong, C.H., Moss, J. CT of Sclerotic Bone Lesions: Imaging Features Differentiating Tuberous Sclerosis Complex with Lymphangioleiomyomatosis from Sporadic Lymphangioleiomyomatosis. *Radiology*. 254, 851-857 (2010).

186- Ashby, D.W., Ramage D. Lesions of the vertebrae and innominate bones in tuberose sclerosis. *Br J Radiol*. 353, 274-7 (1957).

187- Amin, S., Slaney K, O'Callaghan FJ. Musculoskeletal involvement in tuberous sclerosis. *Arch Dis Child.* 0:1 (2016).

188-Dimsdale, H. Tuberose Sclerosis with Intracranial Calcification and Lesions of the Bone. *Proc R Soc Med*. 40, 81-2 (1946).

189- Rafal, R.B., Ndzengue, A., Jaffe, E.A. Tuberous Sclerosis: Computed Tomography Diagnosis. *The Journal of Emergency Medicine*. 44, 259-261 (2013).

190- Morris, BS., Garg, A. Jadhav PJ. Tuberous sclerosis: A presentation of less-commonly encountered stigmata. *Australasian Radiology.* 46, 426–430 (2002).

191- Arbelaez, A., Castillo, M. Skull fibrous plaque in a patient with tuberous sclerosis. *American Journal of Roentgenology*.172, 1456-1457 (1999).

192- Smith T.K., Gregersen, G.G., Samilson, R.L. Orthopaedic Problems Associated with Tuberous Sclerosis. *J Bone Joint Surg Am* Jan. 51, 97-102 (1969).

193- Stosic-Opincal, T., Peric, V., Lilic, G., Gavrilovic, S., Milakovic, B., Grujicic, D. Spine MRI Findings in a Patient with Tuberous Sclerosis: A case Report-Part II. *Spine*. 30, 992-993 (2005).

194- Rado', J.P., Haris, A. Metabolic Bone Disease (Anticonvulsant Osteomalacia) and Renal Tubular Acidosis in Tuberous Sclerosis. *Internal Medicine.* 32, 574-579 (1993).

195- Tashiro M., Hirose W., Hanabusa H., Takahashi T., Kanki H., Asaba Y., Hieda H., Sugi T., Tokura Y., Watanabe K., Kawagoe M. Pancytopenia in tuberous sclerosis. *Med Sci Monit.* 7, 444-7 (2001).

196- Song, L., Zhang, Y, Zhang, W. Bone scintigraphy may help differentiate bone sclerotic lesions from osteoblastic metastases in tuberous sclerosis patients with concomitant pulmonary adenocarcinoma. *Clin Imaging.* 37, 382–5 (2013).

197- Pui, M. H., Kong, H. L., Choo, H. F. Bone changes in tuberous sclerosis mimicking metastases. *Australasian Radiology*. 40, 77–79 (1996).

198- Jonard, P., Lonneux, M., Boland, B., Malghem, J., Jamar, F.O. Tc-99m HDP Bone Scan Showing Bone Changes in a Case of Tuberous Sclerosis or Bourneville's Disease. *Clinical Nuclear Medicine*. 26, 50-52 (2001).

199- Parida, GK**.,** Dhull, VS**.,** Karunanithi, S**.,** Arora, S**.,** Sharma, A**.,** Shamim, SA**.** Accurate Characterization of Skeletal Lesions in Tuberous Sclerosis Complex Using 99mTc M DPSPECT/CT. *Clin Nucl Med*. 40, e444-5 **(**2015).

200- Gallagher, A., Kovach, A., Stemmer-Rachamimov, A., Rosenberg AE., Eskandar E., Thiele, E.A. Metaplastic bone in a cortical tuber of a young patient with tuberous sclerosis complex. *Neurology*. 76, 1602-1604 (2011).

201- Boronat, S., Barber, I., Pargaonkar, V., Chang, J., Thiele, EA. Sclerotic bone lesions at abdominal magnetic resonance imaging in children with tuberous sclerosis complex. *Pediatr Radiol*. 46, 689–694 (2016).

202- Gasparetto, E.L., Neto, A.D.C., Bruck, I., Antoniuk S. Tuberous Sclerosis and Fibrous Dysplasia. *AJNR Am J Neuroradiol.* 24, 835–837 (2003).

203- Breningstall, G.N., Faerber, E.N., Kolanu, R. Fibrous dysplasia in a patient with tuberous sclerosis. *J Child Neurol*. 3, 131–134 (1988).

204- Li, P., Boronat, S., Geffrey, AL., Barber, I., Grottkau, BE., Thiele, EA. Rib and vertebral bone fibrous dysplasia in a child with tuberous sclerosis complex. *Am J Med Genet.* 167A, 2755–2757 (2015).

205- Onda, H., Lueck, A., Marks, P.W., Warren, H.B., Kwiatkowski D.J. Tsc2(+/-) mice develop tumors in multiple sites that express gelsolin and are influenced by genetic background. J Clin Invest. 104, 687–95 (1999).

206- Charles, J.F., Hsu, L-Y., Niemi, EC., Weiss, A., Aliprantis, A.O., Nakamura, M.C. Inflammatory arthritis increases mouse osteoclast precursors with myeloid suppressor function. *The J Clin Invest*. 122, 4592–605 (2012).

207- Hernandez, O., S. Way, S., McKenna, J. 3rd, Gambello, M.J. Generation of a conditional disruption of the Tsc2 gene. *Genesis*, 45,101-106 (2007).